การหาสภาวะที่เหมาะสมในการอบมอลต์ด้วยไมโครเวฟควบคู่กับการอบลมร้อนโดยพิจารณาการใช้พลังงานและปริมาณสารปนเปื้อนและการจำลองการกระจายอุณหภูมิในมอลต์ระหว่างการให้ความร้อนด้วยไมโครเวฟ

นางสุธิดา อัครชนียากร

วิทยานิพนธ์นี้เป็นส่วนหนึ่งของการศึกษาตามหลักสูตรปริญญาวิทยาศาสตรดุษฎีบัณฑิต
สาขาวิชาเทคโนโลยีทางอาหาร ภาควิชาเทคโนโลยีทางอาหาร
คณะวิทยาศาสตร์ จุฬาลงกรณ์มหาวิทยาลัย
ปีการศึกษา 2553

OPTIMIZATION OF COMBINED MICROWAVE-HOT AIR ROASTING OF MALT IN TERMS OF ENERGY CONSUMPTION AND NEO-FORMED CONTAMINANTS CONTENT AND SIMULATION OF THE TEMPERATURE DISTRIBUTION IN MALT DURING THE MICROWAVE HEATING

Mrs. Suthida Akkarachaneeyakorn

A Dissertation Submitted in Partial Fulfillment of the Requirements
for the Degree of Doctor of Philosophy Program in Food Technology
Department of Food Technology
Faculty of Science
Chulalongkorn University
Academic Year 2010

Thesis Title	Optimization of Combined Microwave-Hot air Roasting of Malt in Terms of Energy Consumption and Neo-Formed Contaminants Content and Simulation of the Temperature Distribution in Malt during the Microwave Heating
By	Mrs. Suthida Akkarachaneeyakorn
Field of Study	Food Technology
Thesis Advisor	Assistant Professor Jirarat Tattiyakul, Ph.D.
Thesis Co-Advisor	Associate Professor Jean-Claude Laguerre, Ph.D.

Accepted by the Faculty of Science, Chulalongkorn University in Partial Fulfillment of the Requirements for the Doctoral Degree

…… Dean of the Faculty of Science
(Professor Supot Hannongbua, Ph.D.)

THESIS COMMITTEE

…….. Chairman
(Professor Vanna Tulyathan, Ph.D.)

……..……. Thesis Advisor
(Assistant Professor Jirarat Tattiyakul, Ph.D.)

…….. Thesis Co-Advisor
(Associate Professor Jean-Claude Laguerre, Ph.D.)

…….. Examiner
(Assistant Professor Pasawadee Pradipasena, Sc.D.)

…….. Examiner
(Sasikarn Kupongsak, Ph.D.)

…….. External Examiner
(Associate Professor Suwit Siriwattanayothin)

สุธิดา อัครชนียากร : การหาสภาวะที่เหมาะสมในการอบมอลต์ด้วยไมโครเวฟควบคู่กับการอบลมร้อนโดยพิจารณาการใช้พลังงานและปริมาณสารปนเปื้อน และการจำลองการกระจายอุณหภูมิในมอลต์ระหว่างการให้ความร้อนด้วยไมโครเวฟ (OPTIMIZATION OF COMBINED MICROWAVE-HOT AIR ROASTING OF MALT IN TERMS OF ENERGY CONSUMPTION AND NEO-FORMED CONTAMINANTS AND SIMULATION OF THE TEMPERATURE DISTRIBUTION IN MALT DURING THE MICROWAVE HEATING) อ.ที่ปรึกษาวิทยานิพนธ์หลัก: ผศ. ดร.จิรารัตน์ ทัตติยกุล, อ.ที่ปรึกษาวิทยานิพนธ์ร่วม Assoc. Prof. Jean-Claude Laguerre, Ph.D. 171 หน้า

งานวิจัยนี้ประกอบด้วยสามส่วน ส่วนแรกมีวัตถุประสงค์เพื่อตรวจสอบการเกิดสีและจลนพลศาสตร์ของการเกิดสารปนเปื้อนในระหว่างการอบมอลต์ด้วยไมโครเวฟควบคู่กับการอบลมร้อน คั่วมอลต์ที่ระดับกำลังไมโครเวฟจำเพาะ (specific microwave power) 2.50 2.75 และ 3.00 วัตต์ต่อกรัม เป็นเวลา 3.4 นาที และคั่วมอลต์ต่อด้วยลมร้อนที่อุณหภูมิ 200 องศาเซลเซียส เป็นเวลา 0 37.5 75 112.50 และ 150 นาที วิเคราะห์การเปลี่ยนแปลงสีซึ่งแสดงด้วยค่าความแตกต่างสี (ΔE) และวิเคราะห์ปริมาณของสารปนเปื้อน ได้แก่ ไฮดรอกซีเมททิลเฟอร์ฟูรัล เฟอร์ฟูรัล ฟูแรน และอะคริลาไมด์ โดยการวิเคราะห์ปริมาณสารปนเปื้อน 2 วิธี คือ ฟลูโอโรเมตริก (fluorometric) และเคมีกายภาพ พบว่าค่า ΔE เพิ่มขึ้นแบบลอการิทึมกับเวลาในการคั่ว ฟูแรนวิเคราะห์โดยวิธีฟลูโอโรเมตริกแปรผันตามเวลาตามรูปแบบของสมการเส้นตรง แสดงว่าการเกิดฟูแรน มีรูปแบบเป็นปฏิกิริยาอันดับศูนย์ และไม่สามารถจำแนกรูปแบบการเกิดไฮดรอกซีเมททิลเฟอร์ฟูรัล เฟอร์ฟูรัล และอะคริลาไมด์ ตามเวลาในการให้ความร้อนได้ ส่วนที่สองมีวัตถุประสงค์เพื่อหาสภาวะที่เหมาะสมในการอบมอลต์ด้วยไมโครเวฟควบคู่กับการอบลมร้อนโดยพิจารณาการใช้พลังงาน และปริมาณสารปนเปื้อน คั่วมอลต์ที่กำลังไมโครเวฟจำเพาะ 2.50 ถึง 3.00 วัตต์ต่อกรัม เป็นเวลา 3.3 ถึง 3.5 นาที อุณหภูมิลมร้อน 180 ถึง 220 องศาเซลเซียส เป็นเวลา 60 ถึง 150 นาที วิเคราะห์ค่าความแตกต่างสี พลังงานที่ใช้โดยเตาอบไมโครเวฟ พลังงานที่ใช้โดยเตาอบลมร้อน พลังงานที่ใช้ทั้งหมด และปริมาณไฮดรอกซีเมททิลเฟอร์ฟูรัล เฟอร์ฟูรัล ฟูแรน และอะคริลาไมด์ เปรียบเทียบกับกระบวนการคั่วด้วยลมร้อนที่อุณหภูมิ 180 องศาเซลเซียส เป็นเวลา 2.5 3.5 และ 5 ชั่วโมง สำหรับการผลิตมอลต์สีกาแฟ ช็อคโกแลต และดำ พบว่าการอบมอลต์ด้วยไมโครเวฟควบคู่กับการอบลมร้อนลดการใช้พลังงานทั้งหมดได้ร้อยละ 40 26 และ 26 ตามลำดับ และสำหรับการผลิตมอลต์สีดำด้วยไมโครเวฟควบคู่กับการอบลมร้อน ลดปริมาณไฮดรอกซีเมททิลเฟอร์ฟูรัล เฟอร์ฟูรัล ฟูแรน และอะคริลาไมด์ ได้ร้อยละ 40 18 23 และ 95 ตามลำดับ ตรวจสอบความถูกต้องของสมการทำนายการเกิดสี พลังงานที่ใช้โดยเตาอบไมโครเวฟ พลังงานที่ใช้โดยเตาอบลมร้อน พลังงานที่ใช้ทั้งหมด ปริมาณไฮดรอกซีเมททิลเฟอร์ฟูรัล และเฟอร์ฟูรัล โดยทำการทดลองที่กำลังไมโครเวฟจำเพาะ 2.50 วัตต์ต่อกรัม เป็นเวลา 3.48 นาที อุณหภูมิลมร้อน 215 องศาเซลเซียส เป็นเวลา 136 นาที ร้อยละผลต่างของค่าที่ทำนายและการทดลองน้อยกว่าร้อยละ 20 ส่วนสุดท้ายจำลองการให้ความร้อนมอลต์ในบีกเกอร์ขนาดเส้นผ่านศูนย์กลาง 7.4 ซม. สูง 9.5 ซม. โดยใช้วิธีไฟไนต์อิลิเมนต์ ทำการทดลองเพื่อตรวจสอบความถูกต้องของแบบจำลองโดยใช้เตาอบไมโครเวฟที่ความถี่ 2,450 เมกกะเฮิร์ต พบว่าความแตกต่างของอุณหภูมิที่กึ่งกลางมอลต์เบดที่ได้จากการคำนวณมีความแตกต่างจากอุณหภูมิที่วัดได้จริงเท่ากับร้อยละ 10 โดยเฉลี่ย เมื่อจำลองการถ่ายโอนความร้อนในมอลต์ 75 กรัม ในระหว่างการให้ความร้อนด้วยไมโครเวฟ แปรกำลังไมโครเวฟจำเพาะ ที่ 2.50 2.75 และ 3.00 วัตต์ต่อกรัม เป็นเวลา 120 นาที และแปรน้ำหนักมอลต์ที่ 75 100 และ 125 กรัม ให้ความร้อนที่กำลังไมโครเวฟ 100 วัตต์ เป็นเวลา 120 นาที พบว่า มอลต์ดูดซับพลังงานไมโครเวฟมากบริเวณกึ่งกลางด้านล่างของเบด เมื่อเพิ่มกำลังไมโครเวฟจำเพาะจาก 2.50 เป็น 3.00 วัตต์ต่อกรัม ค่าการดูดซับพลังงานไมโครเวฟเพิ่มจาก 2.06×10^6 วัตต์ต่อลูกบาศก์เมตร เป็น 2.48×10^6 วัตต์ต่อลูกบาศก์เมตร การเพิ่มน้ำหนักมอลต์จาก 75 เป็น 125 กรัม มีผลให้ค่าอุณหภูมิสูงสุดในมอลต์เบดลดลงจาก 288.17 องศาเซลเซียส เป็น 53.11 องศาเซลเซียส ปริมาณไฮดรอกซีเมททิลเฟอร์ฟูรัล และอะคริลาไมด์ที่จุดร้อนเร็วในมอลต์ 75 กรัม ที่ระดับกำลังไมโครเวฟจำเพาะ 2.50 2.75 และ 3.00 วัตต์ต่อกรัม เพิ่มขึ้นตามเวลาและอุณหภูมิ

ภาควิชา : เทคโนโลยีทางอาหาร ลายมือชื่อนิสิต .....

สาขาวิชา : เทคโนโลยีทางอาหาร ลายมือชื่ออาจารย์ที่ปรึกษาวิทยานิพนธ์หลัก .....

ปีการศึกษา : 2553 ลายมือชื่ออาจารย์ที่ปรึกษาวิทยานิพนธ์ร่วม .....

4873874023 : MAJOR FOOD TECHNOLOGY
KEYWORDS: OPTIMIZATION / COMBINED MICROWAVE HOT AIR PROCESS / NEO-FORMED CONTAMINANT / KINETICS / MALT

SUTHIDA AKKARACHANEEYAKORN : OPTIMIZATION OF COMBINED MICROWAVE-HOT AIR ROASTING OF MALT IN TERMS OF ENERGY CONSUMPTION AND NEO-FORMED CONTAMINANTS CONTENT AND SIMULATION OF THE TEMPERATURE DISTRIBUTION IN MALT DURING THE MICROWAVE HEATING. THESIS ADVISOR : ASST.PROF. JIRARAT TATTIYAKUL, Ph.D., THESIS CO-ADVISOR : ASSOC. PROF. JEAN-CLAUDE LAGUERRE, Ph.D., 171 pp.

This research consists of three parts. The first part aimed to determine color development and kinetics of Neo-Formed Contaminants (NFCs) formation during combined microwave-hot air roasting of malt. Malts were roasted at different specific microwave powers (2.50, 2.75, and 3.00 $W \cdot g^{-1}$) for 3.4 min followed by hot air roasting at 200 °C for 0, 37.5, 75, 112.50, and 150 min. Changes in color represented by color difference (ΔE) and formation of NFCs including hydroxymethylfurfural (HMF), furfural, furan, and acrylamide were analyzed by using fluorometric and physico-chemical method. The browning (ΔE) of malts increased logarithmically with roasting time. Furan determined by the fluorometric method increased linearly with time which indicated that the formation of furan followed a zero order kinetic model. The changes in HMF, furfural, and acrylamide with roasting time could not be fitted with any kinetic model. The second part aimed to optimize the process of combined microwave-hot air roasting of malt in terms of energy consumption and NFCs formation. Malts were roasted by combined microwave-hot air at various specific microwave powers (SP = 2.50 to 3.00 $W \cdot g^{-1}$), microwave heating times (t_{mw} = 3.3 to 3.5 min), oven temperatures (T_{oven} = 180 to 220 °C), and oven heating times (t_{oven} = 60 to 150 min). The response variables; color, energy consumption by microwave (E_{mw}) and oven (E_{oven}), total energy consumption (E_{total}), and quantity of HMF, furfural, furan, and acrylamide were determined. Comparing with conventional processes (T_{oven} = 180 °C, t_{oven} = 2.5, 3.5, and 5 hours for coffee, chocolate and black malts, respectively) combined microwave-hot air reduced E_{total} by 40, 26, and 26% for coffee, chocolate and black malt, respectively, and reduced HMF, furfural, furan, and acrylamide contents in black malt by 40%, 18%, 23% and 95%, respectively. The proposed quadratic models of color, E_{mw}, E_{oven}, E_{total}, HMF and furfural contents were experimentally validated. The experiment was carried out using the following parameters: SP = 2.50 $W \cdot g^{-1}$ for 3.48 min, T_{oven} = 215 °C for 136 min. Percentage difference ($\%D$) values between the predicted values and the experimental ones were less than 20%. In the last part, microwave heating of malts in a beaker (7.4 cm diameter and 9.5 cm height) was simulated using finite element method. The model was experimentally validated by heating malts in a lab scale microwave oven operated at 2,450 MHz. The average value of difference $\%D_{avg}$ between the measured and the simulated temperature at the center of the bed was +10%. Heat transfer to a 75-g malt bed subjected to various microwave powers (2.50, 2.75, and 3.00 $W \cdot g^{-1}$) for 120 seconds and malt beds (75, 100, and 125 g) subjected to microwave heating at 100 W for 120 seconds was simulated. The simulation results in all cases showed that absorbed microwave energy concentrated near the center of a malt bed. Increasing microwave power from 2.50 $W \cdot g^{-1}$ to 3.00 $W \cdot g^{-1}$ resulted in an increase in absorbed power from 2.06×10^6 $W \cdot m^{-3}$ to 2.48×10^6 $W \cdot m^{-3}$, whereas increasing malt weight from 75 to 125 g resulted in a reduction in maximum temperature of malt bed from 288.17 °C to 53.11 °C. HMF and acrylamide contents were predicted from formation kinetic model and temperature of malt bed. HMF and acrylamide content at the hot spot in a 75-malt subjected to microwave heating at 2.50, 2.75, and 3.00 $W \cdot g^{-1}$ increased as a function of time and temperature.

Department : Food Technology ..... Student's Signature .....

Field of Study : Food Technology ..... Advisor's Signature .....

Academic Year : 2010 ..... Co-Advisor's Signature .....

ACKNOWLEDGEMENTS

I would like to thank to my parents and family for their support and encouragement.

I would like to express my sincere appreciation to Asst. Prof. Dr. Jirarat Tattiyakul and Assoc. Prof. Dr. Jean Claude Laguerre for their suggestions and patience during my research and studies. I would also like to thank Prof. Dr. Vanna Tulyathan, Asst. Prof. Dr. Pasawadee Pradipasena, Dr. Sasikarn Kupongsak, and Assoc. Prof. Suwit Siriwattanayothin for their invaluable comments.

I would like to thank Dr. Benjamin Neugnot, Dr. Patrick Boivin, Dr. Francisco J. Morales, Dr. Ines Birlouez-Aragon, and Dr. Jad Rizkallah for their support.

I am grateful to the National Science and Technology Development Agency, Ministry of Science and Technology, Thailand and ICARE project, a European Collective Research Project (516415) for the funding support for this study.

My appreciation also goes to technicians in the STAI Department, LaSalle Beauvais France and in the Food Technology Department, Faculty of Science, Chulalongkorn University for their help.

CONTENTS

Pages

Pages

Pages

Pages

LIST OF TABLES

Pages

Pages

LIST OF FIGURES

Pages

Pages

Pages

Pages

LIST OF SYMBOLS

$\boldsymbol{A}$	reactants
$\boldsymbol{B}$	the magnetic field vector ($Wb \cdot m^{-2}$)
B_0	intercept
B_{ij}	parametric coefficient of the model
Cp	specific heat ($J \cdot kg^{-1} \cdot °C^{-1}$)
$\boldsymbol{D}$	electric flux density ($C \cdot m^{-2}$) = εE
D	moisture diffusivity ($m^2 \cdot s^{-1}$)
$\% D_{avg}$	average value of difference in %
d_p	penetration depth (m)
E	electric field ($V \cdot m^{-1}$)
Ea	activation energy ($kJ \cdot mole^{-1}$)
E_{mw}	energy consumption of microwave oven (kJ)
E_{oven}	energy consumption of hot-air oven (kJ)
E_{total}	total energy consumption (kJ)
e	a mathematical constant = 2.718
f	frequency (GHz)
$\boldsymbol{H}$	magnetic field intensity ($A \cdot m^{-1}$)
h	heat transfer coefficient ($W \cdot m^{-2} \cdot K^{-1}$)
$\boldsymbol{J}$	current density ($A \cdot m^{-2}$)
j	the imaginary portion $= (-1)^{1/2}$

k	thermal conductivity ($W \cdot m^{-1} \cdot K^{-1}$)
k_c	reaction rate constant $(mol \cdot cm^{-3})^{1-n}/sec$
M	moisture content ($kg \cdot m^{-3}$)
n	order of reaction
N	number of experiment
P	power generation of the product (W)
P_a	power absorbed (W)
P_i	the incident power (W)
P_{mw}	microwave power input (W)
P_0	microwave power transmitted into a sample (W)
P_r	the reflected power (W)
P_{trans}	power transmitted through a sample (W)
P_v	the power absorbed per unit volume ($W \cdot cm^{-3}$)
P_x	power generation in x direction (W)
P_y	power generation in y direction (W)
P_z	power generation in z direction (W)
$P(z)$	power as a function of distance into the material (W)
Q	heat generation ($W \cdot m^{-3}$)
SP	specific microwave power ($W \cdot g^{-1}$)
T	temperature (°C)
T_a	air temperature in microwave cavity (°C)
$T_{experiment}$	experimental temperature (°C)

T_s	surface temperature of food (°C),
$T_{simulation}$	simulated temperature (°C)
T_0	initial temperature (CC)
t	time (s)
t_{mw}	processing time by microwave (hr)
V	volume (m^3)
w	weight of malt (g)
X_i	coded values of independent variables
Y_k	experimental responses
z	distance (m)
ΔL	L-value difference = $L_{not\text{-}treated\ malt}$ - L_{sample}
Δa^*	a^*-value difference = $a^*_{not\text{-}treated\ malt}$ - a^*_{sample}
Δb^*	b^*-value difference = $b^*_{not\text{-}treated\ malt}$ - b^*_{sample}

Greek letters

α	attenuation factor (m^{-1})
α_d	thermal diffusivity ($m^2 \cdot s^{-1}$)
β	angle coordinate (degrees)
ε	complex permittivity = $\varepsilon' + j\varepsilon''$
ε_0	permittivity of free space = $8.86 \cdot 10^{-12}$ F/m
ε′	permittivity or dielectric constant

ε''	dielectric loss factor
λ_0	wave length of microwave (m)
μ	complex permeability
μ'	magnetic permeability
μ''	magnetic loss factor
ρ	density of food ($kg \cdot m^{-3}$)
σ	electric conductivity (S/m)
ϕ	angle coordinate (degrees)

Subscripts

i, and j	the number of dependent variables = 1, 2, 3, or 4
k	the number of independent variables = 1, 2, 3,…,or 8

CHAPTER I

INTRODUCTION

In the brewing industry, speciality malts or colored malts have been used to give particular colors and flavors to beers. High temperature needs to be attained during roasting of malt in order to get desirable color and flavor. Neo-formed contaminants (NFCs) are the products of Maillard reaction in thermally processed foods. NFCs found in carbohydrate-rich foods are, for example, hydroxymethylfurfural (HMF), furfural, furan, and acrylamide. The presence of NFCs in food is a major concern for humans because of their ability to induce cancer and heritable mutations in laboratory animals.

Microwaves can penetrate inside materials and deposit energy, hence heat can be generated throughout the entire volume of material. Indeed, the transfer of energy does not rely on diffusion of heat from the surface, it is possible to achieve rapid heating that reduces processing time and enhances overall quality of the heated products. Usually, the industry of roasting of the malt implements high temperature air to achieve coloration of malt. It is ordinarily a long, slow process because of the resistance of the hulls to the passage of moisture. This research proposes a new procedure based on the combination of microwaves and hot air to produce colored malt. This new procedure allows energy saving, while getting a product with desirable color, and avoiding the formation of carcinogenic and toxic substances such as NFCs. In addition, the study of the effect of thermal treatment on color development and kinetics of NFCs formations has been performed.

Simulation of the temperature distribution in malt during the microwave heating by mathematical models, provides an insight into the microwave cooking process. Product developers will be able to test the effects of the changes in the food formulations without delay or without the cost of having to work on product samples. Thus, the mathematical modeling minimizes laborious and time consuming work.

1.1 OBJECTIVES

The objectives of this study were:

1. To determine color development and kinetics data of NFCs during combined microwave-hot air heating process.

2. To determine the effect of specific power, microwave processing time, oven temperature, and oven processing time on energy consumption and NFCs content during combined microwave-hot air roasting.

3. To determine the optimum conditions for the production of coffee, chocolate and black malts by using Response Surface Methodology (RSM) analysis.

4. To compare energy consumption and NFCs content during roasting of malt by hot air-only and combined microwave-hot air processes.

5. To simulate energy transfer in a malt bed subjected to microwave heating process.

6. To study the effect of microwave power and weight of malt bed on energy distribution inside a malt bed.

1.2 OUTLINE

This thesis consists of five chapters. Chapter 2, “A Comprehensive Review” describes the theoretical background of microwave, Maillard reaction, and information on NFCs. Chapter 3, “Color Development and Kinetics of Neo-Formed Contaminants Analysis during Combined Microwave-Hot Air Roasting in Malt” deals with the determination of color development and kinetics data of NFCs during combined microwave-hot air roasting process. Chapter 4, “Optimization of Combined Microwave – Hot Air Roasting of Malt Based on Energy Consumption and Neo-Formed Contaminants Content” deals with the determination of predictive equations for color development, energy consumption, and NFCs content in malt. Chapter 5, “Simulation of the temperature distribution in malt during microwave heating” deals with the measurement of physical thermal and dielectric properties of malt and the simulation of heat distribution in malt bed subjected to different heating conditions.

CHAPTER II

A COMPREHENSIVE REVIEW

Microwave ovens have become increasingly popular as a means of heating or warming foods in households. To design an optimum process for microwave heating, it is necessary to understand the theory of microwave heating and the factors affecting heat transfer such as physical properties, thermal properties of food products and microwave oven, and the operating conditions of the microwave oven.

2.1 Microwave theory

Microwaves are electromagnetic waves that have a frequency range from 0.3 GHz to 300 GHz with corresponding wavelengths ranging from 1 meter to 1 millimeter. Microwaves are coherent and polarised in contrast to visible waves (excluding lasers). They obey the laws of optics and can be transmitted, absorbed or reflected depending on the type of material.

The frequencies for microwave heating come under the rules of the Federal Communications Commission which provide certain frequencies for industrial, scientific, and medical (ISM) uses. The commission has assigned for ISM frequencies which conform to the International Radio Regulations adopted in Geneva in 1959. These frequencies are 915, 2,450, 5,800, and 22,125 MHz (Decareau, 1985). Household microwave ovens operate at 2,450 MHz which corresponds to a wavelength of 12.2 centimeters (Buffler, 1993) and microwave power output in the 500-1,000 Watt range.

2.1.1 Microwave generator

Microwaves are generated by a magnetron. A magnetron is a circular symmetrical tube like diode that consists of a cathode as the central axis of the tube and an anode around the circumference. Magnetron contains a space called resonant cavitiy. Resonant cavities act as tuned circuits and generate electric fields. These cavities also determine the output frequency of the microwave. Magnetron has an antenna connected to an anode and it extends into resonant cavities. Antenna is used for transmitting microwave from the magnetron to waveguide (Figure 2.1). The magnetic field is created by a magnetic field that surrounds the magnetron. When power is applied, an electron-emitting material at the cathode becomes excited and emits electrons into the vacuum space between the cathode and anode. The energy of the electrons is caught in the fields. The excess microwave energy travels as waves and are extracted by the antenna. The antenna transmits the oscillating waves to the waveguide where they travel into the oven cavity. The metallic walls of the waveguide are nearly perfect electric conductors and microwaves propagate with low transmission losses. As the waves enter the cavity, they are dispersed by a stirrer (Figure 2.1). This action minimizes hot and cold spots in the oven cavity (Gunasekaran, 2002).

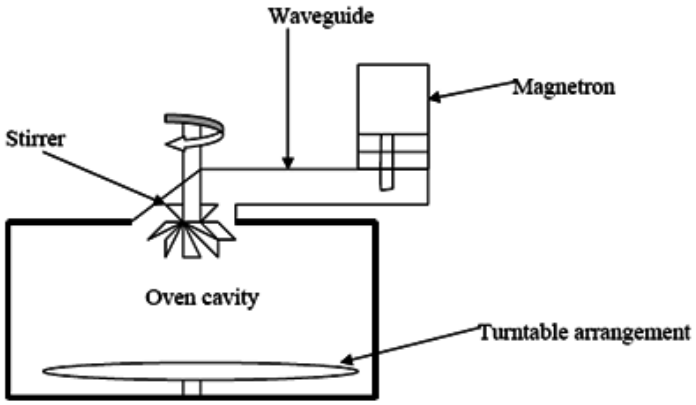

Figure 2.1 Major components of a typical microwave oven.

Source: Guanasekaran (2002)

In conventional thermal processing, energy is transferred to the material through convection, conduction, or radiation of heat from the surfaces of the material. In contrast, microwave energy is delivered directly to materials through molecular interaction with the electromagnetic field. In conventional heating methods, energy is transferred due to thermal gradients but microwave heating is the conversion of electromagnetic energy to thermal energy through direct interaction of the incident radiation with the molecules of the target material. The difference in the way that energy is delivered can result in many potential advantages for using microwaves for processing materials. Microwaves can penetrate materials and deposit energy which means that heat can be generated throughout the volume of the material. This transfer of energy does not rely on diffusion of heat from the surfaces, thus achieving rapid heating that reduces processing time and enhances overall quality. In addition to volumetric heating, microwaves can be used to heat low thermal conductivity products. It is also possible to have selective heating which is able to heat target compounds.

The main disadvantage of microwave heating is non-uniformity. The waves are only coming from one direction, from left to right and front to back in the microwave oven as shown in Figure 2.2a and 2.2b. Combining the two waves, as shown in Figure 2.2c, the amplitudes of all internal rays add or subtract at all positions within the slab. This phenomenon causes hot and cold spots inside an oven cavity.

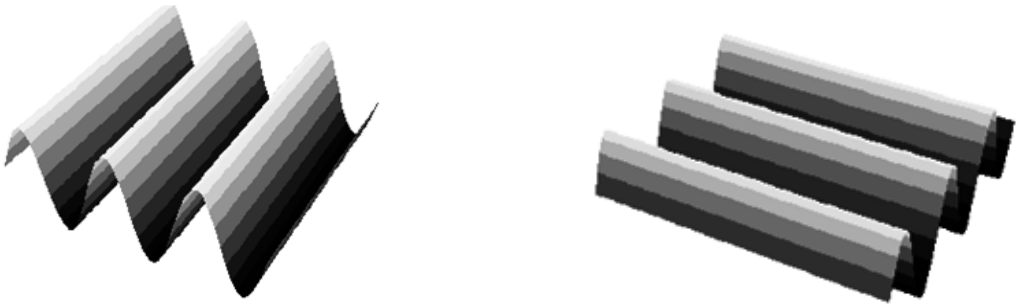

(a) (b)

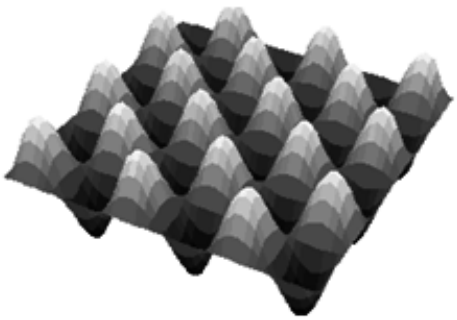

(c)

Figure 2.2 Wave goes from left to right and front to back in the microwave oven (a) and (b), and combining the two waves (c) causes hot and cold spots inside an oven cavity.

Source: National Science Foundation (2005)

2.1.2 Interaction of microwave with materials

In microwave heating, the heating effect in food products is the result of two mechanisms, which are ionic interaction and dipolar interaction.

2.1.2.1 Ionic interaction

Most food products contain water with varying amounts of dissolved salts such as sodium, potassium, and calcium chloride. When these salts dissolve, the molecule ionizes or separates into two charged particles or ions which interact with the electric field. The energy transfer to the ions and then to neighboring atoms or molecules is one mechanism of microwave heating. The interaction with sodium and chlorine ions is shown in Figure 2.3.

In the enclosed cavity of a microwave oven, the field extends in the three perpendicular oven directions: Any charged particle found in the oven, or in any material placed in the oven, experiences a force alternating in the three orthogonal directions at 2.45 billion times per second. The net force will first accelerate the particle in one direction and then in the opposite, with particles of opposite charges being accelerated in opposite directions. The accelerating particle collides with an adjacent particle, it will impart kinetic energy to it resulting in an increase in particle's temperature. As the second, more agitated, particle interacts with its neighbors, it transfers agitation or heat to them, until all neighboring particles have their temperature increased. By this mechanism, energy from the oscillating microwave electric field in the microwave oven cavity is imparted to charged particles in terms of physical agitation. This increased energy of agitation, or heat, is then transferred to other parts of the material.

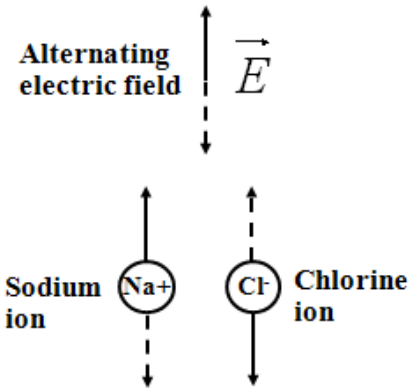

Figure 2.3 Inonic interaction.

2.1.2.2 Dipolar interaction

The water molecules prevalent in most foods and many materials are made up of two hydrogen atoms and an oxygen atom. The structure of the molecule is in the form of a V as shown in Figure 2.4, with the two hydrogen atoms attached to the oxygen atom making an angle of 105º. The hydrogen atoms consist of a positive charge, and the oxygen atom consists of two negative charges. The charges are physically separated and in this form are called a dipole. This dipole is the equivalent of an electric compass needle and acts in an electric field in the same way that a magnetic compass needle acts in a magnetic field. If these water molecules are placed in a region of an oscillating electric field, they will experience a torque or rotational force attempting to orient them in the direction of the field.

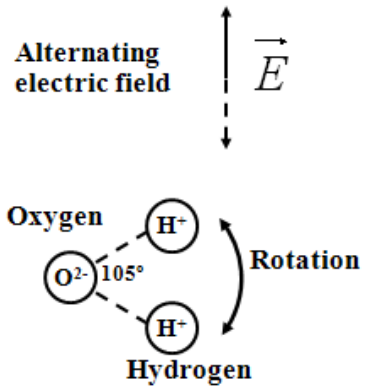

Figure 2.4 Dipolar interaction.

Before the microwave electric field is applied, all the water molecules in the food are thermally agitated in a random fashion corresponding to the initial temperature of the sample to be heated. When the field is applied, the molecules all attempt to orient themselves in the initial field direction. As they do, they collide randomly with their neighbors. When the field reverses, they attempt to reverse direction and further collisions occur. These collisions add to the background thermal agitation, then perceived as an increase in temperature.

2.1.3 Dielectric properties

Microwave radiation is part of the electromagnetic spectrum, it behaves like the visible light radiation. Similar to the laws of optics, materials interact with microwaves in three ways. Firstly, they reflect microwave radiation impinging on them. Secondly, they transmit microwaves that have entered into them. Finally, they absorb some of the microwave energy being transmitted through them.

Mathematical equations developed by Maxwell predict the complete behavior of electromagnetic radiation's interaction with matter for any type of material in any geometry. In order to do this, two pairs of parameters describing the

material are required. These pairs are known as the complex permeability (μ) and the complex permittivity (ε).

$$\mu = \mu' - j\mu'' \quad (2.1)$$

$$\varepsilon = \varepsilon' - j\varepsilon'' \quad (2.2)$$

Complex permittivity is the dielectric property that describes food behavior under an electromagnetic field (Metaxas and Meredith, 1993). The real part of complex permittivity is called the dielectric constant (ε'), and the imaginary part is called dielectric loss (ε″).

To understand how microwaves interact with materials, consider a plane wave impinging on an infinite slab of material. A plane wave is defined as microwave radiation whose electric field's direction in space are all parallel. Such is the case for an electromagnetic wave far from its generating antenna or as exists in an empty oven cavity with the microwaves bouncing from wall to wall. For small loads in a microwave oven, the assumption of plane waves impinging on the food may have somewhat more validity than for large loads, particularly if the load is thin and flat. For larger loads the assumption is inaccurate but still gives a basis for visualization.

2.1.3.1 Reflection, absorption, refraction

When a microwave wave strikes a food sample, it can be reflected, absorbed, refracted.

2.1.3.1.1 Reflection

During a microwave radiation incident upon a slab from a direction perpendicular to its surface, part of energy is reflected. The extent of

energy reflected from the surface, P_r, is dependent on the slab's dielectric constant ε′. The principal determining factor for the magnitude of reflection comes from the dielectric constant (ε′) of the material. Errors due to neglecting ε″ are less than 5% for virtually all foods. Neglecting the loss factor, an approximate relation for the reflection of microwave power reflected from an infinite-slab food surface is;

$$P_r = \left(\frac{\sqrt{\varepsilon'} - 1}{\sqrt{\varepsilon'} + 1} \right)^2 \qquad (2.3)$$

2.1.3.1.2 Absorption

P_r is the reflected power, the amount transmitted into the medium, P_0, is given by P_0 = 1- P_r**.** The equation for microwave power absorption by a product is shown in Equation 2.4.

$$P_v = 2\pi f \varepsilon_0 \varepsilon'' E^2 \qquad (2.4)$$

2.1.3.1.3 Refraction

For microwave radiation incident on a surface at an oblique angle (ϕ), the reflected wave is at the same angle (Figure 2.50). The transmitted wave is refracted toward a line perpendicular to the surface (normal direction) at an angle β. The magnitude of β is given by Snell's law:

$$\sin \beta = \sin \phi / (\varepsilon')^{1/2} \qquad (2.50)$$

Equation 2.50 is approximate; a correct equation includes the loss factor. Examining the initial reflected ray shows that if the absorption of the medium is not too great, a portion of the microwave power reaches the opposite side of the slab. At this interface a portion of the wave is reflected internally according to Equation 2.50, and a portion is transmitted out the opposite side. This reflection process continues until there is essentially no remaining microwave power at an interface; that is, the power has been essentially all been absorbed during the multiple reflections.

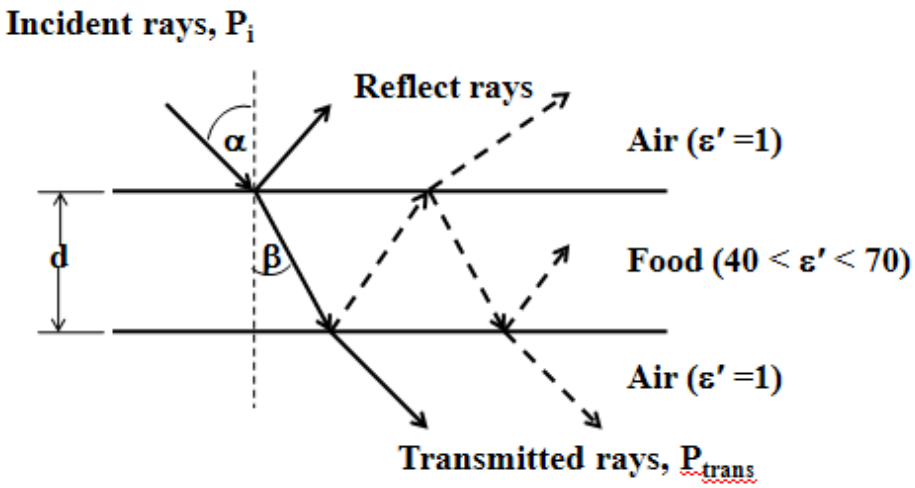

Figure 2.50 Reflection, absorption, and transmission of microwaves in a dielectric medium.

Source: Buffler (1993)

2.1.3.1.4 Transmission

The power reflected from the surface by an oblique incident wave shown in Figure 2.50 consists of the sum of the initially reflected wave plus all the waves emanating from that surface produced by the internal multiple

reflections. Some power also escapes from the opposite side of the slab during these multiple reflections. The total power transmitted through the product, P_{trans}, is the sum of the power emanating at each internal reflection. The same analysis holds for perpendicular incidence, $\alpha = 0^{o}$, as previously discussed. Energy, and thus power, is conserved; in other words, it must all be reflected, absorbed, or transmitted through the slab. The refraction of power transmitted is thus:

$$P_{trans} = 1 - P_r - P_a \qquad (2.6)$$

2.1.3.2 Factors affecting dielectric properties

Dielectric properties of food, which describe how materials interact with electromagnetic radiation, exert a great impact on heat generation and transfer inside the foods during microwave heat treatment. Knowledge of dielectric properties is important in the selection of proper packaging materials and cooking utensils and in the design of microwave heating equipment. The capability of foods to store electromagnetic energy is described by their dielectric constant (ε') while the ability to dissipate electromagnetic energy into heat is described by their dielectric loss factor (ε″). Both dielectric properties are influenced by food composition, product temperature, and microwave frequency.

2.1.3.2.1 Food composition

The dielectric properties of food products are primarily determined by their chemical composition and, to a much lesser extent, by their physical structure. The effect of water and salt content depends to a large extent on the manner in which the molecules are bound or restricted in their movement by other

food components. In general, ε' is directly proportional to water content while ε″ varies with the proportion of water, salt and fat content, temperature, and microwave field frequency. It has been reported that the amount of free water greatly affects ε' since the microwave heating effect is by means of free water rotation in an oscillating field (Ryynanen, 1995). At low or moderate salt contents, ε' is hardly modified granted that the amount of water is unchanged. In contrast, at higher salt concentrations, water molecules are bound and lose their ability to reorient themselves in response to the changing electromagnetic field direction resulting in a lower ε'. However, higher salt contents cause an increase in free charge density, hence an enhanced conductivity and an elevation of ε″ (Figure 2.6).

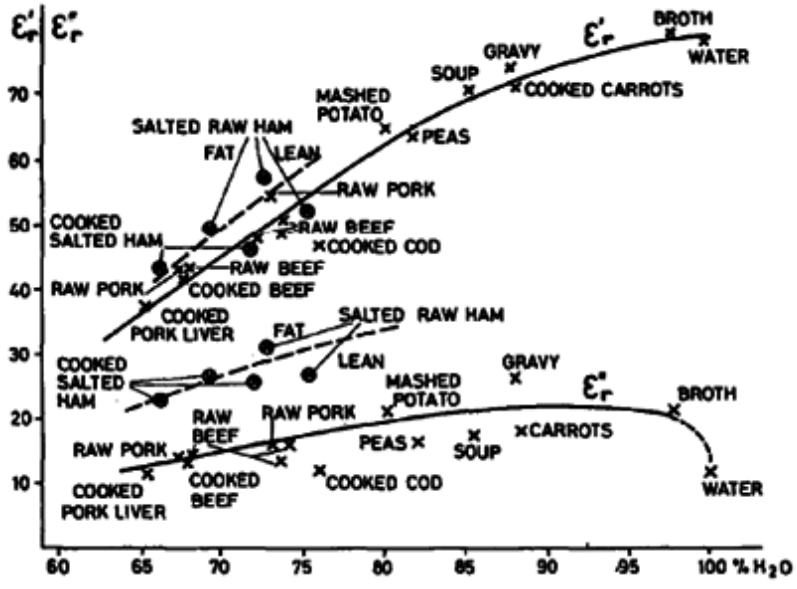

Figure 2.6 Relationship between water content and dielectric data at 20 °C and 2800 MHz.

Source: Ryynanen (1995)

2.1.3.2.2 Product temperature

The dielectric properties of food at low temperatures are influenced by the amount of free (or mobile) water and ions. During thawing of foods with high water content, a sharp increase in ε' and ε″ is observed in the melting zone. After melting, ε' decreases with further temperature increase. This is because the random thermal motions of the molecules oppose the orienting action created by the electromagnetic field. Therefore, as temperature increases, the efficiency of polarization of free water by the electromagnetic field decreases giving rise to a decrease in ε'. For pure water, ε″ decreases rapidly with increasing temperature. It has been observed that at a higher microwave frequency, only salty foods show an increase in ε″ with temperature (Ryynanen, 1995). As the food becomes saltier such as cooked ham, the ionic effect comes into play, reducing the drop-off of ε″ with temperature (Figure 2.7).

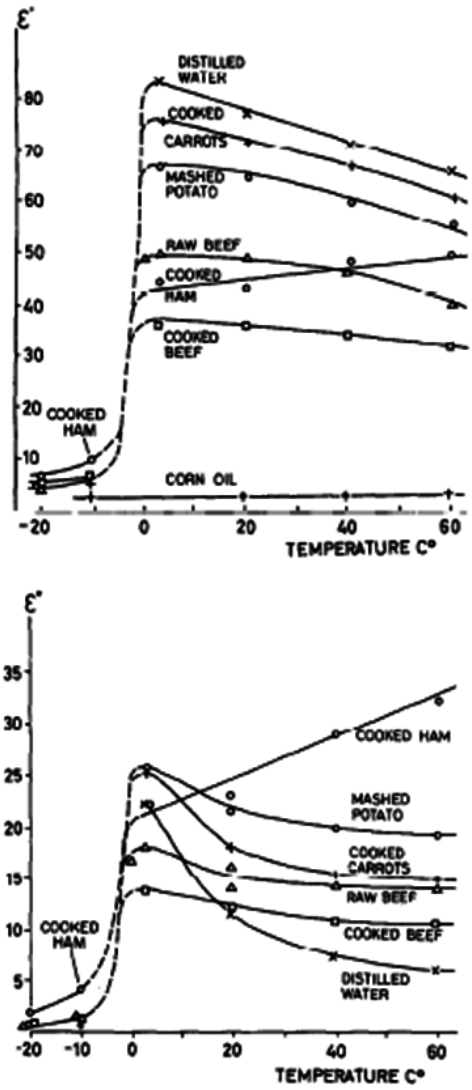

Figure 2.7 Temperature dependence of ε' and ε" for various food substances at 2800 MHz.

Source: Ryynanen (1995)

The large differences in both dielectric and thermal properties between frozen and thawed foods can cause difficulties in thawing. The thawed part of a food has a higher ε' and ε″ thus, lower characteristic impedance than the frozen part. This effect is known as runaway heating, which means that the warm

part is rapidly heating while there is still some ice left in the rest of the food (Ryynanen, 1995). The dielectric parameters of frozen food are complicated because they depend not only on the amount of unfrozen water, which changes with temperature, but also on its location and salinity (Buffler, 1993).

2.1.3.2.3 Microwave frequency

In foods having high salt contents, ionic losses are much higher and dipole losses are much lower at 915 MHz than at 2450 MHz. This is because, at lower frequencies, ions have more time to migrate back and forth with the change of field direction contributing to an increase in ε″. On the other hand, loss due to dipolar movement is more important when moving towards higher frequencies, resulting in a lower ε″ (Buffler, 1993). At very high frequencies, molecules just quiver instead of rotating (Sharma, *et al*., 2000). ε' is mainly influenced by dipolar movement. As long as the polar molecule can rotate freely, the dipole moment, which is a measure of ε', is fully effective and ε' remains constant (Buffler, 1993). However, study (Westphal and Sils, 1972) has shown that, in sea ice, ε' slightly decreases with increasing frequency (Table 2.1).

Table 2.1 Dielectric constant of sea ice

Temperature (°C)	Frequency (MHz)		
	500	1000	2700
20	3.20	3.20	3.20
30	3.18	3.17	3.17
40	3.16	3.16	3.16
50	3.15	3.15	3.14
60	3.14	3.14	3.13

Source: adapted from Mudgett (1995)

2.1.4 Penetration depth

The penetration depth, d_p, is the depth at which the microwave power decreases to 1/e or 36.8% of its original power. Since microwave energy is absorbed as it penetrates the food, effective heating will not take place at greater depths (Sharma *et al*., 2000). The equation describing the power at any point within an infinite slab of material for an incident plane wave is

$$\frac{P(z)}{P_0} = e^{-z/d_p} \qquad (2.7)$$

2.1.5 Factors affecting heat transfer by microwave

Temperature distribution inside the product subjected to microwave heating is non-uniform. There are several factors that affect heat generation and transfer in food heated in a microwave oven. The factors widely studied include

physical properties, e.g. the size and shape of food, thermal properties of food, e.g. thermal conductivity (k) and specific heat (C_p), and the operating conditions of the microwave oven, e.g. microwave frequency, microwave power cycling, and rotation of food.

2.1.5.1 Physical properties of food

2.1.5.1.1 Size

The size of a food product affects the depth of microwave penetration, heating rate and uniformity. Irregular shaped products are subjected to non-uniform heating due to the difference in product thickness (Mudgett, 1995). Romano *et al*. (2005) solved the mathematical model of microwave heating by using FEMLAB®, release 3.00 with the Chemical Engineering Module. The authors considered the problem in two-dimensional symmetry and used the Finite Element Method (FEM) to solve the problem. Cylindrical samples of potato were considered and the results presented in their study showed that, as the cylinders dimensions increased, the maximum temperature moved from the axis towards the external surface. These results agree with a previous study by Oliveira and Franca (2002).

2.1.5.1.2 Shape

Microwave energy generates hot spots or maximum temperature values in the center of spheres. In cylinders, microwaves generate non uniform radial distribution with the surface reaching the highest temperature values. However, microwave energy generates maximum temperature values in the center of spheres and cylinders when the microwave penetration depth is approximately 1.5 times the food's diameter (Buffler, 1993). In cube and slab geometries, microwave energy concentrates in the corners. The corners are normally vulnerable to heating

because they are exposed to microwaves from many directions resulting in overheating and, hence, non-uniform doneness. These findings agreed with a previous study by Campanone and Zaritzky (2005).

2.1.5.2 Thermal properties

2.1.5.2.1 Thermal conductivity

The thermal conductivity of a material is a measure of its ability to conduct heat. Although thermal conductivity depends mostly on composition, the percentage of void space, shape, size and arrangement of void spaces and homogeneity of the food can affect the heat flow paths through the material (Sweat, 1995). The thermal conductivity of food plays an important role in microwave heating. High thermal conductivity materials dissipate heat faster than low thermal conductivity materials during microwave heating. Food with high thermal conductivity will take less time to attain uniform temperature during the holding period.

2.1.5.2.2 Specific heat

Specific heat indicates how much heat is required to change the temperature of a material. Specific heat can be raised by increasing solid content by adding components like salt or protein.

In general, heat transfer rates are higher for foods possessing higher thermal conductivity and lower specific heat values. However, foods that have a very high *k* (highly conductive materials) are not suitable for being heated in a microwave oven because they reflect nearly all of the incident microwave energy on its surface. This causes power output loss and overheating of the magnetron that, in turn, shortens the magnetron's operating life or possibly damage it.

High thermal diffusivity ($\alpha_d=k/(\rho \cdot Cp)$) aids in heat distribution inside foods. Thus, the more frozen water, which has the high value of α_d, contained in foods, the faster heat will move away from the point where energy is deposited. However, heating rate of frozen water by the microwave oven is low because of the frozen water has low dielectric constant and dielectric loss (where the molecules are not free to rotate).

2.1.5.3 The operating conditions of the microwave oven

2.1.5.3.1 Microwave frequency

Oliveira and Franca (2002) simulated cylindrical shrimp sample having a radius of 1.6 centimeters, irradiated at 915 MHz and 2450 MHz and a microwave power of 3.00 $W \cdot cm^{-2}$. The initial temperature of the sample was at 27 ^{0}C. The sample irradiated at 2450 MHz was heated for 1 minute, and the sample irradiated at 915 MHz was heated for 30 seconds. For the samples irradiated at 915 MHz, higher temperature values were attained in comparison to the samples heated at 2450 MHz. The energy absorption was more effective at lower frequencies. The relative dielectric loss values were higher at 915 MHz compared to 2450 MHz, indicating that dissipation of electromagnetic energy into heat was more effective at lower frequencies.

2.1.5.3.2 Microwave power cycling

Taher and Farid (2001) investigated the microwave thawing of a 1.5 kg frozen minced beef sample in a plastic circular tray (235 millimeters in diameter and 40 millimeters height) placed in the center of a microwave oven cavity. The sample irradiated at 2450 MHz with a 650 W output was heated from the topside only. The cyclic on-off operation of the microwave rating was 100 % and 28 % (a 7 second power-on followed by an 18 second power-off).

The result showed that the cyclic 28% operation decreased the rate of mean temperature change, thus increasing heating uniformity when compared with continuous heating.

2.1.5.3.3 Rotation of food

Oliveira and Franca (2002) studied the effect of rotation on a sample by simulating an irregular beef sample (3.2 centimeters × 1.6 centimeters). The sample was irradiated at 2800 MHz for 1 minute. The authors found that the difference between the maximum and minimum temperatures for the static sample was 90°C and that the difference between the maximum and minimum temperatures for the rotated sample was 43°C. Rotating the sample led to a significant decrease in temperature gradients which, when coupled with power cycling, further reduced the non-uniformity in microwave heating. Moreover, the authors found that a cylindrical beef sample of 0.8 centimeter in radius heated at 2800 MHz with power cycling mode and rotation had a 72% reduction in the difference between maximum and minimum temperatures when compared to a static sample using continuous heating.

Geedipalli *et al*. (2007) studied the role of rotation of a potato sample in improving uniformity of food in a microwave oven. The sample cube (3.6 centimeters × 4.7 centimeters × 2.1 centimeters) was irradiated at 2450 MHz. The initial temperature of the air and food inside the oven was constant at 25 °C. The results showed that the turntable helped in increasing the temperature uniformity of the potato by about 40 %.

2.2 Maillard Reaction

The Maillard reaction is a non-enzymatic browning reaction, caused by the condensation of an amino group and a reducing compound, resulting in complex biological changes in the food system. The Maillard reaction occurs when foods are either heated or during storage. The positive contributions of the Maillard reaction are flavor generation and color development. The negative aspects are off-flavor development, flavor loss, discoloration, loss of nutrition value and formation of toxic Maillard reaction products (Lingnert *et al*., 2002). Therefore, the aim of the food manufacturer is to find an optimum balance between the positive and negative aspects. The Maillard reaction is favored in systems with intermediate moisture content with a_w values between 0.5 and 0.8, temperatures over 50 °C and a slightly acidic pH (pH 4-7) (Capuano *et al*., 2008). The Maillard reaction takes place in three major stages and is dependent on factors such as concentrations of reactants and reactant type, pH, time, temperature and water activity. The early stage (step 1) involves the condensation of a free amino group (from free amino acids and/or proteins) with a reducing sugar to form Amadori or Heyns rearrangement products. The advance stage (step 2) is a degradation of the Amadori or Heyns rearrangement products via different alternative routes involving deoxyosones, fission or Strecker degradation. A complex series of reactions including dehydration, elimination, cyclization, fission, and fragmentation results in a pool of flavor intermediates and flavor compounds as illustrated schematically in Figure 2.8. The final stage (stage 3) of the Maillard reaction is characterized by the formation of brown nitrogenous polymers and co-polymers. While the development of color is an important feature of

the reaction, relatively little is known about the chemical nature of the compounds responsible. Color compounds can be grouped into two general classes: low molecular weight color compounds, which comprise two to four linked rings, and the melanoidins, which have much higher molecular weights (Lingnert *et al*., 2002).

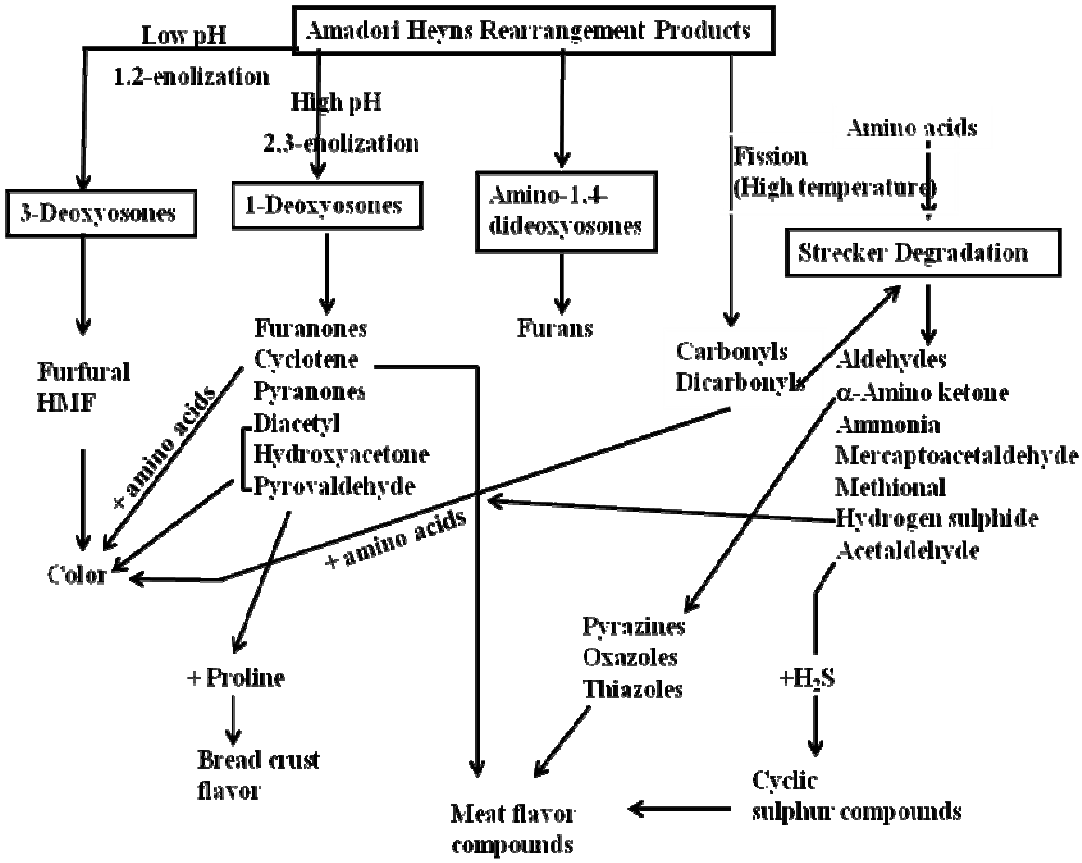

Figure 2.8 Pathways of the formation of key flavor intermediates and products in the Maillard reaction.

Source: Mlotkiewics (1998)

2.2.1 Controlling factors of the Maillard reaction products

Maillard reaction can be controlled through starting reactants, water activity, pH, and temperature and time.

2.2.1.1 Starting reactants

The starting reactants of the Maillard reaction are reducing sugar and amino acids/proteins. The Maillard reaction requires reducing sugar, i.e. sugar containing keto- or aldehydes (free carbonyl groups). All monosaccharides and sugars, except for sucrose, are reducing sugars. In oligosaccharides and starch only the end-terminal monosaccharide is a reducing sugar. Starch and sugars, such as sucrose, lactose and maltose, can easily hydrolyse upon heating above 100 °C at a slightly acidic pH, resulting in the formation of monosaccharides (reducing sugar). Thus, thermal processing often results in a continuous supply of reducing sugar formed from complex carbohydrates.

The reactivity of amino acids has been performed on free amino acids in diluted aqueous solutions. Amongst the amino acids studied, lysine was the most reactive. In proteins and peptides, only free amino groups i.e. N-terminal α-amino groups and Ω-amino groups can react (Mlotkiewics, 1990). The richest sources of lysine are found in red meat, fish, and diary products (University of Maryland Medical Center, 2010).

2.2.1.2 Water activity

Water has both an inhibitory and an accelerating impact on the Maillard reaction. Water acts partly as a reactant, partly as a solvent and as a transporting medium of reactants. In the initial step of the Maillard reaction, three moles of water are formed per mole of carbohydrate, thus the reaction occurs less readily in foods with a high water activity (a_w) value because the dilution of the reagents. At low a_w, the mobility of reactants is limited, despite their presence at

increased concentrations resulting in the reduction of browning rate (Mlotkiewics, 1990; Lingnert *et al*., 2002; Nursten, 2005).

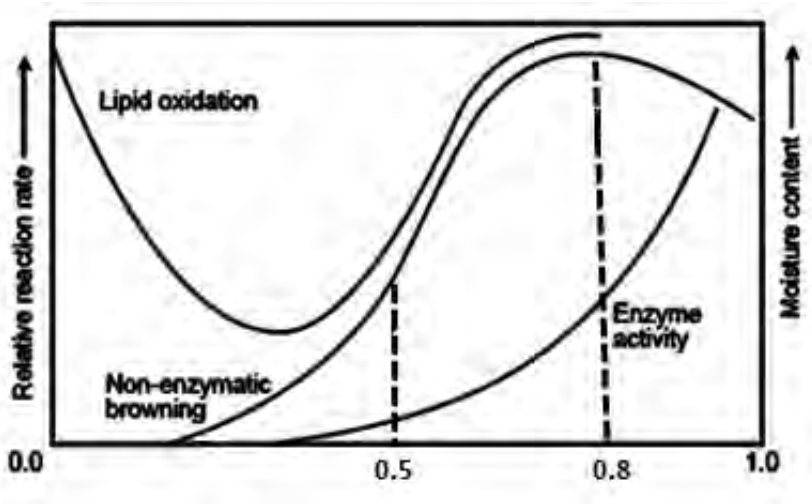

Figure 2.9 Reaction rates of non-ezymatic browning, lipid oxidation, and enzyme activity in food as a function of water activity.

As shown in Figure 2.9, the Maillard reaction occurs most rapidly at intermediate a_w values (0.5 to 0.8) (Nursten, 2005). Dried foods and intermediate-moisture foods have a_w values in this range and it is here that the a_w value is of the most significance to the reaction. However, a_w values for maximum browning rate are affected by other components of the system. Humectants, such as salt, sugar, and glycerol, can lower the a_w value for maximum browning.

2.2.1.3 pH

Since the Maillard reaction itself has a strong influence on pH, it is hard to evaluate the pH influence. Low pH values (pH < 7) favor the formation of furfurals (from the Amadori rearrangement products), while the routes for reductones

and fission products are preferred at a high pH. The reactivity of sugar and amino group is highly influenced by pH. The open chain form of sugar and the unprotonated form of amino group, considered to be the reactive forms, are favoured at high pH. The most desirable meaty and pot-roasted aroma was obtained at pH 4.7, but pH had a less dramatic effect on aroma than did temperature, time or water content (Lingnert *et al*., 2002). Liu *et al*. (2008) studied the effect of pH on color in the galactose and glycine model system. The authors indicated that the rate of color formation could be reduced by decreasing pH of the system.

2.2.1.4 Temperature

Temperature dependency of chemical reactions is often expressed as the activation energy (E_a). Activation energy data for the Maillard reaction have been reported within the wide range of 10 to 160 kJ·mole^{-1}, depending on which effect of the reaction has been measured (Lingnert *et al*., 2002). The activation energy is also highly dependent on pH. The temperature dependence of the Maillard reaction is also influenced by the participating reactants so it is difficult to isolate the effect of temperature as a single variable (Lingnert *et al*., 2002). The rate of reaction increases with temperature (Matins *et al*., 2001). An increase in temperature leads to an increase of the reactivity between sugar and amino group. The temperature dependence of the reaction rate constant k is often described by the well-known Arrhenius equation as shown in Equation 2.8;

$$k = A^* \exp(\frac{E_a}{RT}) \qquad (2.8)$$

2.3 Neo-Formed Contaminants

Neo-Formed Contaminants (NFCs) are the products of the Maillard reaction in food processing and/or storage, particularly at high temperatures, of foods that contain carbohydrates and protein. NFCs in foods are, for example, HMF, furfural, furan, and acrylamide. The reductor sugars and proteins are the main compounds involved in the initial stage of the Maillard reaction (Gasper and Lopes, 2009). In the advanced stages of the Maillard reaction, undesirable compounds such as HMF, furfural, furan, and acrylamide can be found. In April 2002 the Swedish National Food Administration (NFA) and researchers from Stockholm University announced their findings that acrylamide, a toxic and potential cancer-causing chemical, is formed in many types of food, processed or cooked at high temperatures (Swedish National Food Administration, 2002). The Food and Agriculture Organization/World Health Organization jointly convened a consultation on the health implications of acrylamide in food (Food and Agriculture Organization/World Health Organization Consultation on Health Implication of Acrylamide in Food, 2002). The consultation concluded that the presence of acrylamide in food is a major concern for humans, based on the ability to induce cancer and heritable mutations in laboratory animals.

2.3.1 Hydroxymethylfurfural

The structure of hydroxymethylfurfural (HMF) is shown in Figure 2.10 and it's molecular formula is $C_6H_6O_3$. HMF is a colourless solid and is highly water-soluble. The molecule is a derivative of furan, containing both aldehyde and alcohol functional groups (Ulbricht *et al*., 1984).

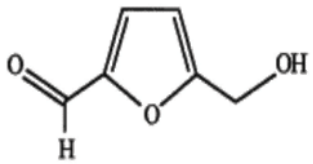

Figure 2.10 Structure of HMF.

HMF has been identified in a wide variety of heat-processed foods including milk, fruit juices, spirits, honey, etc (Chemical Research in Toxicology, 2009). The Council of the European Union (2001) established a maximum HMF quality level in honey (40 $mg \cdot kg^{-1}$) and in apple juice (50 $mg \cdot kg^{-1}$). No limits of HMF have been established for other foods (Gasper and Lopes, 2009). *In vitro* studies have shown that HMF is weakly carcinogenic (Chemical Research in Toxicology, 2009) . HMF is formed from reducing sugars by acid-catalyzed dehydration and in the Maillard reaction. It is an intermediate breakdown product of hexose decomposition and is a reactive substance that can participate in numerous chemical reactions such as those involving polymerization (Ulbricht *et al*., 1984; Gökmen, 2006; Chemical research in toxicology, 2009). HMF in foods has been analysed using liquid chromatography/mass spectrometry (LC-MS) as described by Gökmen (2006). This method can quantitatively determine the HMF levels in food with a detection limit of 0.005 $\mu g \cdot g^{-1}$. The determination of HMF levels in food was purify the sample by solid-phase extraction (SPE) with commercial cartridges or liquid-liquid extraction with dichloromethane. HMF in foods has also been analysed using gas chromatography/mass spectrometry (GC-MS), as described by Teixidó *et al*. (2006).

2.3.2 Furfural

The structure of furfural is shown in Figure 2.11 and its molecular formula is $C_5H_4O_2$. Furfural is colorless with a melting point of -38.7 °C, and a boiling point of 161.7 °C (International Agency for Research on Cancer, 1994a).

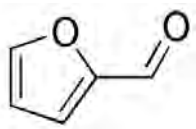

Figure 2.11 Structure of furfural.

Furfural occurs naturally and is formed during the processing and domestic preparation of a broad range of foods. It is also carried over into food from its use as an extraction solvent or as a component of flavor mixtures. The maximum level of furfural intake being no more than 0.5 to 1% of the intake from other food sources (Kroes, 1999). Furfural is a volatile component in a wide range of fruits and vegetables (International Agency for Research on Cancer, 1995).

Compounds or physical factors assessed by IARC (International Agency for Research on Cancer) are classified into four groups, based on the existing scientific evidence for carcinogenicity, which are group 1 "Carcinogenic to humans", group 2A "Probably carcinogenic to humans", group 2B "Possibly carcinogenic to humans", group 3 "Unclassifiable as to carcinogenicity in humans", and group 4 "Probably not carcinogenic to humans". For group 1 "Carcinogenic to humans", there is enough evidence to conclude that it can cause cancer in humans. For group 2A: "Probably carcinogenic to humans", there is strong evidence that it can cause cancer in humans, but at present it is not conclusive. For group 2B: "Possibly carcinogenic

to humans", there is some evidence that it can cause cancer in humans but at present it is far from conclusive. For group 3: "Unclassifiable as to carcinogenicity in humans", there is no evidence at present that it causes cancer in humans. For group 4: "Probably not carcinogenic to humans", There is strong evidence that it does not cause cancer in humans. Furfural has been classified as a carcinogen group 3 (International Agency for Research on Cancer, 1994a). Furfural was tested for carcinogenicity by oral administration in one study in mice (Arts *et al*., 2004)and one study in rats (Parkash and Caldwell, 1994). In the mice study, it increased the incidence of hepatocellular adenomas and carcinomas in males and hepatocellular adenomas and forestomach papillomas in females. In the rat study the male rats had a low incidence of cholangiocarcinomas, which occur rarely. In a two-stage assay on mouse skin, furfural had a weak initiating activity (International Agency for Research on Cancer, 1994a). Furfural and HMF are derived from hydrolysis of pentose sugars and hexose sugars, respectively. They occur in many foods such as cereals, biscuits, bread, and honey (Gaspar and Lopes, 2009). Methods used in the analysis of furfural are gas chromatography/mass spectrometry (GC-MS) and high-performance liquid chromatography (HPLC). The determination of furfural in processed citrus juices by solid-liquid extraction of the juice, followed by HPLC, with detection at 280 nanometer was carried out by Lo Coco *et al*. (1994).

2.3.3 Furan

Furan (C_4H_4O) is a colorless liquid with a strong ether-like odour. It has a boiling point of 31.4 °C (International Agency for Research on Cancer, 1994b). The structure of furan is shown in Figure 2.12.

Figure 2.12 Structure of furan.

In spring 2004, Food and Drug Administration scientists announced the discovery of the substance furan in an unexpected number of foods. Furan forms as a result of traditional heat treatment techniques, such as the long established methods of food preparation and preservation of retorting foods in cans and jars. It has been found in such foods as soups, sauces, beans, pasta meals, and baby foods (Food and Drug Administration, 2004). Furan is considered to be carcinogenic in rats and mice and has been classified as "possibly carcinogenic to humans" (group 2B) (International Agency for Research on Cancer, 1994b). The primary source of furans in food is thermal degradation and rearrangement of organic compounds, particularly carbohydrates. A variety of experimental systems, including the heating of sugars (eg., glucose, lactose, fructose, xylose, rhamnose), the heating sugars in the presence of amino acids or protein (e.g., alanine, cysteine, casein) (Yaylayan, 2003), and the thermal degradation of ascorbic acid have been used to produce furans in food (Fendor *et al*., 2010). Furan is also formed from unsaturated fatty acids (Mark *et al*., 2006). The Food and Drug Administration/Center for Food Safety and Applied Nutrition (CFSAN) developed gas chromatography/mass spectrometry (GC-MS) methodologies for furan analysis in foods. Semi-solid and solid foods are weighed into headspace vials, diluted with either water or saturated NaCl solution, fortified with an internal standard (*d4*-furan), and the vials are sealed. Liquid foods are

weighed into headspace vials, fortified with internal standard (*d4*-furan), and the vials are sealed. Automated headspace sampling followed by gas chromatography/mass spectrometry (GC-MS) analysis is used to detect furan and *d4*-furan in the scan mode. Furan is quantified by using a standard additions curve, where the concentration of furan in the fortified test portions is plotted versus the furan/*d4*-furan response factors (Food and Drug Administration, 2006).

2.3.4 Acrylamide

Acrylamide (CH_2=CH-CO-NH_2; 2-propenamide) with a molecular weight of 71 appears as a white crystalline solid. It is odourless and has a high solubility in water which is 2155 $g \cdot l^{-1}$ water (25 °C). It has a melting point of 84.5 °C and its boiling point is 192.6 °C at atmospheric pressure (Lingnert *et al*., 2002). The structure of acrylamide is shown in Figure 2.13.

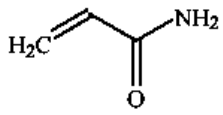

Figure 2.13 Structure of acrylamide.

Acrylamide has been reported to be present in a great number of vegetables including: potatoes, carrots, radish, lettuce, Chinese cabbage, parsley, onions, spinach and rice (Lingnert *et al.*, 2002). In one gram of samples, 1.5 to 100 nanograms (ng) of acrylamide could be detected (Lingnert *et al.*, 2002). Average intakes for the general population were estimated to be in the range of 0.3 to 0.8 micrograms (μg) of acrylamide intake per kilogram of body weight per day. Levels of acrylamide in beer had a low value (<0.03 $mg \cdot kg^{-1}$) (Food and Agriculture

Organization/World Health Organization Consultation on Health Implication of Acrylamide in Food, 2002). However, due to the high level of consumption, it could potentially impose risks to consumers, a concern that should be investigated. Acrylamide is genotoxic *in vivo* of somatic cells and germ cells and therefore has the potential to induce heritable damage at the genetic and chromosomal level. It is known to be metabolised to glycidamide, a chemically reactive epoxide that forms DNA adducts. Glycidamide is also genotoxic. Both acrylamide and glycidamide cause damage to genes by virtue of their binding to DNA (Food and Agriculture Organization/World Health Organization Consultation on Health Implication of Acrylamide in Food, 2002). There is a good deal of literature on acrylamide causing DNA damage in germ cells. It has been found that acrylamide induces tumors in both rats and mice, at a number of different sites, a fact that is consistent with the genotoxic mode of action of the chemical (Food and Agriculture Organization/World Health Organization Consultation on Health Implication of Acrylamide in Food, 2002; Yener and Kahpci, 2009). The International Agency for Research on Cancer (IARC) classified acrylamide as "probably carcinogenic to humans" (group 2A) (International Agency for Research on Cancer, 1994). The no-observed-adverse-effect level of acrylamide neurotoxicity in rats was 0.50 $mg \cdot kg^{-1}$ body weight per day (Dybing and Sanner, 2003). Food and Agriculture Organization/World Health Organization Consultation on Health Implication of Acrylamide in Food (2002) stated that the magnitude of the cancer risk posed by acrylamide in food was not quantified. Quantitative measurements of human cancer risks using experimental animal carcinogenicity data have been attempted using different models (Kaldor, 1992). However, the consultation did not reach a consensus on how quantitative risk

assessment based on animal data should be used to estimate human cancer risk from acrylamide in food.

The major mechanistic pathway for the formation of acrylamide in foods so far established is via the Maillard reaction. Zyzak *et al.* (2003) proposed a mechanism of acrylamide formation, shown in Figure 2.14. The α-amino group of free asparagine reacts with a carbonyl source, forming a Schiff base. Under heat, the Schiff base decarboxylates (facilitated by delocalization of negative charge, which Schiff base formation allows), forming a product that can react in one of two ways. It can hydrolyze to form 3-aminopropionamide that can further degrade via the elimination of ammonia to form acrylamide when heated. Alternatively, the decarboxylated Schiff base could decompose directly to form acrylamide via elimination of an imine.

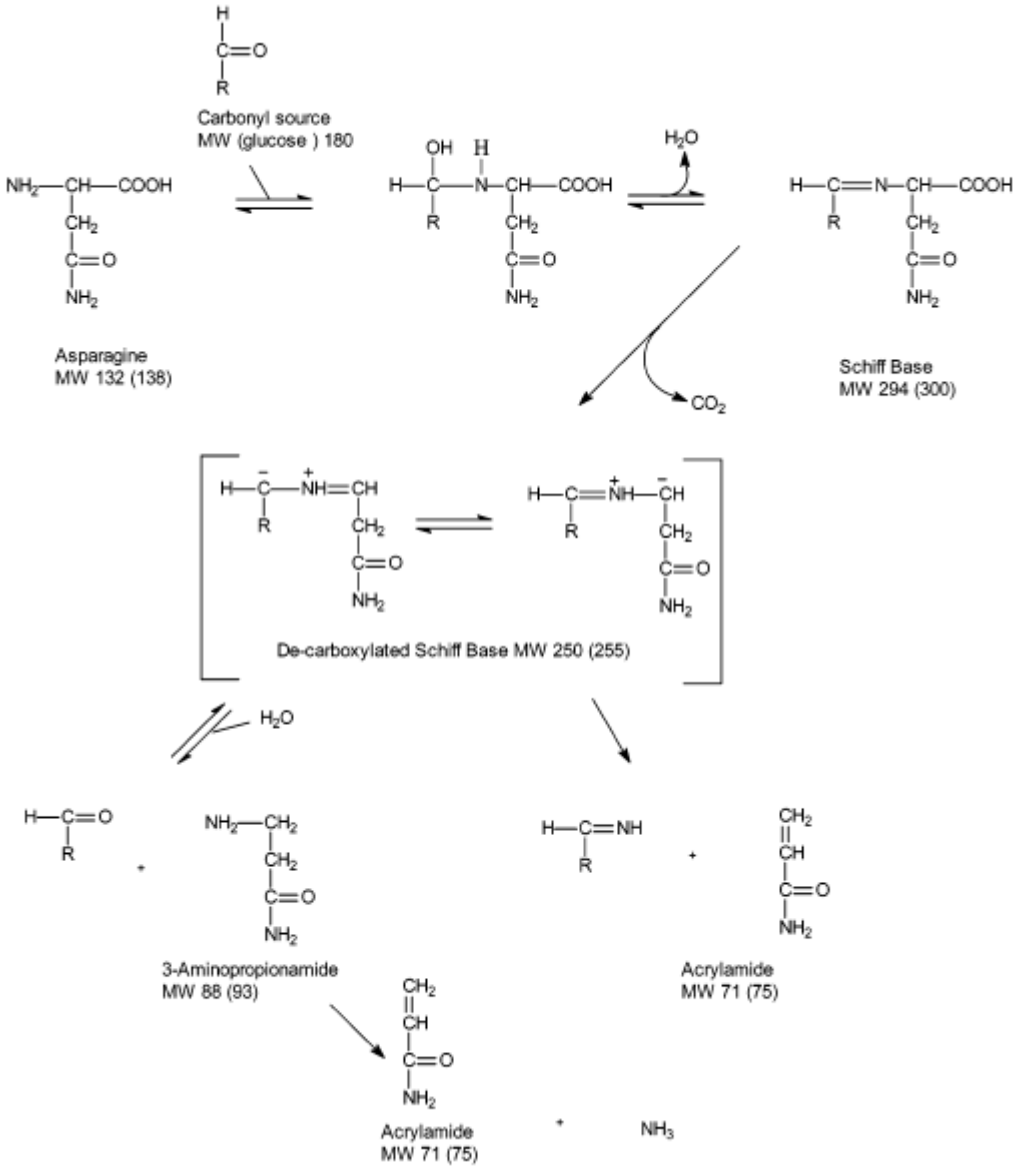

Figure 2.14 Mechanism of acrylamide formation in heated foods.

Source: Zyzak *et al*. (2003)

Mainly two methods of acrylamide analysis (Liquid Chromatography-Mass Spectrometry (LC-MS) or Gas Chromatography-Mass Spectrometry (GC-MS) are used by laboratories world wide (Taeymans *et al.*, 2004). Limits of quantification range from 0.03 to 0.05 $mg \cdot kg^{-1}$ for LC-MS down to 0.01 to 0.03 $mg \cdot kg^{-1}$ for GC-MS. However, it is quite clear that for the analysis of acrylamide at <0.030 $mg \cdot kg^{-1}$ level,

GC-MS after bromination is the best approach. This approach has the advantage of adequate sensitivity with multiple ion confirmation. A further advantage of this technique is that a relatively simple bench-top GC-MS can be employed for acrylamide analysis. Application of GC-MS-MS or coupling to a high resolution MS would even further lower the detection limit of certain foods, approaching the range of 0.001 to 0.002 $mg \cdot kg^{-1}$ (Taeymans *et al.*, 2004). Analysis by LC-MS-MS involves direct determination of underivatized acrylamide. The LC-MS-MS method was more lenient with respect to direct measurement without prior derivatization and no increasing in temperature during the chromatographic separation (Eriksson, 2005). While GC-MS techniques are either based on bromination of the analyte or direct analysis without derivatization. The latter approach is less laborious and in both reported cases, employs liquid–liquid extraction of the analysis. In the method reported by Biedermann *et al.* (2002), the determinative step is either positive ion chemical ionization in the selected ion monitoring (SIM) mode or electron impact ionization, achieving a level of detection of around 50 and <0.01 $mg \cdot kg^{-1}$, respectively.

CHAPTER III

KINETICS OF NEO-FORMED CONTAMINANTS FORMATION DURING COMBINED MICROWAVE-HOT AIR ROASTING OF MALT

3.1 INTRODUCTION

Neo-formed contaminants (NFCs) are substances formed during the Maillard and oxidation reactions occurring in food subjected to heat treatment (Rizkallah *et al*., 2008). Some of these molecules are suspected of being mutagenic and/or carcinogenic to humans, especially hydroxymethylfurfural (HMF), furfural, furan and acrylamide (International Agency for Research on Cancer, 1994c; Food and Agriculture Organization/World Health Organization Consultation on Health Implication of Acrylmide in Food, 2002; Swedish National Food Administration, 2002; Dybing *et al*., 2005; Food and Drug Administration, 2005; Chemical Research in Toxicology, 2009). In the brewing industry, colored malts have been used to give particular colors and flavors to beers. Colored malt is produced by roasting. The Maillard reaction, which causes non-enzymatic browning, is one of the main chemical events occurring during malt roasting. It affects the quality of processed food products, in particular the sensory attributes, such as color and flavor. However, the Maillard reaction can also have negative effects on the nutrition value as well as on the formation of toxic compounds (Martins *et al*., 2001). The Maillard reaction has been extensively characterized and found to be highly influenced by the type of substrate, temperature, water activity, and pH (Heldman and Lund, 1992; Martins and Boekel, 2005; Rufián-Henares *et al*., 2008). A precise control of the Maillard reaction is fundamental to the production of heated foods and the quantification of

appropriate Maillard reaction products is frequently used for monitoring the development of the reaction. HMF is naturally formed as an intermediate Maillard reaction product from the dehydration of hexose sugars under mild acidic conditions. Formation of HMF in foods is especially dependent on temperature and pH (Gökmen, 2006). Furfural is formed by the Maillard reaction from pentose sugars (Gökmen, 2006). Furan can be mainly formed during the heating of foods via the Maillard reaction between sugars and amino acids (Yaylayan *et al*., 2003), thermal degradation of ascorbic acid (Fendor *et al*., 2010), and unsaturated fatty acids (Mark *et al*., 2006). The formation of acrylamide in foods occurs as a result of a reaction between amino acid asparagines and reducing sugars at typical cooking temperatures (Zyzak *et al*., 2003). This mechanism involves the formation of a Schiff base followed by decarboxylation and the elimination of either ammonia or a substituted imine under heat to yield acrylamide. The acrylamide formation depends on the concentration of the precursors as well as the processing conditions (Gökmen *et al*., 2006). The formation of color, widely known as browning, is the result of the Maillard reaction. The formation of color in food samples during heating process depends on temperature and water activity (Purlis, 2010). Combined microwave-hot air heating is an alternative to conventional malt roasting in order to minimize NFCs levels in malt without affecting consumer acceptability or generating further unknown contaminants with potential health concerns (Birlouez-Aragon *et al*., 2010). Knowledge of NFCs formation kinetics to describe and predict changes during malt roasting process in order to minimize NFCs while retaining typical color and flavor is useful for the brewing industry.

Objectives

The objective of this study was to follow the process of malt coloration and kinetics of NFCs formation during combined microwave-hot air roasting process in order to minimize NFCs while retaining malt color.

3.2 LITERATURE REVIEW

Maillard reaction induces browning and has an effect on flavor and nutritive value of foods especially in heated food (Boekel, 2006). Heating at high temperatures, between 90 and 220 °C, may lead to the formation of toxic compounds (Claeys *et al*., 2005b). The Maillard reaction is actually a complex network of various reactions involving reactants and products with high reactivity. The reaction begins with condensation between a reducing sugar (e.g. glucose) and a compound having a free amino group such as lysine. The condensation product (N-substituted glycosylamine) is then rearranged to form the Amadori product (1-amino-1-deoxy-2-ketose) which is subsequently degraded into different compounds depending on the pH of the system. At pH 7 or below, HMF (when hexoses are involved) or furfural (when pentoses are involved) are formed via enolization. Both of these are highly reactive compounds that take part in further reactions, i.e, condensation and polymerization, leading to the formation of melanoidins, other brown polymers and aromatic substances (Hodge, 1953). This is the route associated with browning development during malt roasting because of the pH range. Other reaction pathways (pH above 7) involve sugar dehydration and fragmentation, amino acid degradation, polymerization, and the formation of melanoidins (Hodge, 1953). The various

possible reaction pathways taking place depend strongly on temperature, pH, and the nature of the reaction, i.e, type of sugar, type of amino acid, or protein (Martins *et al*., 2001). The level of the Maillard reaction products including color, HMF, furfural, furan and acrylamide are the net result of complex reactions (Martins *et al*., 2001).

3.2.1 Kinetic models of food

Levenspiel (1972) and Martins *et al*. (2001) have given a detailed explanation on the use of kinetics in food applications. Rate law which governs the reaction rate of reactant A, in a closed system with only one compound reacting, is shown in Equation 3.1.

$$-\frac{d[A]}{dt} = k_c[A]^n \qquad (3.1)$$

By integration of the differential equation with respect to time, a zero-order reaction model, a first-order reaction model, and a second-order reaction model resulted as shown in Equation 3.2, 3.3, and 3.4, respectively.

$$[A] = [A]_0 - k_c t \qquad (3.2)$$

$$[A] = [A]_0 \exp(-k_c t) \qquad (3.3)$$

$$\frac{1}{[A]} = \frac{1}{[A]_0} + k_c t \qquad (3.4)$$

where, [*A*] = concentration of reactant A ($mol \cdot l^{-1}$); $[A]_0$ = initial concentration of reactant A ($mol \cdot l^{-1}$); k_c = reaction rate constant $mol^{1-n} \cdot l^{n-1} \cdot s^{-1}$; *t* = time (s); n = order of a reaction.

3.2.2 Kinetics of color development

The degree of browning is used to analytically assess the extent to which the Maillard reaction has taken place in food. Color formation depends on the precursors, thermal processing parameters, and pH (Martins *et al*., 2001). The melanoidin was mainly built up from sugar degradation products, formed in the early stages of the Maillard reaction, polymerized through aldo-type condensation and linked by amino compounds (Martins and Boekel, 2005).

Liu *et al*. (2008) studied kinetic of color development of Maillard reaction in galactose and glycine model system during heating at 60, 75, and 90 ºC. The result indicated that color development followed first-order kinetics. Pulris (2010) reviewed kinetic models for browning development. In Broyart *et al*. (1998), browning kinetics during baking of crackers at 240 °C hot air temperature was first order, where the color was expressed as an L-value. Likewise, in Zanoni *et al*. (1995), the browning kinetic of bread crusts during baking at 200 and 250 °C hot air temperature was also first order, where the color was expressed as ΔE-parameter.

3.2.3 Kinetics of NFCs formation

Claeys *et al*. (2005b) studied the effect of temperature and time on the formation of acrylamide in potato strips heated at 200 °C in an oven. The authors found that level of acrylamide increased with temperature and time. However, after reaching a maximum, the level of acrylamide decreased. The authors concluded that

the decrease of acrylamide was caused by the reaction of acrylamide with reactive compounds and the kinetic of acrylamide formation was first order because the level of acrylamide increased log-linearly as a function of time. After prolonged heating, a log linear of the acrylamide content was observed. The authors purposed the kinetic model of acrylamide formation as two consecutive reactions consisting of a first order formation rate constant (k_F) and a first order elimination rate constant (k_E) as shown in Equation (3.5)

$$\text{Reactant} \xrightarrow{k_F} \text{Acrylamide} \xrightarrow{k_E} \text{Acrylamide-protein or Acrylamide degradation product} \quad (3.5)$$

HMF and acrylamide are considered as heat-induced markers for a wide range of carbohydrate-containing foods. They are used for monitoring the heating process applied to cereal products (Capuano *et al*., 2008). Amino acids, serine and cysteine, are major reactants for furan formation (Crews and Castle, 2007) and amino acid asparagine is a major reactant of acrylamide formation (Taeymans *et al*., 2004). Ameur *et al*. (2006) studied the kinetic of HMF and color formation in cookies during baking at 200, 250, and 300 °C. The authors stated that the formation of HMF, as well as color development, in the cookies followed a first-order kinetic. Capuano *et al*. (2008) studied the effect of time and temperature of baking on color, HMF, and acrylamide levels in bread crisp. The authors reported that the browning color was related to the total heat charge absorbed by the bread slice during toasting. Higher temperatures resulted in a more intense browning for the same final moisture content. They also found that HMF formation followed a first order kinetic. Moreover, HMF

formation was highly correlated with the browning level and it was strongly affected by the moisture content. Acrylamide formation was found to follow a zero order kinetic (Capuano *et al*., 2008). Knol *et al*. (2009) used empirical models with the logistic-exponential model to fit the formation of acrylamide in potato crisp. The authors found that acrylamide formation follow logistic-exponential model, which indicated that the reaction was of logistic-exponential kinetic type.

3.3 MATERIALS AND METHODS

In this study, the heat treatment is carried out in two steps: the first one is pre-heating by microwave whose role is to enable a rapid rise in temperature, that is, from ambient temperature to around 180°C. The second step is the hot air roasting of malt in a domestic hot air oven in order to achieve malt coloration.

3.3.1 Materials

Barley malts were obtained from the French Institute of Brewing and Malting, Nancy, France. The average initial moisture content of the malt was 5.36% (wet basis).

3.3.2 Heating experiment

Kinetics of NFCs formation during roasting of malt by combined microwave-hot air was carried out as follows: 75 g of malt weighed in a 250 cm^3-beaker was firstly microwave pre-heated at different specific powers (2.50, 2.75, and 3.00 $W \cdot g^{-1}$) for 3.4 minutes in a lab scale microwave oven (Microondes Énergie Système, Villejuif, France) equipped with a 1,860 W-microwave generator (magnetron) and running at 2,450 MHz (Figure 3.1). The malts were then quickly arranged in a single layer on a 40 cm × 40 cm tray and submitted to hot air roasting at

200 °C in a 2,800 W-domestic hot air oven (FB 970 C2/E IX, Ariston, Fabriano, Italy) for various heating times (0, 37.5, 75, 112.5, and 150 minutes). The experiments were carried out under the following conditions: triplicate experiments for heating times at 0 and 150 minutes and duplicate experiments for heating times at 37.5, 75, and 112.5 minutes. After heating, the malts were transferred to a beaker and immediately cooled in an ice-water bath until the core temperature reached 21 °C.

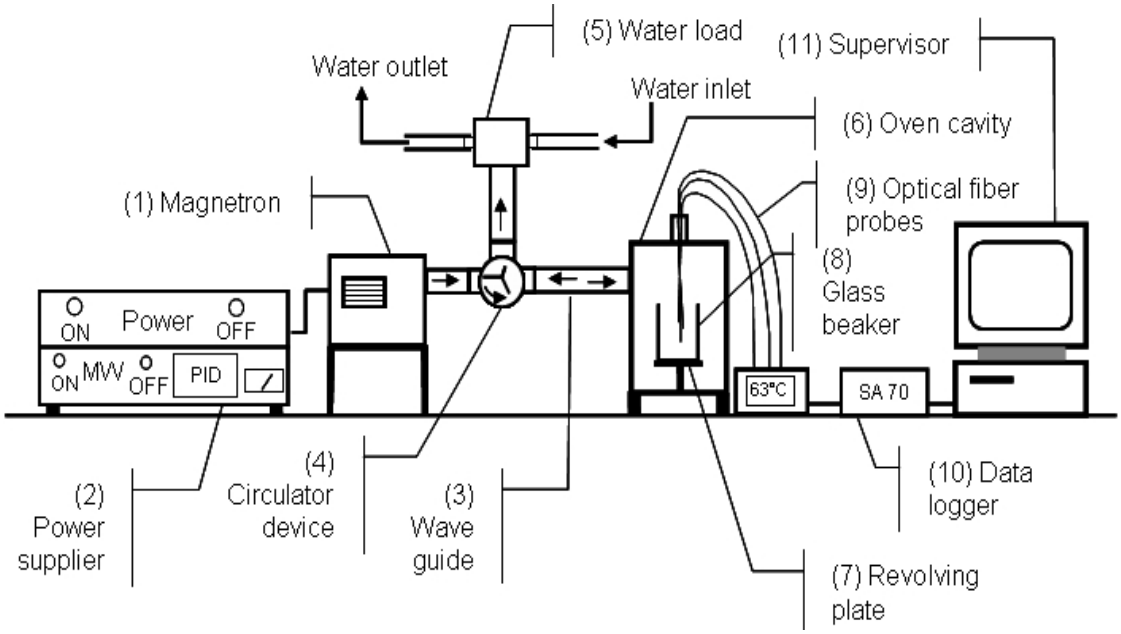

Figure 3.1 A lab scale microwave oven equipped with a 1,860 W-microwave generator (magnetron) and interfaced with data logger.

3.3.3 Color determination

Color of ground malt was determined by L, a^*, b^* color space (tristimulus) coordinates in terms of L (L = 0 yields black and L = 100 indicates white), a^* (negative values indicate green while positive values indicate magenta), and b^* (negative values indicate blue and positive values indicate yellow) values, using a

Minolta colorimeter CR300 (Minolta, Carrières Sur Seine, France). The colorimeter was calibrated against a standard calibration plate. The measurements of color were triplicated and the average values of L, a^*, and b^* were reported. The color difference parameter; ΔE, was calculated from L, a^* and b^* value using Equation 3.6.

$$\Delta E = \sqrt{(\Delta L)^2 + (\Delta a^*)^2 + (\Delta b^*)^2} \qquad (3.6)$$

where, $\Delta L = L_{not\text{-}treated\ malt} - L_{sample}$; $\Delta a^* = a^*_{not\text{-}treated\ malt} - a^*_{sample}$; $\Delta b^* = b^*_{not\text{-}treated\ malt} - b^*_{sample}$.

3.3.4 NFCs content determination

NFCs content including HMF, furfural, furan, and acrylamide content were evaluated by the fluorometric method described in 3.3.4.1 and the physico-chemical analysis method described in 3.3.4.2. The fluorometric method is an indirect method to determine NFCs content. This method is based on the sample's fluorescence properties (Lichtman and Conchello, 2005). The physico-chemical analysis using High Performance Liquid Chromatography (HPLC) is a direct analysis method to determine NFCs content.

3.3.4.1 Fluorometric method

The fluorometric method is an indirect method to measure NFCs content. This method is based on the sample's fluorescence properties. Fluorescence profile is influenced by particle size distribution, moisture content, the reflection, and refraction of light at the surface of sample (Symons and Dexter, 1991). The

fluorometric method was an alternative method for the determination of NFCs content in food industry because it is fast, cost effective, pollution free, non destructive and it does not need any extraction step (Rizkallah *et al*., 2008). The fluorescence synchronous spectra of NFCs which are HMF, furfural, furan and acrylamide in malt samples were acquired using a fluorescence spectrophotometer (Cary Eclipse, Varian, Melbourne, Australia). The fluorescence synchronous spectra were directly measured on ground malt placed in 1 × 1 × 4.5 cm^3 acrylic cuvettes (Sarstedt®, France). Excitation spectra were recorded between 280 and 550 nm and the emission synchronous delta ($\Delta=\lambda_{em}-\lambda_{exc}$) varied between 0 and 180 nm. Steps for excitation and emission synchronous Δ set at 4 nm. The multiway arrays of two dimensional fluorescence data were decomposed by means of multiway parallel factor analysis (PARAFAC) models. The NFCs content was predicted using the fluorescence model developed by Rizkallah *et al*. (2008).

3.3.4.2 Physico-chemical analysis

HMF and furfural were quantified by HPLC according to the method described by Rufián-Henares *et al*. (2006). HMF and furfural were quantified using the external standard method within the range 0.05 to 10 $mg{\cdot}l^{-1}$ and 0.5 to 10 $mg{\cdot}l^{-1}$ for HMF and furfural, respectively. Sample reporting levels of HMF or furfural outside the calibration range were additionally diluted 10-fold in mobile phase. The limit of quantification for HMF and furfural were 2 $mg{\cdot}kg^{-1}$ and 15 $mg{\cdot}kg^{-1}$, respectively. All chemicals used were of an analytical grade and were obtained from Sigma-Aldrich (St. Louis , MO , USA). For the acrylamide analysis, the calibration curve was carried out by using d3-acrylamide in water as the internal standard. The internal standard was obtained from Polymer Source (St. Louis , MO ,

USA). d3-acrylamide and 40 mL of water were added to 4 g of ground malt. The mixture was shaken for 2 hours and centrifuged at 15000 × g and 20 °C for 10 minutes. The supernatant was purified by solid-phase extraction (SPE) on an Isolute Multimode (Hewgoed, Mid-Glamorgan, UK), cartridge. The purified sample was filtered on regenerate cellulose with 25 µm pore size. Acrylamides were determined in the filtrate by LC-MS-MS in MRM mode with a Waters Alliance™ 2690 HPLC system and a Waters Quattro Micro™ mass spectrometer in MRM-ESI+ mode. Calibration ranged from 0 to 500 $\mu g \cdot l^{-1}$ corresponding to 0 to 5000 $\mu g \cdot l^{-1}$ for malt.

3.4 RESULTS AND DISCUSSION

3.4.1 Relation between color and roasting time

Because of the heterogeneity of the roasted malt grain, the color measurements are carried out on whole grain sample after milling. The color was expressed as a color difference between roasted and unroasted malt (ΔE parameter) according to Equation 3.6.

Figure 3.2 shows the relationship between color values (ΔE) of malt, which are roasted at different specific microwave powers (2.50, 2.75, and 3.00 $W \cdot g^{-1}$) for 3.4 min and at 200 °C oven temperature as a function of roasting time. The first point of this graph corresponds to ΔE of malts at the end of the microwave pre-heating step. Brown pigments with low and high molecular weight are formed in the advanced stage of the Maillard reaction. The development of color is an evidence and extremely important indicator of the extent of the advanced Maillard reaction. The colors of malt during that reaction ranged from pale yellow to very dark brown (Heldman and Lund, 1992; Rufián-Henares *et al*., 2008). Figure 3.2 shows that at

each roasting condition, ΔE increased as a logarithmic function of roasting time. During roasting of malt, water activity of the malt decreased, this, coupled with a high temperature input (>150 °C) provided optimum conditions for the formation of the Maillard reaction products and intense brown color. As can be seen in Figure 3.2, ΔE increased rapidly for the first 30 minutes of roasting by hot air and then continued to increase slightly.

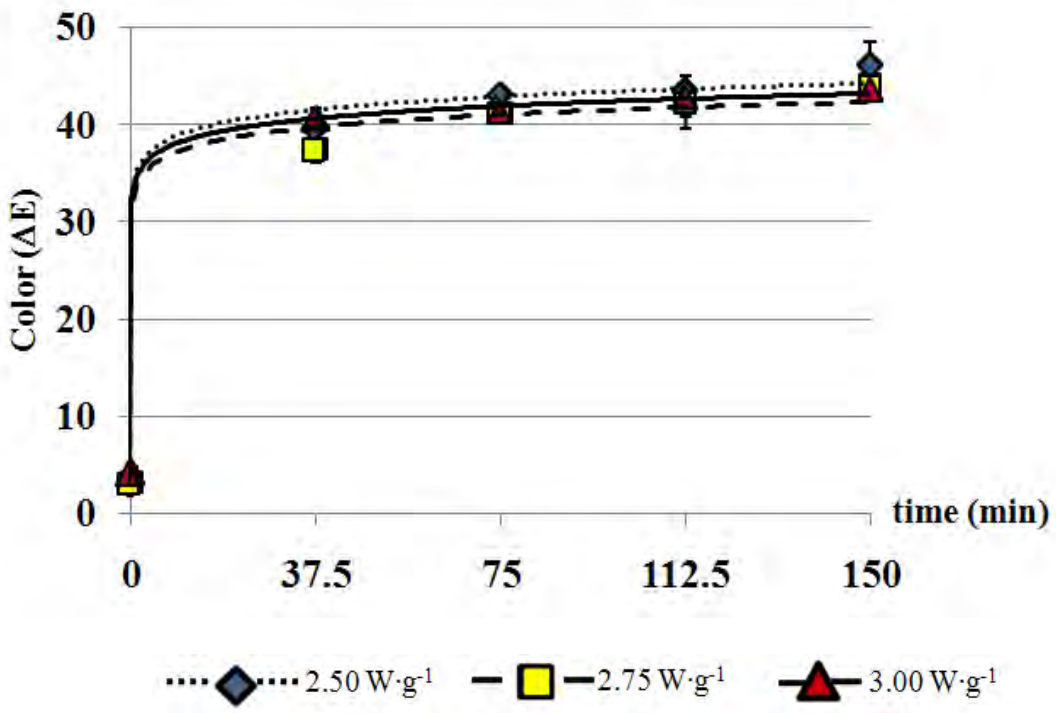

Figure 3.2 Color (ΔE) of malt roasted at different specific microwave powers (2.50, 2.75, and 3.00 $W \cdot g^{-1}$) for 3.4 min and at 200 °C oven temperature as a function of roasting time.

ΔE is very well correlated to roasting time (R^2 = 0.9945, 0.9929, 0.9996 at 2.50, 2.75, and 3.00 $W \cdot g^{-1}$, respectively for 3.4 minutes followed by hot air roasting at 200 °C). The fitted equations to predict color (ΔE) during roasting malt for each specific microwave power are given below:

At 2.50 $W \cdot g^{-1}$ specific microwave power:

$$\Delta E = 1.9583\ln(t) + 34.492, \quad R^2 = 0.9945 \qquad (3.7)$$

At 2.75 $W \cdot g^{-1}$ specific microwave power:

$$\Delta E = 1.865\ln(t) + 32.999, \quad R^2 = 0.9929 \qquad (3.8)$$

At 3.00 $W \cdot g^{-1}$ specific microwave power:

$$\Delta E = 1.8512\ln(t) + 33.958, \quad R^2 = 0.9996 \qquad (3.9)$$

Where: t is roasting time (min).

Equations 3.7 to 3.9 can be used to predict the end point of the roasting process in the production of colored malt. ΔE values of desirable coffee, chocolate and black malt were 50.41, 54.37 and 59.72, respectively. As shown in Table A.1 of Appendix A, roasting time significantly influenced the malt color whereas specific microwave power did not affect the malt color at 95% confidence level.

3.4.2 Kinetics of NFCs data during combined microwave-hot air roasting process of malt

Table 3.1 shows HMF, furfural, and acrylamide content, quantified by the physico-chemical method, of unroasted malt and malt after pre-heating by microwave at various specific microwave powers. The results clearly demonstrated that an increase in microwave specific power caused an increase in HMF, furfural, and acrylamide. Increasing microwave specific power from 2.50 $W \cdot g^{-1}$ to 3.00 $W \cdot g^{-1}$ resulted in a 2-fold and 1.5-fold increase in HMF and acrylamide, respectively, and an

80-fold increase in furfural. HMF, furfural, and acrylamide formations were related to the total heat charge absorbed by the malts. Due to higher thermal input, starch and non-reducing sugars may be hydrolyzed, giving rise to the formation of reducing sugars that can participate in Maillard Reaction. Therefore, the formation of HMF, furfural, and acrylamide tended to increase with increasing specific microwave powers.

Table 3.1 HMF, furfural, and acrylamide content, quantified by physico-chemical method, of unroasted malt and malt after pre-heating by microwave at various specific powers.

Conditions of microwave pre-heating	HMF ($mg \cdot kg^{-1}$)	Furfural ($mg \cdot kg^{-1}$)	Acrylamide ($mg \cdot kg^{-1}$)
1. Unroasted malt	1.9	Not detected	Not detected
2. Specific power 2.50 $W \cdot g^{-1}$*	60.37	1.83	1.6×10^{-4}
3. Specific power 2.75 $W \cdot g^{-1}$*	110.59	6.85	1.9×10^{-4}
4. Specific power 3.00 $W \cdot g^{-1}$*	127.35	146.51	2.4×10^{-4}

* microwave heating time of 3.4 minutes

In this study, kinetic experiments were carried out to explore effect of heating on NFCs during combined microwave-hot air process. The accumulation of HMF, furfural, and acrylamide content identified by the fluorometric method and physico-chemical method during the roasting of malt at different specific microwave powers (2.50, 2.75, and 3.00 $W \cdot g^{-1}$) for 3.4 min and 200 °C hot air temperature are shown in Figures 3.3 to 3.11. Figure 3.12 shows the accumulation of furan content

identified by the fluorometric method during the roasting of malt at different specific microwave powers for 3.4 min and 200 °C hot air temperature. The first point of these graphs corresponds to the end of the microwave preheating step. From Figures 3.3 to 3.11 the physico-chemical method provided higher HMF, furfural, and acrylamide content than fluorometric method. The HMF content, identified by the physico-chemical method, shown in Figure 3.3 to 3.5, was defined for two stages. The first stage was the initial increasing from 0 minute until 37.5 minutes for 2.50 $W \cdot g^{-1}$ specific microwave power preheating and from 0 minute until 75 minutes for 2.75 and 3.00 $W \cdot g^{-1}$ specific microwave power preheating, respectively. HMF was mainly formed through the 1,2 enolisation of Amadori compounds under acid condition (Delgado-Andrade *et al*., 2010; Matins *et al*., 2001). The second stage was the subsequent decreasing stage until 150 minutes because of HMF degradation under high temperature and long time condition. This finding is similar to the results from previous investigations by Delgado-Andrade *et al*. (2010) and Rufián-Henares *et al*., (2006). For HMF content, identified by the fluorometric method for 2.50, 2.75, and 3.00 $W \cdot g^{-1}$ specific microwave powers preheating (Figures 3.3 to 3.5), the results did not follow the same trend with the change in HMF content with heating time, which was identified by the physico-chemical method. This might be due to the insufficiency in size reduction and non-uniformity in size of ground malt which affected the fluorescence profile that consequently affected the result from the fluorometric method. Therefore, the degree of refinement of sample in milling step was important for obtaining a good result. Moreover, it is important for the measurement of the fluorescence spectra as soon as possible after sample milling to ensure that there is no change in moisture content of ground malt. From Figures 3.6

to 3.8, the furfural content identified by the fluorometric method and physico-chemical method for 2.50, 2.75, and 3.00 $W \cdot g^{-1}$ specific microwave power preheating were found to increase with roasting time for all cases except furfural, identified by fluorometric method for 3.00 $W \cdot g^{-1}$ specific microwave power preheating as shown in Figure 3.8. An increase of furfural content is formed by Amadori compound. In addition, furfural may be formed from HMF degradation under high temperature conditions (Delgado-Andrade *et al*., 2010; Rufián-Henares *et al*., 2006). Figure 3.9 shows the acrylamide content, identified by the physico-chemical method at 2.50 $W \cdot g^{-1}$ specific microwave power preheating. The results show that acrylamide content increased with roasting time until 112.5 minutes then gradually decreased. The decrease of acrylamide was caused by the reaction of acrylamide with reactive compounds (Claeys *et al*., 2005b). Likewise, Knol (2009) concluded that acrylamide was not an end product in the Maillard reaction. The degradation of acrylamide may result from the polymerization of acrylamide and amino acid. Capuano *et al*. (2008) purposed the kinetic model of acrylamide formation for prolonged heating as two consecutive reactions consisting of formation reaction and degradation reaction. Figures 3.10 and 3.11 show the acrylamide content, identified by the physico-chemical method at 2.75, and 3.00 $W \cdot g^{-1}$ specific microwave power preheating. The results show that acrylamide content increased with roasting time for the entire heating process. The fluctuation of acrylamide content identified by the fluorometric method for preheating at 2.50, 2.75, and 3.00 $W \cdot g^{-1}$ specific microwave power, shown in Figures 3.9 to 3.11, was observed.

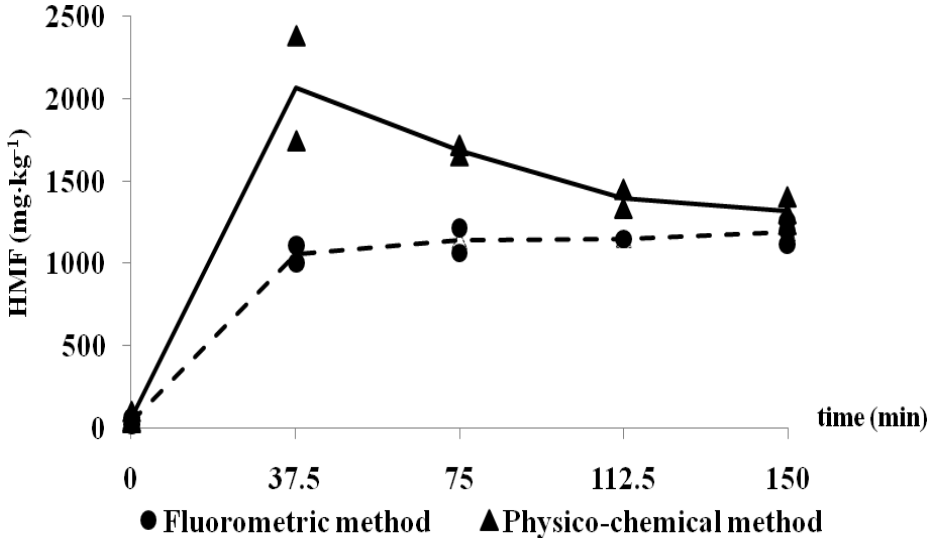

Figure 3.3 Accumulation of HMF content identified by the fluorometric method and physico-chemical method during the roasting of malt at 2.50 $W \cdot g^{-1}$ specific microwave power for 3.4 min and 200 °C hot air temperature.

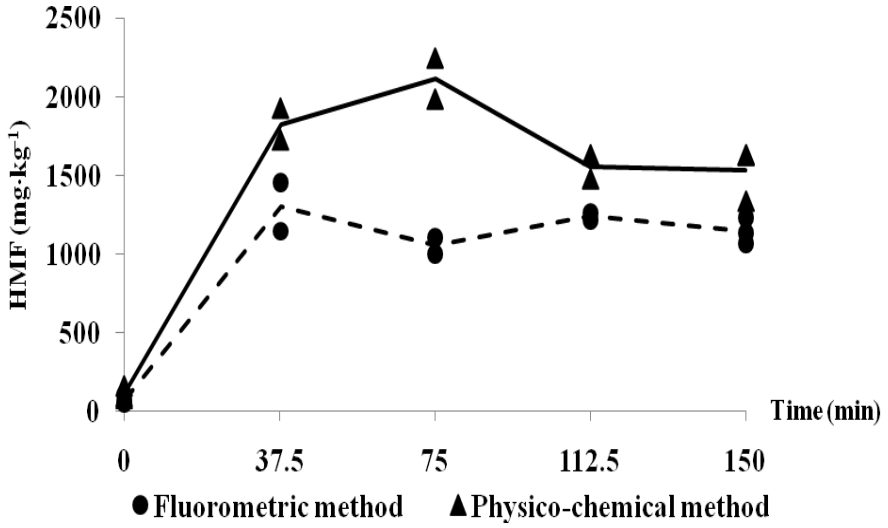

Figure 3.4 Accumulation of HMF content identified by the fluorometric method and physico-chemical method during the roasting of malt at 2.75 $W \cdot g^{-1}$ specific microwave power for 3.4 min and 200 °C hot air temperature.

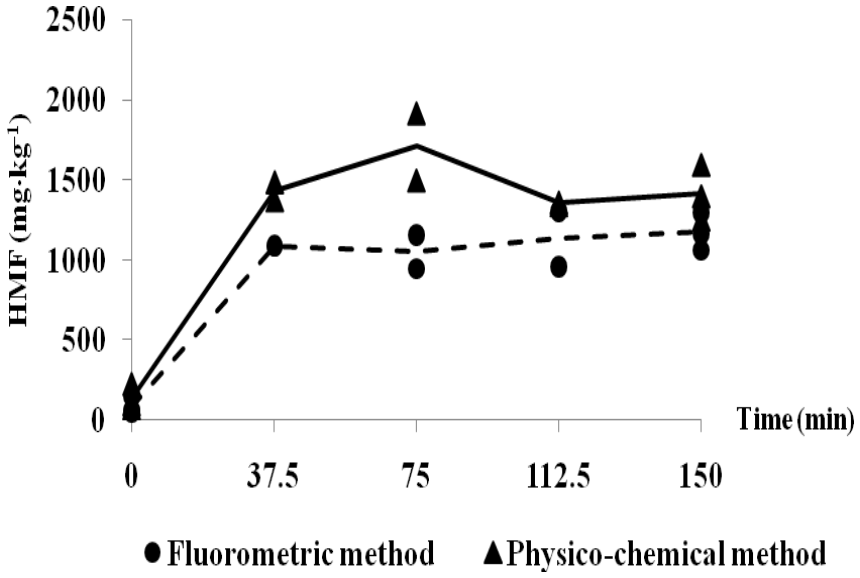

Figure 3.5 Accumulation of HMF content identified by the fluorometric method and physico-chemical method during the roasting of malt at 3.00 $W \cdot g^{-1}$ specific microwave power for 3.4 min and 200 °C hot air temperature.

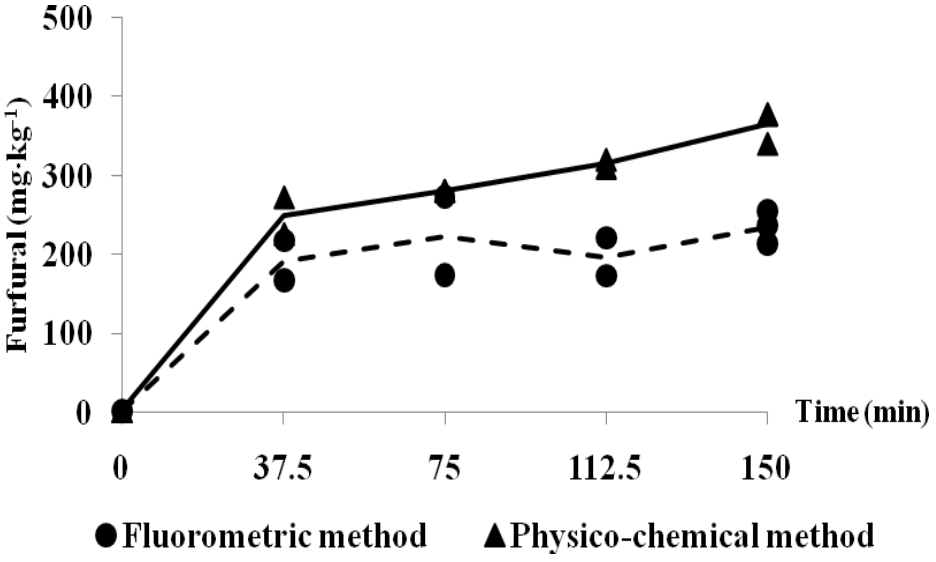

Figure 3.6 Accumulation of furfural content identified by the fluorometric method and physico-chemical method during the roasting of malt at 2.50 $W \cdot g^{-1}$ specific microwave power for 3.4 min and 200 °C hot air temperature.

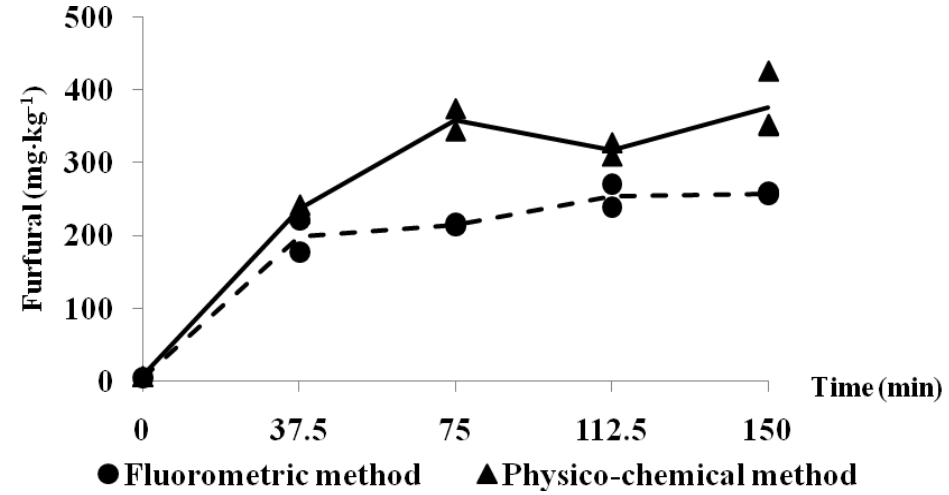

Figure 3.7 Accumulation of furfural content identified by the fluorometric method and physico-chemical method during the roasting of malt at 2.75 $W \cdot g^{-1}$ specific microwave power for 3.4 min and 200 °C hot air temperature.

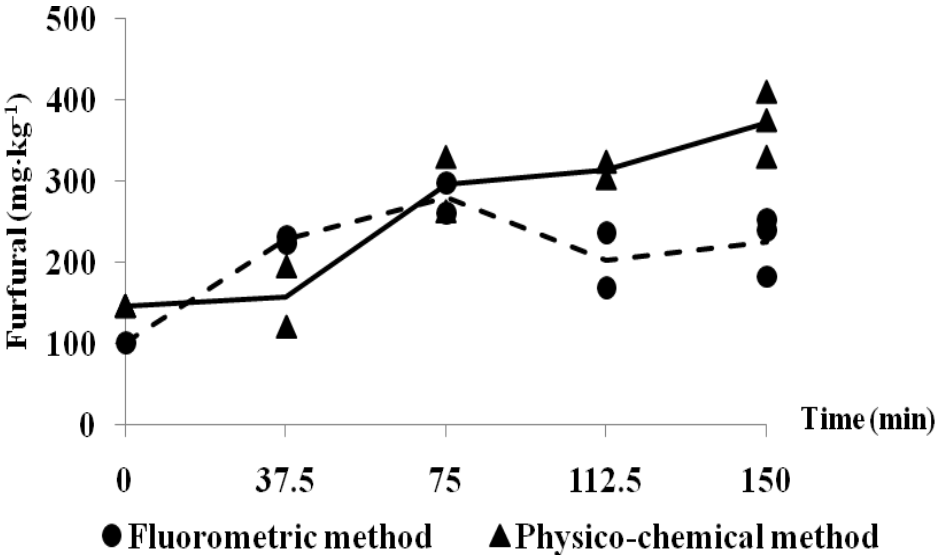

Figure 3.8 Accumulation of furfural content identified by the fluorometric method and physico-chemical method during the roasting of malt at 3.00 $W \cdot g^{-1}$ specific microwave power for 3.4 min and 200 °C hot air temperature.

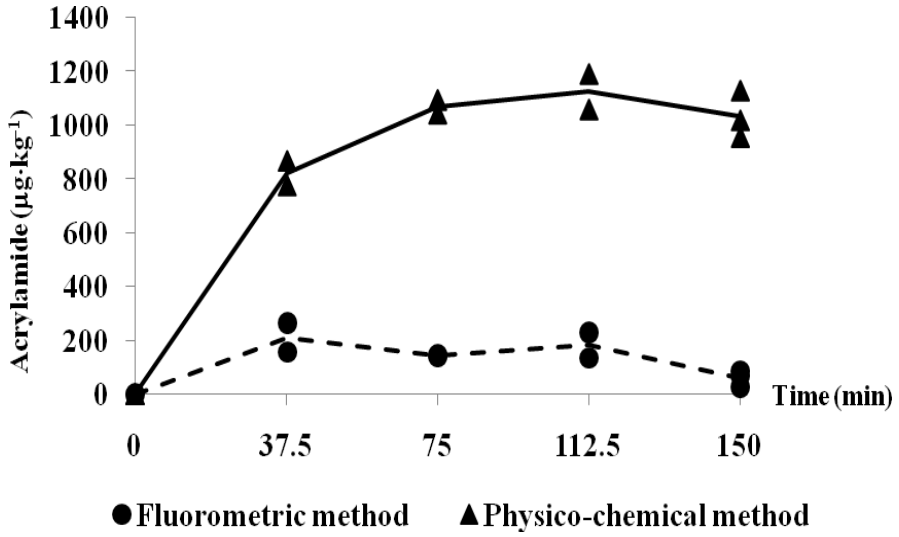

Figure 3.9 Accumulation of acrylamide content identified by the fluorometric method and physico-chemical method during the roasting of malt at 2.50 $W \cdot g^{-1}$ specific microwave power for 3.4 min and 200 °C hot air temperature.

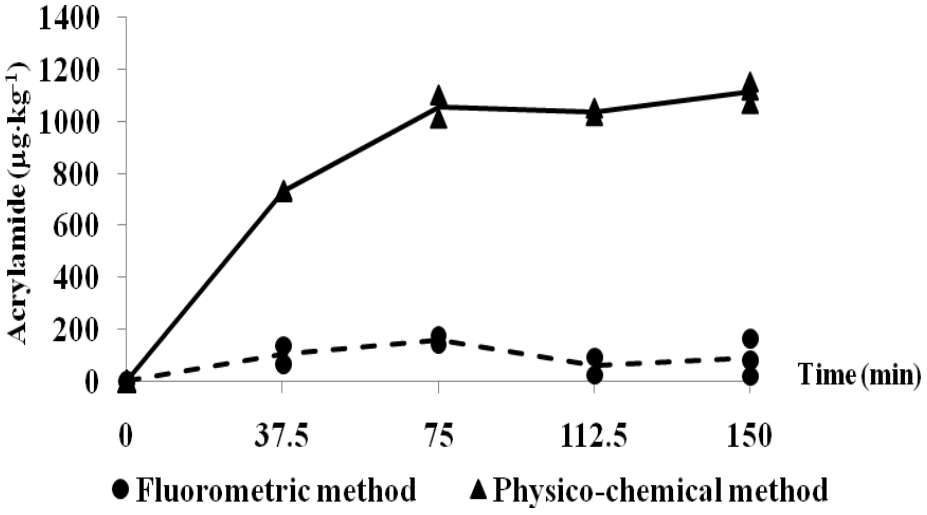

Figure 3.10 Accumulation of acrylamide content identified by the fluorometric method and physico-chemical method during the roasting of malt at 2.75 $W \cdot g^{-1}$ specific microwave power for 3.4 min and 200 °C hot air temperature.

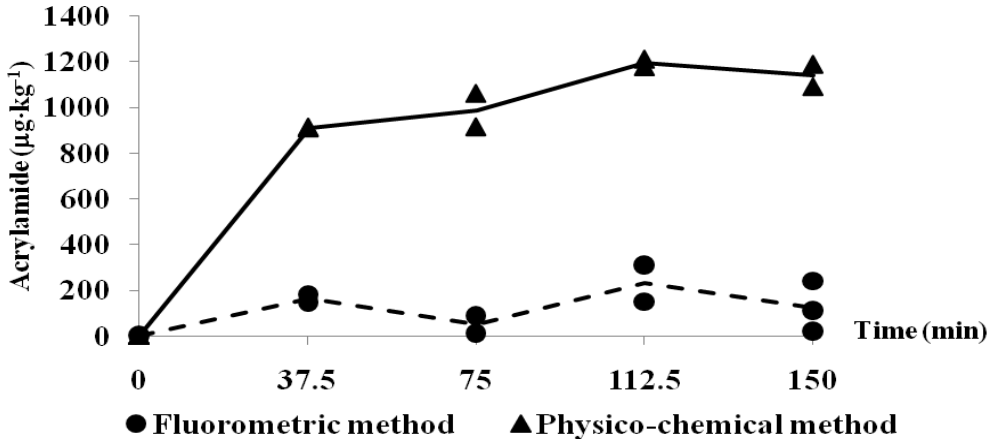

Figure 3.11 Accumulation of acrylamide content identified by the fluorometric method and physico-chemical method during the roasting of malt at 3.00 $W \cdot g^{-1}$ specific microwave power for 3.4 min and 200 °C hot air temperature.

Figure 3.12 shows furan content, identified by the fluorometric method at 2.50, 2.75, and 3.00 $W \cdot g^{-1}$ specific microwave power preheating. Furan could not be measured by the physico-chemical method because of a limited quantity of the samples. The furan content during roasting at 2.50 $W \cdot g^{-1}$ specific microwave power pre-heating was found to increase with roasting time until 75 minute. After 75 minutes, furan content decreased with roasting time and finally gradually increased during hot air roasting. A 2.75 and 3.00 $W \cdot g^{-1}$ specific microwave powers preheating, furan was found to increase with roasting time for the entire heating process. Considering the standard error of the analyses it can be concluded that furan content follows the same evolution whatever the microwave specific power.

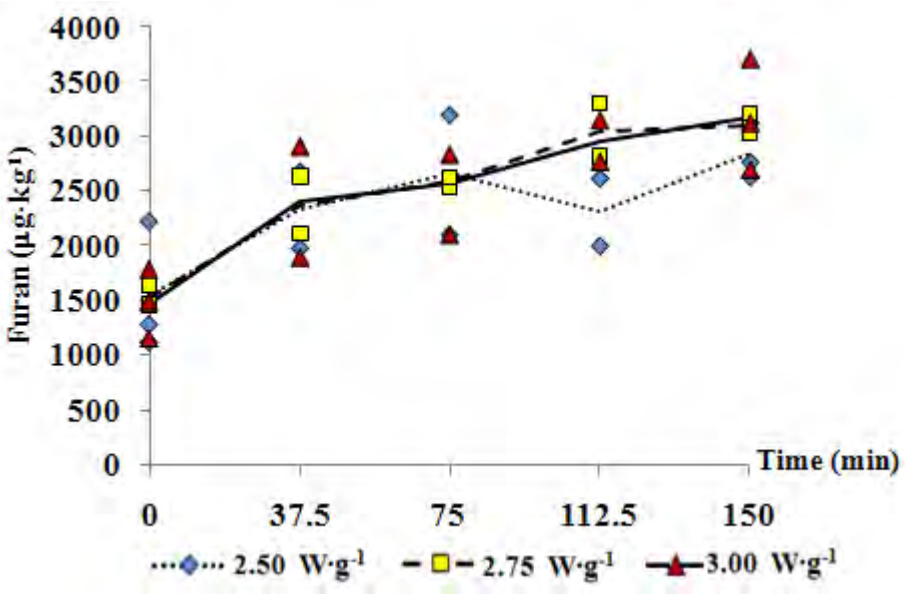

Figure 3.12 Accumulation of furan content during the roasting of malt at different specific microwave powers for 3.4 min and 200 °C hot air temperature. The data on furan was obtained by the fluorometric method.

For all experiments, preheated malts were roasted in a domestic oven at 200 °C hot air temperature. Regardless of the specific microwave power used in the preheating step, malts were subjected to heating at the same temperature for 150 minutes. Therefore, we expected to find a linear relationship with the same trends (decreasing or increasing behavior) between chemical indicators (HMF, furfural, furan, and acrylamide) and roasting time for the three specific microwave powers. The effect of specific microwave power should be observed only on the original point.

In order to identify kinetics order for NFC formation or degradation, the heating in domestic oven was considered over a range from 37.5 to 150 minutes. Figure 3.13 shows results of the curve fitting for furan identified by the fluorometric

method during roasting at 2.50, 2.75, and 3.00 $W \cdot g^{-1}$ specific microwave power for 3.4 min and 200 °C hot air temperature. From Figure 3.13, it appears that the furfural content as a function of roasting time for all specific microwave powers could be fitted using a linear model with satisfactory correlation coefficient (R^2 between 0.77 and 0.95). As expected, the slopes of each specific microwave power value were close to each other. Therefore furan formation in malt during combined microwave-hot air roasting followed a zero-order kinetic. Figures 3.14 to 3.22 show results of curve fitting for HMF, furfural, and acrylamide identified by the fluorometric method and physico-chemical method during roasting at 2.50, 2.75, and 3.00 $W \cdot g^{-1}$ specific microwave powers for 3.4 min and 200 °C hot air temperature. In Figures 3.14 to 3.22, the experimental data on HMF content identified by the physico-chemical method with a specific microwave power of 2.50 $W \cdot g^{-1}$, furfural content identified by the physico-chemical method with a specific microwave power of 2.50 and 3.00 $W \cdot g^{-1}$, and acrylamide content identified by the physico-chemical method with a specific microwave power of 2.75 $W \cdot g^{-1}$ could be fitted using a linear model with quite satisfactory correlation coefficient (R^2 between 0.70 and 0.89), while HMF content identified by the physico-chemical method with a specific microwave power of 2.75 and 3.00 $W \cdot g^{-1}$, furfural content identified by the physico-chemical method with a specific microwave power of 2.75 $W \cdot g^{-1}$, and acrylamide content identified by the physico-chemical method with a specific microwave power of 2.50 and 3.00 $W \cdot g^{-1}$ could not be fitted to any model (R^2 between 0.06 and 0.62). Moreover, HMF, furfural, and acrylamide content identified by the fluorometric method for all specific microwave powers could not be fitted to any model (R^2 less than 0.52) except for furfual identified by the fluorometric method with a specific microwave power of

2.75 $W \cdot g^{-1}$ that could be fitted using a linear model (R^2 equal 0.83). From this study, the change in HMF, furfural, and acrylamide identified by the physico-chemical and fluorometric method could not be adequately fitted with any kinetic model. There was, thus, no conclusive trend for the formation kinetics of these substances. More experiments are suggested. This issue should be addressed in the trial design of future prospective studies on kinetics of NFCs formation during combined microwave-hot air roasting of malt. According to Carabasa-Giribet and Ibarz-Ribas (2000), HMF formation for aqueous model systems containing glucose and aspartic acid, glutamic acid or asparagine followed a zero order kinetic while Ameur et al. (2006) stated that the formation of HMF in cookies followed a first-order kinetic. Capuano *et at*. (2008) reported that acrylamide formation in toasted bread slices followed a zero-order kinectic.

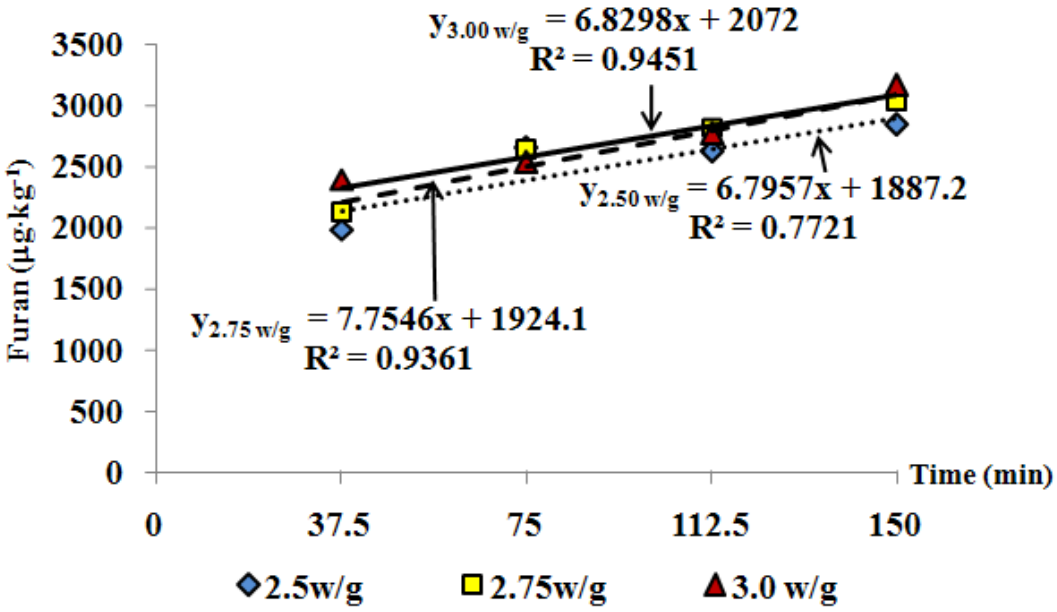

Figure 3.13 Representative results of curve fitting for furan during roasting at various specific microwave powers for 3.4 min and 200 °C hot air temperature. The data on furan was obtained by the fluorometric method.

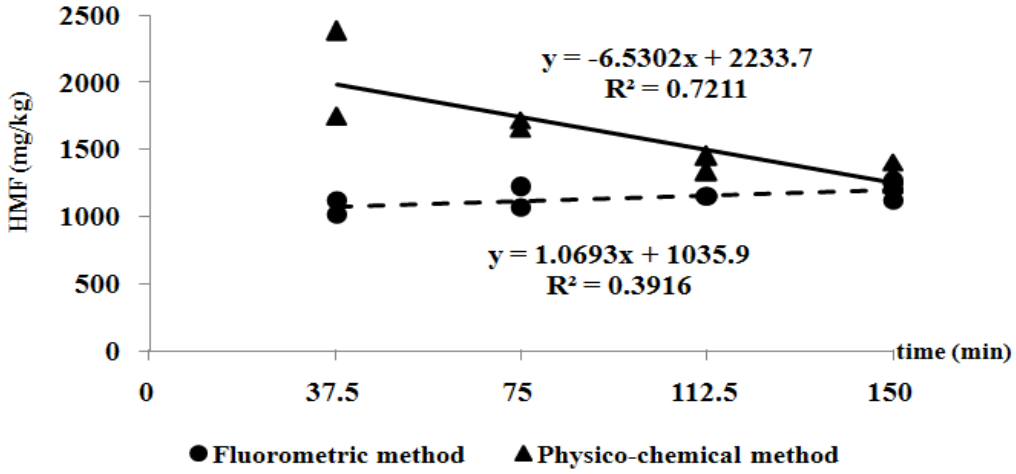

Figure 3.14 Representative results of curve fitting for HMF identified by the fluorometric method and physico-chemical method during roasting at 2.50 $W \cdot g^{-1}$ specific microwave powers for 3.4 min and 200 °C hot air temperature.

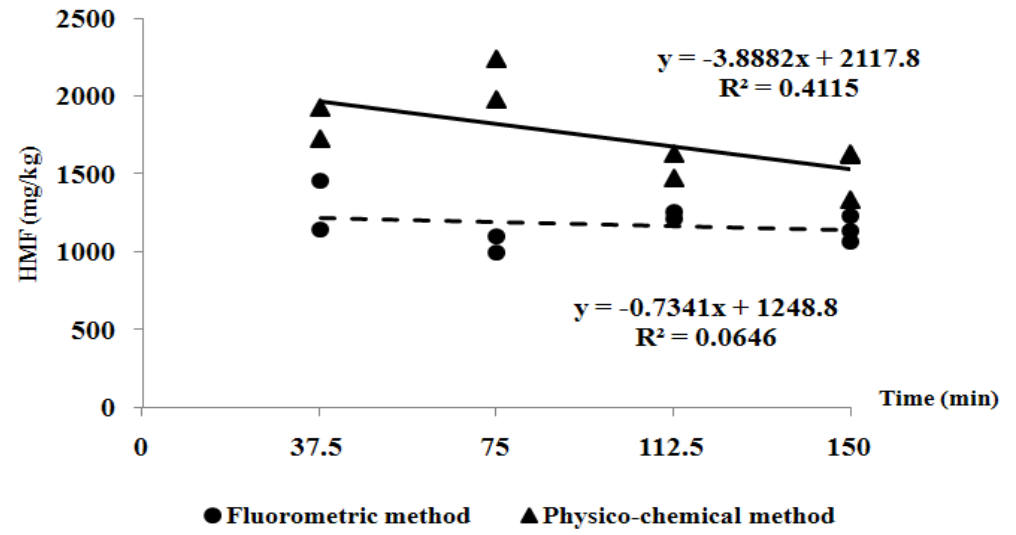

Figure 3.15 Representative results of curve fitting for HMF identified by the fluorometric method and physico-chemical method during roasting at 2.75 $W \cdot g^{-1}$ specific microwave powers for 3.4 min and 200 °C hot air temperature.

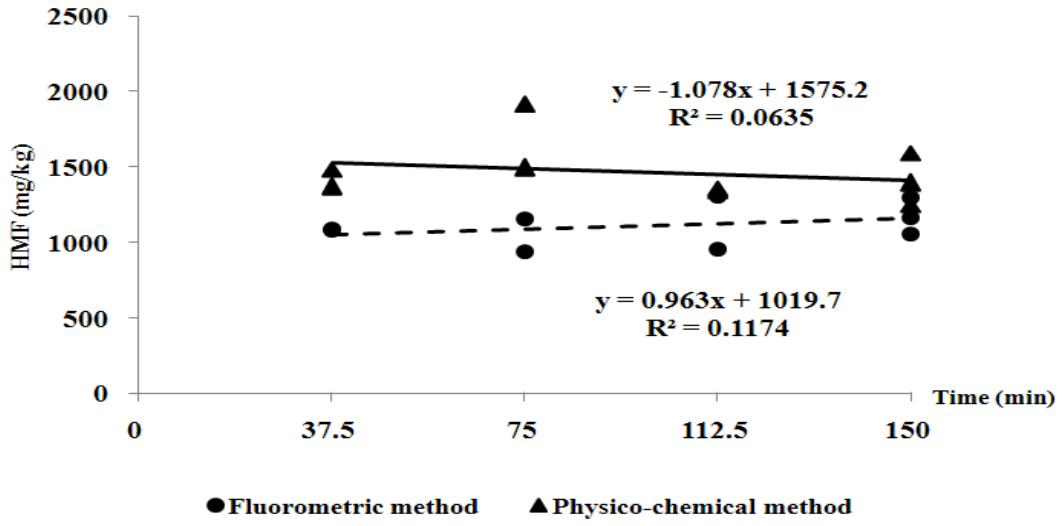

Figure 3.16 Representative results of curve fitting for HMF identified by the fluorometric method and physico-chemical method during roasting at 3.00 $W \cdot g^{-1}$ specific microwave powers for 3.4 min and 200 °C hot air temperature.

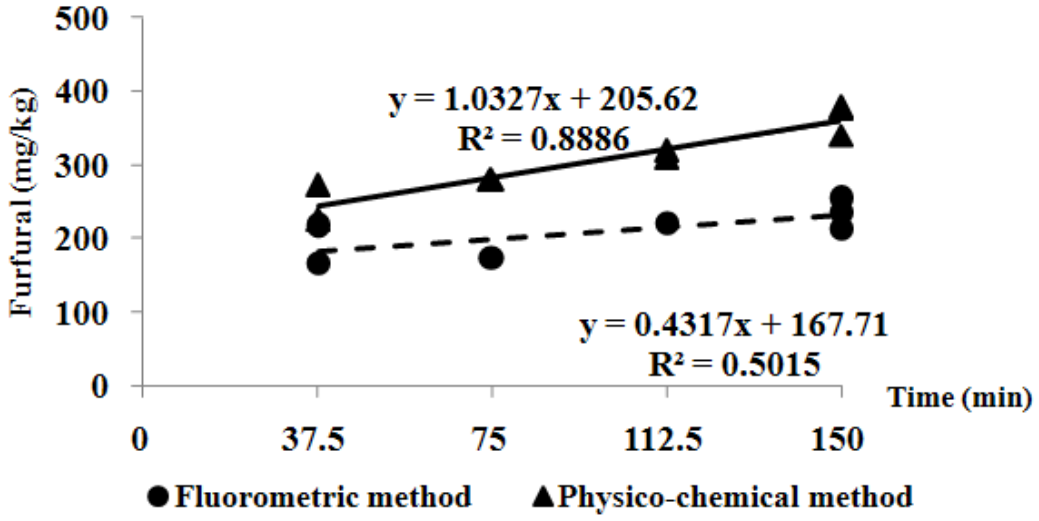

Figure 3.17 Representative results of curve fitting for furfural identified by the fluorometric method and physico-chemical method during roasting at 2.50 $W \cdot g^{-1}$ specific microwave powers for 3.4 min and 200 °C hot air temperature.

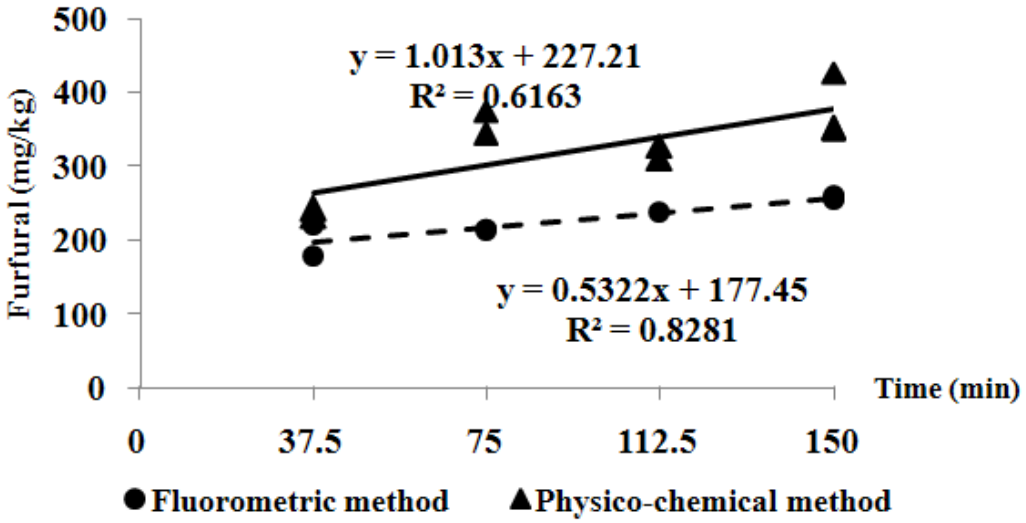

Figure 3.18 Representative results of curve fitting for furfural identified by the fluorometric method and physico-chemical method during roasting at 2.75 $W \cdot g^{-1}$ specific microwave powers for 3.4 min and 200 °C hot air temperature.

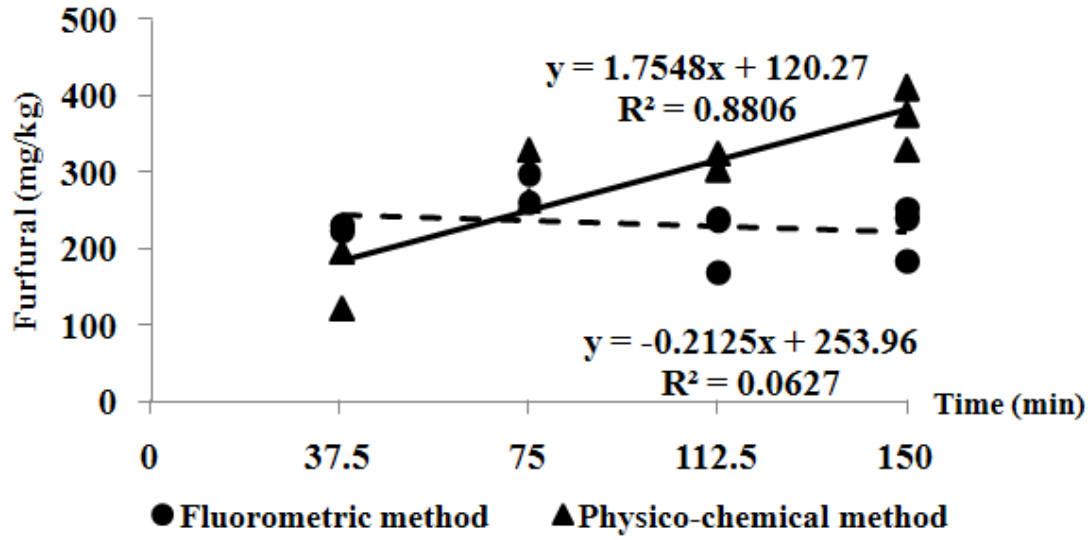

Figure 3.19 Representative results of curve fitting for furfural identified by the fluorometric method and physico-chemical method during roasting at 3.00 $W \cdot g^{-1}$ specific microwave powers for 3.4 min and 200 °C hot air temperature.

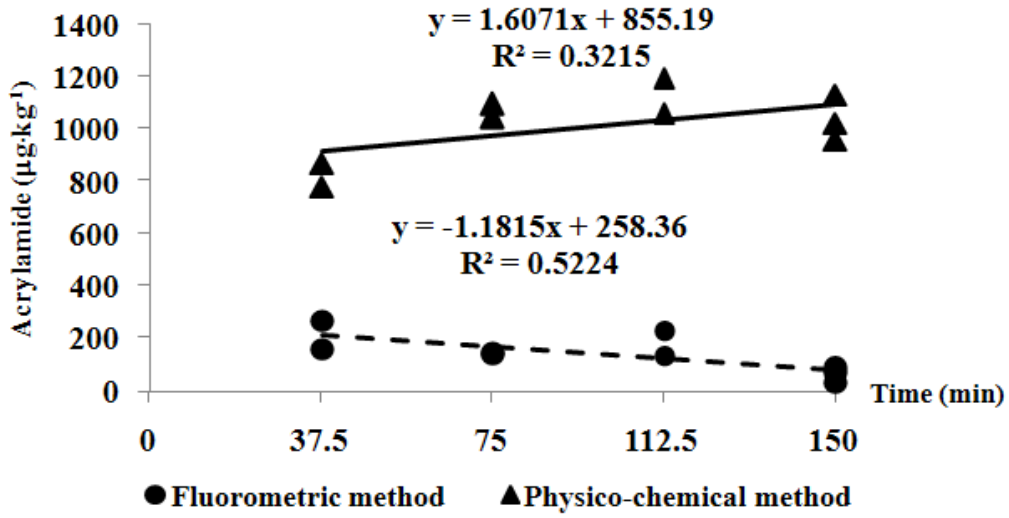

Figure 3.20 Representative results of curve fitting for acrylamide identified by the fluorometric method and physico-chemical method during roasting at 2.50 $W \cdot g^{-1}$ specific microwave powers for 3.4 min and 200 °C hot air temperature.

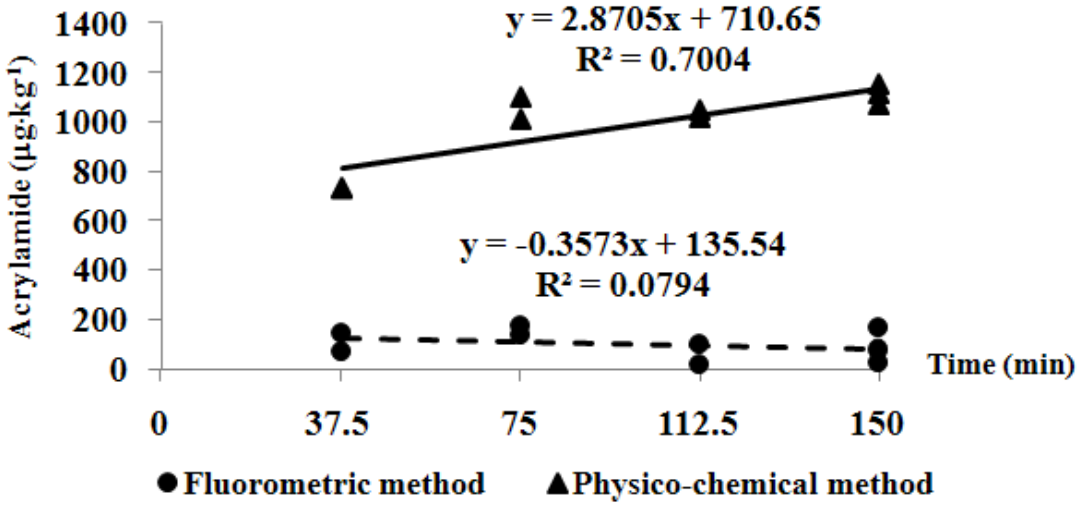

Figure 3.21 Representative results of curve fitting for acrylamide identified by the fluorometric method and physico-chemical method during roasting at 2.75 $W \cdot g^{-1}$ specific microwave powers for 3.4 min and 200 °C hot air temperature.

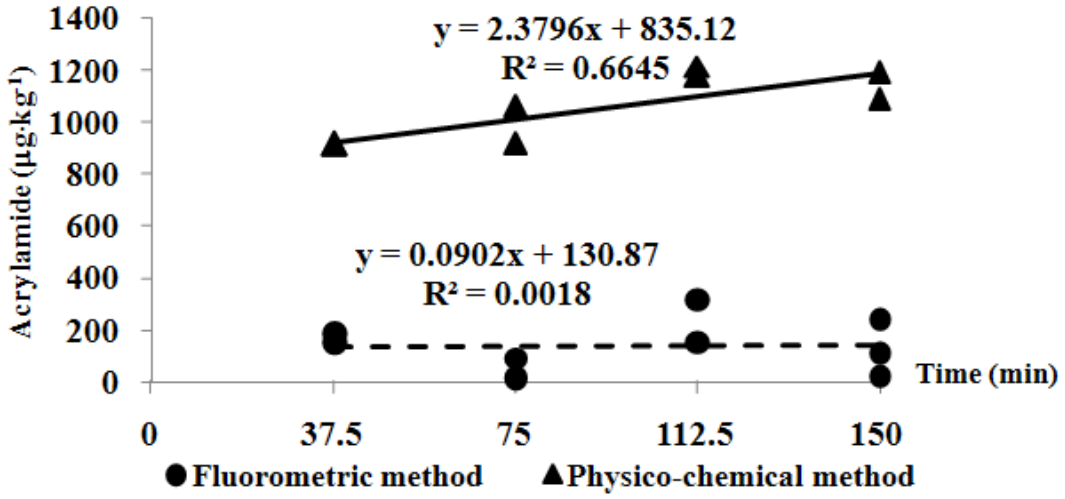

Figure 3.22 Representative results of curve fitting for acrylamide identified by the fluorometric method and physico-chemical method during roasting at 3.00 $W \cdot g^{-1}$ specific microwave powers for 3.4 min and 200 °C hot air temperature.

3.5 CONCLUSIONS

The predictive equations for color development during roasting used as indicators to characterize and identify the end point of the roasting process in the production of colored malts were determined. The level of furfural determined by the fluorometric method increased linearly as a function of time which indicated that the formation of furfural followed a zero order kinetic model. There is no conclusive trend for the formation kinetics of HMF, furfural, and acrylamide.

CHAPTER IV

OPTIMIZATION OF COMBINED MICROWAVE-HOT AIR ROASTING OF MALT IN TERMS OF ENERGY CONSUMPTION AND NEO-FORMED CONTAMINANTS CONTENT

4.1 INTRODUCTION

In the brewing industry, speciality malts or colored malts have been used to give particular colors and flavors to beers. Speciality malts or colored malts are malts which have a coffee, chocolate or black color (Hough *et al*., 1971; Lewis and Young, 2002; Briggs *et al*., 2004). High temperatures need to be attained during the roasting of malt in order to get a desirable color and flavor. During conventional roasting processes, moisture is initially removed from the surface of the grain causing water to move from the interior of the product to the dried surface through a diffusion process. This phenomenon is time and energy consuming. In a microwave drying system, the product heating is associated with a volumetric heat generation which leads to higher internal temperatures resulting in an increase in internal vapor pressure. In the case of water rich products this helps to push liquid flow towards the surface, making it possible for higher drying rates (Prabhanjan *et al*., 1995; Mujumdar, 2000; Sharma *et al*., 2000). In a conventional roaster, it takes several hours for the temperature to reach 200^{o}C in the malt beds. Microwave heating, however, requires only a few minutes to achieve the temperature at this level.

Neo-formed contaminants (NFCs) are the product of the Maillard reaction taking place during the heating of foods. The Maillard reaction occurs because of a condensation reaction between free amino acids and reducing sugars. It comprised

three basic steps. The initial reaction is the condensation of an amino acid with a simple sugar, which loses a molecule of water to form N-substituted aldosylamine. N-substituted aldosylamine is unstable and undergoes Amadori rearrangement to form 1-amino-1-deoxy-2-ketoses which can undergo complex subsequent dehydration, fission and polymerization. The Maillard reaction is dependent on factors such as concentrations of reactants, reactant type, pH, time, temperature, and water activity. Free radicals and antioxidants are also involved (Mlotkiewicz, 1998).

NFCs found in foods are, for example, hydroxymethylfurfural (HMF), furfural, furan, and acrylamide (Food and Agriculture Organization/World Health Organization Consultation on Health Implication of Acrylamide in Food, 2002; Zyzak *et al*., 2003). It is well known that NFCs occur during the heating of foods especially those processed at vigorous heat conditions (over 100^{o}C). The presence of NFCs in food is a major concern for humans because of its ability to induce cancer and heritable mutations in laboratory animals (Food and Agriculture Organization/World Health Organization Consultation on Health Implication of Acrylamide in Food, 2002; Swedish National Food Administration, 2002; Dybing *et al*., 2005). Since microwave heating can generate heat from inside food pieces, when using in combination with convention heating it can improve heat transfer and, thus, reduce heating time compared to hot air only, therefore, it may be beneficial to produce colored malt by using combined microwave-hot air roasting to achieve a desirable malt color and avoid the formation of carcinogenic and toxic substances such as NFCs.

Objectives

The objectives of this study were to compare energy consumption and NFCs formation during the roasting of malt by hot air-only and combined microwave-hot air processes as well as to determine the effect of specific power, microwave processing time, oven temperature, and oven processing time on energy consumption and NFCs content during combined microwave-hot air roasting. Response Surface Methodology was used in order to obtain quadratic models in order to predict optimal conditions for producing coffee, chocolate and black colored malt with the combined microwave-hot air process.

4.2 LITERATURE REVIEW

Malt roasting by means of hot air is ordinarily a long and slow process because of the resistance of the hulls to the passage of moisture. The temperature profile in grain drying shows a positive gradient from surface to center (Decareau, 1985). The major disadvantages of hot air roasting are deterioration of flavor, color, and nutrients, low energy efficiency and lengthy drying times (Maskan, 2000). The desire to eliminate this problem, prevent significant quality loss, and achieve fast and effective thermal processing have resulted in the use of microwave processes. Roasting of malt by microwaves generates internal heat. Microwaves can easily penetrate the inert dry layers to be absorbed directly by the moisture and the quick energy absorption causes rapid increases in temperatures (Prabhanjan *et al*., 1995). Therefore, microwave energy should be applied in the first stage for increasing the temperature, followed by hot air roasting for flavor and color development.

4.2.1 Heating of food by combined microwave-hot air

Microwave heating applications are widely used in combination with hot air. In an air-drying system, hot air removes water in its free state on the surface of the product, whereas microwave energy removes free water in the product (Alibas, 2007). A combined microwave-conventional heating process can reduce surface moisture more efficiently when compared to microwave-only heating (Decareau, 1985). The lower relative humidity of the hot air favors the mass transfer at the surface of the product. There have been researches showing an improvement in the quality of finished products when microwaves are used in combination with other conventional drying processes such as infrared heating (Datta and Ni, 2002), hot air drying (Bouraoui *et al*., 1993; Prabhanjan *et al*., 1995; Maskan, 2000; Sharma and Prasad, 2001; Alibas, 2007), and vacuum drying (Mujumdar, 2000). The qualities of dry mushrooms were found to be superior to those dried under conventional methods (Funebo and Ohlsson, 1998). Microwave dried garlic cloves were found to have better flavor and color with higher vitamin C retention and water uptake (Sharma and Prasad 2001; Sharma and Prasad 2006). It was also possible to obtain good quality dried carrots (Prabhanjan *et al*., 1995), mushrooms (Funebo and Ohlsson, 1998), pumpkin slices (Alibas, 2007), potato slices (Bouraoui *et al*., 1994), meat, cookie dough (Decareau, 1985), skimmed milk, whole milk, casein powers (Al-Duri and McIntyre, 1992), butter and fresh pasta (Decareau, 1985) by using microwaves combined with conventional drying. Combined microwave-hot air-drying resulted in a reduction in the drying time to an extent of 80 to 90% for garlic cloves and 25 to 90% for carrots when compared to conventional hot air drying (Prabhanjan *et al*., 1995; Sharma and Prasad, 2001).

4.2.2 Factors influencing the NFCs formation in food

Temperature and time are two factors that are consistently identified in the formation of NFCs in food. Given these important factors, various ways of preparing food, with the exception of boiling, have not been eliminated as contributing to NFCs formation. In fact, recent evidence tends to indicate that it is the actual temperature and time, rather than the method, which contributes to NFCs formation in food (Martin *et al*., 2001; Gökmen *et al*. 2006). Knowing the mechanisms of NFCs formation, including possible reactants and precursors, is critical information for identifying possible ways of reducing or minimizing that formation. It is also recognized that home and commercial food preparation methods need to be considered.

Claeys *et al*. (2005b) studied the effect of the process parameters (temperature and time), and the reactants (glucose and asparagines) on acrylamide levels in French fries, potatoes, and wheat flour. The authors found that acrylamide formation is positively correlated with temperature and time, reducing sugar and amino content. In addition, the authors suggested that pre-treatment such as blanching potatoes could reduce the formation of acrylamide during heating by extracting reducing sugars and asparagines. Blanching renders the membranes permeable, thus facilitating the extraction of the acrylamide precursors.

Gökmen *et al*. (2006) studied the effect of frying time and temperature on acrylamide formation in French fries during frying at 150, 170 and 190 °C. The result showed that the amount of acrylamide increased not only with increasing temperature, but also with the time of frying. However, frying temperature appeared to have a greater effect on acrylamide formation when compared to frying time.

Erdoğdu *et al*. (2007) showed that microwave application prior to frying resulted in a marked reduction of the acrylamide levels on the whole potato strips. When potato strips were subjected to frying after a microwave pre-cooking step, acrylamide content in the whole potato strip was reduced by 36% at 150 °C, 41% at 170 °C and 60% at 190 °C.

Ameur *et al*. (2007) studied the influence of the type of sugar, baking temperature and a_w on HMF formation in cookies. The authors reported that HMF started to accumulate at a_w between 0.5 and 0.7 depending on the temperature and followed a first order kinetic, highly dependent on the baking temperature and type of sugar. The authors stated that fructose was more efficiently transformed to HMF than does glucose. The higher conversion of fructose into HMF due to a fructose-specific reaction pathway involving a 1,2-endiol intermediate in acidic media.

4.2.3 Response Surface Methodology (RSM)

There are several experimental design models that can help reduce the number of experiments and that can be used in different cases. If it is necessary to detect influential factors, experimental designs for first-order models (factorial designs) can be used. To approximate a response function or to optimize a process, experimental designs for second-order models should be used (Ferreira *et al*., 2004).

The most popular first-order design is the two-level full (or fractional) factorial, in which every factor is experimentally studied at only two levels. Due to their simplicity, full factorial designs are very useful for preliminary studies or in the initial steps of an optimization. However, since only two levels are used, the models that can be fitted to these designs are somewhat restricted. Consequently, a more

sophisticated model is required, one that employs more than two factor levels to allow the fitting of a full quadratic polynomial (Ferreira *et al*., 2004).

RSM is a collection of mathematical and statistical techniques that are useful for the modeling and analysis of problems in which a response of interest is influenced by several variables. The objective of RSM is to determine the optimum operating conditions for the system or to determine a region of the factor space in which operating requirements are satisfied (Montgomety, 1997). The main advantage of RSM is the reduction of the experimental trials needed to evaluate multiple parameters and their interactions (Simsek *et al*., 2007).

A central composite design (CCD) combines a two-level full or fractional factorial design with additional points and with at least one point at the center of the experiment region. CCD would be selected to obtain properties such as rotatability or orthogonality (Montgomety, 1997; Ferreira *et al*., 2004). CCD consist of a 2^k factorial, $2k$ axial runs, and n_c center runs, where k is the number of variables and n_c is the number of center points (Montgomety, 1997).

An alternative and very useful experimental design for second-order models is the Box-Behnken design (BBD). BBD is a rotatable second-order design based on three-level incomplete factorial designs. The special arrangement of the BBD levels allows the number of design points to increase at the same rate as the number of polynomial coefficients. BBD is formed by combining 2^k factorials with incomplete block designs (Montgomety, 1997). The number of experimental points (N) is defined by the expression $N = 2k(k\text{-}1) + C_0$, where k is the number of variables and C_0 is the number of center points (Mozzo, 1990; Ferreira *et al*., 2004). Table 4.1 shows Box-Behnken matrix for three factors with triplicate at center point.

Table 4.1 Box-Behnken matrix for three factors.

run no.	x_1	x_2	x_3	x_4
1	-1	-1	0	0
2	1	-1	0	0
3	-1	1	0	0
4	1	1	0	0
5	0	-1	-1	0
6	-1	0	-1	0
7	1	0	-1	0
8	0	1	-1	0
9	0	-1	1	0
10	-1	0	1	0
11	1	0	1	0
12	0	1	1	0
13	0	0	0	0
14	0	0	0	0
15	0	0	0	0

Source: adapted from Mozzo (1990)

4.3 MATERIALS AND METHODS

4.3.1 Materials

Barley malts were obtained from the French Institute of Brewing and Malting, Nancy, France. Average initial moisture content of the malt was 5.36% (wet basis).

4.3.2 Drying experiment

In each experiment, 75 g of malt was weighed in a 250 cm^3-beaker which was then subjected to microwave treatment. This lab-scale microwave pilot plant (Microondes Énergie Système, Villejuif, France) was presented in Figure 3.1. Three fiber optic probes were used to measure temperature at the center of the malt bed during the treatment. All data were collected on a data logger (SA 70, AOIP, Ris Orangis, France) controlled by Labview® supervisor software (National Instruments,

Nanterre, France). Microwave heating was done at 2.50, 2.75, and 3.00 $W \cdot g^{-1}$ specific microwave power. Specific microwave power is defined as the ratio of the microwave power input to the mass of the malt sample. Therefore microwave power inputs were adjusted at 187.5, 206.25, and 225 W, respectively.

After microwave heating, the sample was quickly transferred to the 2,800 W-domestic oven (FB 970 C2/E IX, Ariston, Fabriano, Italy) and heated at 180, 200 and 220℃ for 60, 105, and 150 minutes. The malts were arranged in one layer on a 40 cm × 40 cm tray. After heating, the malts were cooled to room temperature (21 °C) in an ice-water bath.

4.3.3 Moisture analysis

Moisture analysis of ground malt was carried out using a hot air oven at 105 ± 2°C (Association of Official Analytical Chemists, 1990 methods 935.29). The analyses were done in triplicate. The average moisture content and standard deviation were recorded.

4.3.4 Color determination

The color of the ground malt was determined as described in Chapter III, section 3.3.3.

4.3.5 NFCs content determination

NFCs content including HMF, furfural, furan, and acrylamide content were evaluated by the fluorometric method and the physico-chemical analysis method as described in Chapter III, section 3.3.4.

4.3.6 Calculation for energy consumption

The roasting of the malt grains was carried out with a combined microwave-hot air process; therefore, the total energy consumption (E_{total}) comprises

two parts, one for the microwaves and the other for the hot air, as indicated in Equation 4.1.

$$E_{total} = E_{mw} + E_{oven} \quad (4.1)$$

The energy consumption of the hot air oven (E_{oven}) was measured by a watt-hour meter. The energy consumption of the microwave oven (E_{mw}) was calculated using Equations 4.2 and 4.3.

$$E_{mw} = P_{mw} \times t_{mw} \times 3.6 \quad (4.2)$$

The value 3.6 in Equation 4.3 is a multiplication factor to convert E_{mw} to kJ units.

$$P_{mw} = SP \times w \quad (4.3)$$

4.3.7 Response Surface Methodology

In this study the Box-Behnken design, a response surface design, was selected to estimate the main effect of the process variables on heat transfer variables during the roasting of malts and to optimize the combined microwave-hot air process. One of the advantages of the Box-Behnken design is its flexibility for regulation because the design employs only three factor levels (-1, 0 and 1). The design also allows the addition of more factors using former experiment data (Mozzo 1990; Montgomery 1997). The independent variables were specific microwave powers (X_1) of 2.50, 2.75, and 3.00 $W \cdot g^{-1}$; microwave heating times (X_2) of 3.3, 3.4, and 3.5 minutes; oven temperatures (X_3) of 180, 200, and 220 °C; and oven heating times (X_4) of 60, 105, and 150 minutes. The dependent variables were color (Y_1), energy

consumption by the microwave (Y_2), energy consumption by the oven (Y_3), total energy consumption (Y_4) and the quantities of HMF (Y_5), furfural (Y_6), furan (Y_7) and acrylamide (Y_8). The design includes 25 experiments with 3 replications of the center point. The Box-Behnken matrix for four factors is shown in Table 4.2. The experiments were carried out in a random order. The levels of Box-Behnken design for each parameter were found from preliminary experiments.

The factor levels were chosen to acquire a range of color from coffee to black malt as shown in Figure 4.1. The quadratic model (Equation 4.4) was used in order to predict each response (Y_k) in all experimental regions as follows:

$$Y_k = B_0 + B_1X_1 + B_2X_2 + B_3X_3 + B_4X_4 + B_{11}X_1^2 + B_{22}X_2^2 + B_{33}X_3^2 + B_{44}X_4^2 + B_{12}X_1X_2 + B_{13}X_1X_3 + B_{14}X_1X_4 + B_{23}X_2X_3 + B_{24}X_2X_4 + B_{34}X_3X_4 \quad (4.4)$$

The transform equations from coded values of independent variables to real values of independent variables were: Specific power ($W \cdot g^{-1}$) = $0.25 \cdot X_1 + 2.75$, Time of microwave (min) = $0.1 \cdot X_2 + 3.4$, Oven temperature (°C) = $20 \cdot X_3 + 200$, and Time of oven (min) = $45 \cdot X_4 + 105$.

Table 4.2 Box-Behnken matrix for four factors.

run no.	x_1	x_2	x_3	x_4
1	-1	-1	0	0
2	1	-1	0	0
3	-1	1	0	0
4	1	1	0	0
5	0	-1	-1	0
6	-1	0	-1	0
7	1	0	-1	0
8	0	1	-1	0
9	0	-1	1	0
10	-1	0	1	0
11	1	0	1	0
12	0	1	1	0
13	0	0	-1	-1
14	0	-1	0	-1
15	-1	0	0	-1
16	1	0	0	-1
17	0	1	0	-1
18	0	0	1	-1
19	0	0	-1	1
20	0	-1	0	1
21	-1	0	0	1
22	1	0	0	1
23	0	1	0	1
24	0	0	1	1
25	0	0	0	0
26	0	0	0	0
27	0	0	0	0
28	0	0	0	0

Source: adapted from Mozzo (1990)

4.3.8 Statistical Analysis

An analysis of variance and response surface regression was performed using the regression module of Microsoft Excel 2003 software. The model was obtained for each dependent variable or response. Factors were rejected when their confidence level was less than 95%.

4.4 RESULTS AND DISCUSSION

In this study, roasting malt by microwave-only has been performed in preliminary experiments. The results showed that it was not possible to obtain homogeneous malt color. The necessity to use high temperature resulted in the use of high specific microwave powers leading to heterogeneity in malt roasting; some grains became black while others were still pale. In order to overcome this a combined microwave-hot air, a two-stage roasting process involving an initial microwave heating, followed by hot air convective roasting has been proposed to give better product quality with a considerable saving in energy and time. Using microwaves for heating the malt in the first step gives a rapid rise in the malt temperature. The sample was then subjected to a holding temperature for a determined period of time in a hot air oven until the end of the treatment. This step allowed malt coloration and flavor development.

The average initial moisture content of the malt used for the entire study was 5.36% (wet basis) and the average final moisture content after combined microwave-hot air treatment was in the 1%-3% (wet basis) range. This is in the same final moisture range from conventional roasting processes (Hough *et al*., 1971; Lewis and Young, 2002).

4.4.1 The relationship between ΔE-value and °EBC

In the brewing industry malt color is usually characterized according to the European Brewing Convention (EBC) color system which consists of comparing color of malt samples after liquid extraction with a set of reference colors. This method is not precise enough to be used as a response in an experimental design. Therefore, the L a^*b^* system was used to specify the color of malt. In this research,

the *ΔE* values of desirable coffee, chocolate and black malt were 50.41, 54.37 and 59.72, respectively, as shown in Figure 4.1. The relationship between the ΔE-value and the °EBC unit is shown in Figure 4.2. The color of malt in the °EBC unit can be predicted from ΔE-value following Equation 4.5 or measured from the experiment. Table 4.3 shows that the predicted °EBC-values were in range of the measured °EBC values. Since the colorimeter method, associated with equation 4.5, which was used to determine the ΔE-value is easier and cheaper than the °EBC determination method, it has the potential to help facilitating the brewing industry in malt color characterization.

Figure 4.1 Colors and the corresponding color difference value (ΔE) of not-treated, coffee, chocolate and black malt.

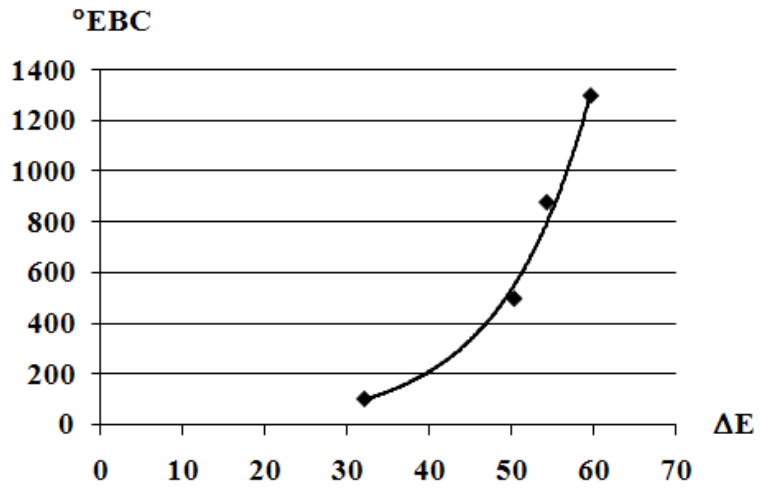

Figure 4.2 Graph relationships between color in ΔE-values and °EBC unit.

$$°EBC = 5.2711e^{0.0924 \cdot \Delta E}, R^2 = 0.9945 \quad (4.5)$$

Table 4.3 Malt color in ΔE-value, predicted °EBC and the measured °EBC of coffee, chocolate and black malts.

	ΔE-value	°EBC from Equation 4.5	Measured °EBC
Coffee malt	50.41	556	400-600
Chocolate malt	54.37	801	800-880
Black malt	59.72	1313	1200-1400

4.4.2 The effect of factors associated with microwave and hot air oven on energy consumption and NFCs content during combined microwave-hot air roasting

The experimental responses studied included: ΔE, E_{mw}, E_{oven}, E_{total}, HMF, furfural, furan, and acrylamide content (Y_1 to Y_8). The values obtained experimentally

are given in Table 4.4. The response surface plots calculated from the quadratic models obtained for the different responses: ΔE, E_{mw}, E_{oven}, E_{total}, HMF, furfural, furan, and acrylamide content are shown in Figures 4.3 and 4.4. At a constant specific microwave power (2.75 $W \cdot g^{-1}$) and microwave heating time (3.4 minutes), the experimental results for the ΔE, E_{oven}, E_{total} tended to increase with oven temperature and oven heating time as shown in Figures 4.3a, 4.3c, and 4.3d. Color products are the high molecular weight compounds referred to as melanoidins, and the low molecular weight colored compounds, containing two or three heterocyclic rings (Ames *et al*., 1998). Figure 4.3a shows that color development increased with increasing temperature and heating time.

Figures 4.4a to 4d show response surface plots of HMF, furfural, furan, and acrylamide concentration at constant specific microwave powers (2.75 $W \cdot g^{-1}$) and microwave heating time (3.4 minutes). HMF, furfural, furan and acrylamide levels tended to increase with increasing temperature and time as shown in Figures 4.4a to 4.4d except acrylamide level which tended to decrease while increasing time as shown in Figure 4.4d.

Table 4.4 ΔE, E_{mw}, E_{oven}, E_{total}, content of HMF, furfural, furan, and acrylamide of malts roasted at various treatment conditions according to the Box-Behnken design.

Treat-ment no.	Color (ΔE)	E_{mw} (kJ)	E_{oven} (kJ)	E_{total} (kJ)	HMF ($mg \cdot kg^{-1}$)	Furfural ($mg \cdot kg^{-1}$)	Furan ($\mu g \cdot kg^{-1}$)	Acrylamide ($\mu g \cdot kg^{-1}$)
1	41.46±0.49	37.13	4685.95	4723.008	1283.2	225.86	2755.37	80.99
2	43.44±0.06	44.55	4685.95	4730.5	1089.9	174.1	2233.5	230.59
3	43.23±0.43	39.38	4685.95	4725.33	1093.34	254.51	3152.13	20.68
4	43.002±0.36	47.25	4685.95	4733.2	1120.33	141.69	1806.01	308.12
5	33.10±0.17	40.84	4037.98	4078.82	1029.73	159.36	1975.4	128.7
6	32.42±0.15	38.25	4037.98	4076.23	1181.77	172.94	2093.3	133.16
7	35.20±0.09	45.9	4037.98	4083.88	1186.27	192.85	2343.77	73.21
8	32.66±0.12	43.31	4037.98	4081.29	1098.27	144.65	1764.93	169.61
9	55.49±0.49	40.84	5387.17	5428.01	1048.41	277.45	3385.17	18.11
10	54.80±0.17	38.25	5387.17	5425.42	968.39	306.49	3782.9	7.56
11	53.99±0.46	45.9	5387.17	5433.007	993.009	301.5	3695.97	11.39
12	53.95±0.08	43.31	5387.17	5430.49	1002.36	312.75	3847.93	7.14
13	31.25±0.47	42.08	2307.42	2349.49	1080.31	158.57	1922.03	123.001
14	42.09±0.15	40.84	2677.69	2718.52	1060.9	227.12	2813.007	32.65
15	38.36±0.63	38.25	2677.69	2715.94	1176.26	245.77	2960.37	29.82
16	41.00±0.14	45.9	2677.69	2723.59	1104.34	188.88	2367.77	89.24
17	40.54±0.43	43.31	2677.69	2721.00	1211.03	197.6	2408.27	149.39
18	51.34±0.19	42.08	3078.38	3120.46	1032.07	307.48	3771.1	8.44
19	34.17±0.64	42.08	5768.55	5810.62	1143.63	79.03	1001.4	513.26
20	44.93±0.19	40.84	6694.21	6735.05	1179.63	235.34	2884.4	46.28
21	47.16±0.40	38.25	6694.21	6732.46	1116.93	254.3	3126.23	28.19
22	45.06±0.60	45.9	6694.21	6740.11	1058.73	252.72	3142.67	20.49
23	46.09±0.47	43.31	6694.21	6737.53	982.49	270.54	3380.17	12.81
24	59.94±3.20	42.08	7695.96	7738.04	1036.17	332.32	4029.77	7.96
25	45.49±0.12	42.08	4685.95	4728.03	1063.83	259.16	3216.63	19.18
26	45.70±0.35	42.08	4685.95	4728.03	1108.57	268.87	3297.13	17.44
27	44.90±0.28	42.08	4685.95	4728.03	1213.2	223.41	2783.23	55.81
28	46.31±0.72	42.08	4685.95	4728.03	1112.6	261.48	3212.503	20.76

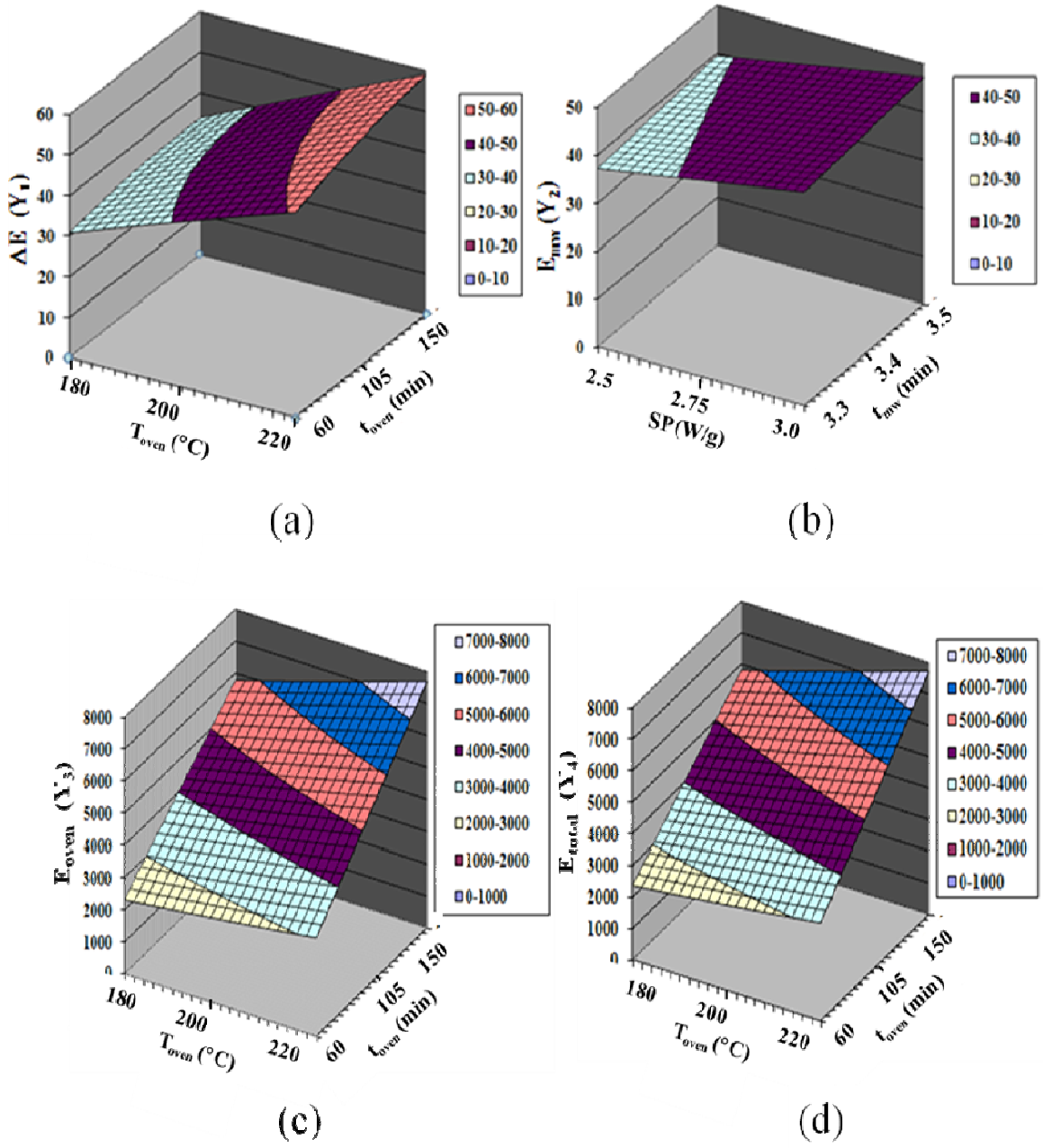

Figure 4.3 Response surface plot of (a) color (ΔE), (b) energy consumption by the microwave (E_{mw}), (c) energy consumption by the oven (E_{oven}), and (d) total energy consumption (E_{total}) as a function of specific microwave powers (SP), microwave heating times (t_{mw}), oven temperatures (T_{oven}) , and oven heating times (t_{oven}). The preheating step was carried out at 2.75 $W \cdot g^{-1}$ specific microwave power for 3.4 minutes.

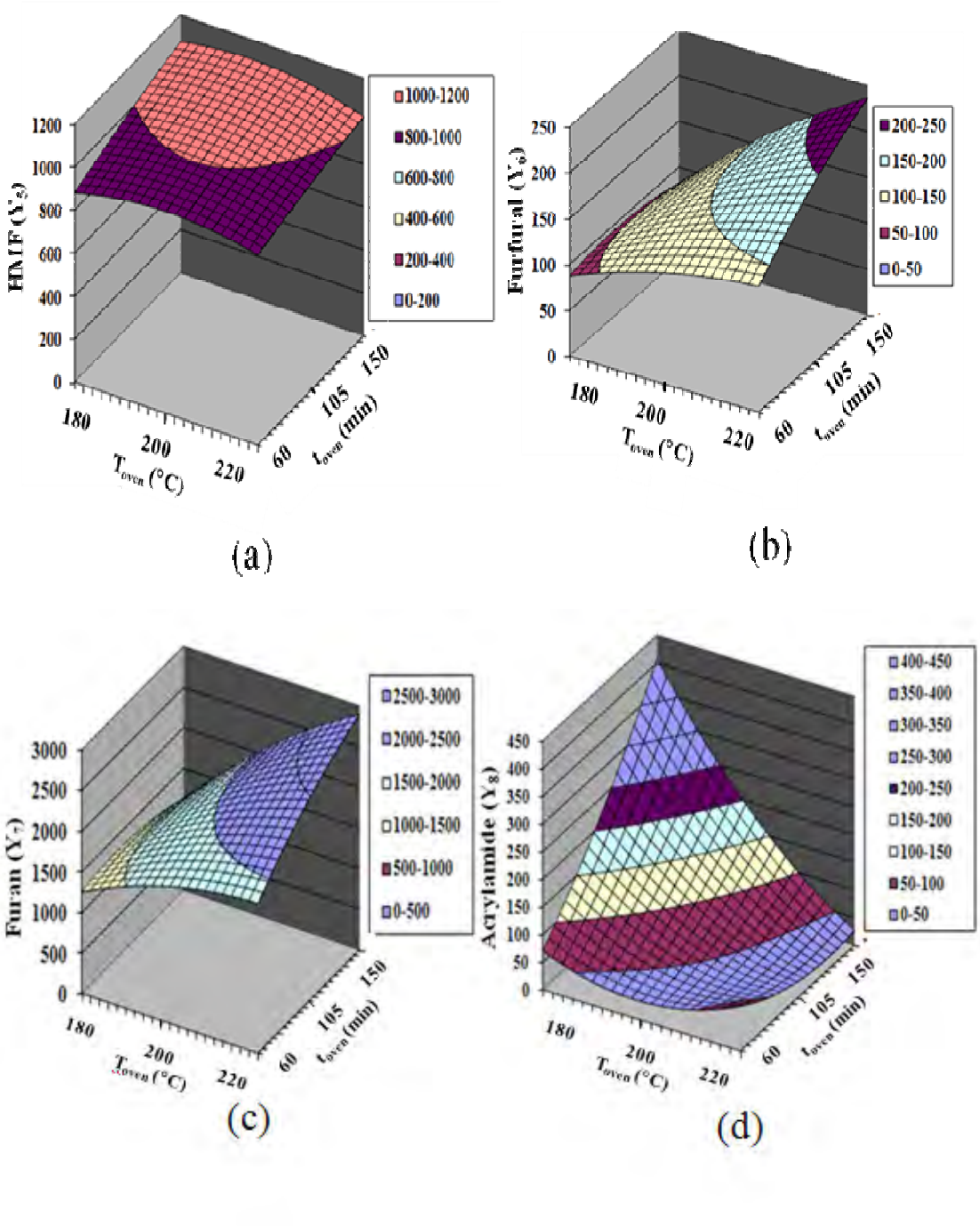

Figure 4.4 Response surface plot showing effect of oven temperature (T_{oven}) and oven heating times (t_{oven}) on the HMF (a), furfural (b), furan (c), and acrylamide (d) content. The preheating step was carried out at 2.75 $W \cdot g^{-1}$ specific microwave power for 3.4 minutes. The HMF, furfural, furan, and acrylamide content were determined by the fluorometric method.

HMF, furfural, furan, and acrylamide have been found to occur during the browning process of the Maillard reaction of reducing sugars with amino acids. Malts have high levels of the precursor reactant of the Maillard reaction, containing 8% to 11% protein and 58% to 60% starch (Hough *et al*., 1971) that can easily hydrolyze upon heating above 100 °C, resulting in the formation of monosaccharides (reducing sugar). During malt roasting process, high oven temperature and a long heating time cause the Maillard reaction as well as the dehydration of sugar which catalyses the reaction to occur. Therefore, the formation of HMF, furfural, and furan, tended to increase with increasing roasting temperatures and time. These results agreed with reports found elsewhere (Eichner and Wolf, 1983; Ulbricht *et al*., 1984; Zyzak *et al*., 2003; Taeymans *et al*., 2004; Eriksson, 2005; Crews and Castle, 2007). The reaction rate of the Maillard reaction is increased 4 fold by every 10 °C increment (Eskin, 1990). Amino acids serine and cysteine are major reactants for furan formation (Crews and Castle 2007) and amino acid asparagine is a major reactant of acrylamide formation (Taeymans *et al*., 2004). Figure 4.4d shows acrylamide formation as a function of oven temperature and heating time for a constant microwave specific power of 2.75 $W \cdot g^{-1}$ and a microwave heating time of 3.4 minutes. It can be seen from this figure that with a low oven temperature, 180 °C, acrylamide content increased dramatically with time. Conversely, with a high oven temperature, at 220 °C, acrylamide content seems to decrease with time. This may be due to the fact that when roasting malts is carried out near burning point (220 °C) of asparagine, asparagine degradation occurs and limits the acrylamide formation. In addition, a prolonged heating time leads to a partial degradation of acrylamide by reaction with other compounds or by polymerization (Capuano, *et al*. 2008) resulting

in a decrease in the acrylamide concentration. Regression and variance analysis result of ΔE, E_{mw}, E_{oven}, E_{total}, HMF, furfural, furan, and acrylamide content as shown in Appendix A., Tables A.2 to A.9. Tables 4.4 and 4.5 show the regression analysis for the eight responses (Y_1 to Y_8). As can be seen in Table 4.5, oven temperature and oven heating time (X_3 and X_4) are the most influencing factors on malt color (Y_1). The positive coefficients for X_3 and X_4 indicate that these factors have a positive effect on the response Y_1, that is, when the oven temperature (X_3) or the oven heating time (X_4) increases, the malt color is enhanced. The linear and interaction effect of specific microwave powers (X_1) and microwave heating times (X_2) significantly affected the energy consumption by the microwave (Y_2). The linear and interaction effect of X_4, and X_3, and the quadratic effect of X_3 significantly affected energy consumption by the oven (Y_3). The linear and interaction effects of X_4, X_3, the quadratic effect of X_3, and the linear effect of X_1 were the most influencing effects with regard to total energy consumption (Y_4). The total energy consumption was not affected by X_2. This was because the time utilized by the microwave (3 to 4 minutes) was much less than that of the hot-air oven (1 to 2.50 h). The positive coefficient of X_1, X_3 and X_4 indicated linear effects on the increase of Y_4.

Table 4.5 shows that only the linear effect of the oven temperature was the primary determining factor of the HMF, furfural, furan, and acrylamide content in malt (Y_5 to Y_8). No significant quadratic and interaction between independent variables for Y_6 to Y_8 was observed. From a statistical point of view, it was shown that, neither specific microwave power nor microwave heating time played a significant role in the alteration of malt color and NFCs formation. As displayed in Table 4.5 and 4.6, Y_1, and $Y_{5\text{-}flu}$ to $Y_{7\text{-}flu}$ models had an insignificant lack of fit test,

which means that Y_1, and $Y_{5\text{-}flu}$ to $Y_{7\text{-}flu}$ models represented the data satisfactorily. On the other hand, the $Y_{8\text{-}flu}$ model had a significant lack of fit, indicating that the model failed to predict the acrylamide formation as a function of X_1, X_2, X_3, and X_4. A lack of fit test for the Y_2, Y_3, and Y_4 models could not be tested because the value of pure error equaled zero. The R^2 values for color (0.99), $E_{microwave}$ (1.00), E_{oven} (1.00), E_{total} (1.00), HMF (0.72), furfural (0.85), and furan (0.86) were in an acceptable range while a lower R^2 values of 0.54 was found for acrylamide content. Low R^2 value indicated that the generated model is inadequate for prediction purposes. Therefore model Y_8 should not be used to predict acrylamide content. Adequate simplified models to predict process response are summarized in Table 4.7.

Table 4.5 Coefficient and analysis of variance of regression models in terms of specific microwave powers, microwave heating times, oven temperatures, and oven heating times for ΔE-value, E_{mw}, E_{oven}, and E_{total}.

Coded Factors	ΔE-value (Y_1)		E_{mw} (Y_2) (kJ)		E_{oven} (Y_3) (kJ)		E_{total} (Y_4) (kJ)	
	B	P-Value	*B*	P-Value	*B*	P-Value	*B*	P-Value
Const.	45.6000	0.0000*	42.0750	0.0000*	4685.9504	0.0000*	4728.0254	0.0000*
X_1	0.3567	0.1556	3.8250	0.0000*	0.0000	1.0000	3.8250	0.0236*
X_2	-0.0850	0.7252	1.2375	0.0000*	0.0000	1.0000	1.2375	0.4218
X_3	10.8892	0.0000*	0.0000	1.0000	674.5956	0.0000*	674.5956	0.0000*
X_4	2.7275	0.0000*	0.0000	1.0000	2012.0684	0.0000*	2012.0684	0.0000*
X_1X_2	-0.5475	0.2045	0.1125	0.0000*	0.0000	1.0000	0.1125	0.9659
X_1X_3	-0.8975	0.0474*	0.0000	1.0000	0.0000	1.0000	0.0000	1.0000
X_1X_4	-1.1850	0.0126*	0.0000	1.0000	0.0000	1.0000	0.0000	1.0000
X_2X_3	-0.2750	0.5140	0.0000	1.0000	0.0000	1.0000	0.0000	1.0000
X_2X_4	0.6775	0.1222	0.0000	1.0000	0.0000	1.0000	0.0000	1.0000
X_3X_4	1.4100	0.0044*	0.0000	1.0000	289.1124	0.0000*	289.1124	0.0000*
X_1X_1	-1.4346	0.0009*	0.0000	1.0000	0.0000	1.0000	0.0000	1.0000
X_2X_2	-1.3271	0.0016*	0.0000	1.0000	0.0000	1.0000	0.0000	1.0000
X_3X_3	-0.2933	0.3966	0.0000	1.0000	26.6274	0.0000*	26.6274	0.0000*
X_4X_4	-1.0908	0.0062*	0.0000	1.0000	0.0000	1.0000	0.0000	1.0000
Lack of fit		0.2678		**		**		**
R^2	0.9944		1.0000		1.0000		1.0000	
CV (%)	1.88		0		0.11		0.11	

X_1 = specific microwave powers (SP), X_2 = microwave heating times (t_{mw}), X_3 = oven temperatures (T_{oven}), and X_4 = oven heating times (t_{oven})

B = parametric coefficient of the model

* Significant at $p \leq 0.05$

** pure error = 0

Table 4.6 Coefficient and analysis of variance of regression models in terms of specific microwave powers, microwave heating times, oven temperatures, and oven heating times for HMF, furfural, furan and acrylamide.

Coded Factors	HMF ($Y_{5\text{-}flu}$) (mg·kg^{-1})		Furfural ($Y_{6\text{-}flu}$) (mg·kg^{-1})		Furan ($Y_{7\text{-}flu}$) (µg·kg^{-1})		Acrylamide ($Y_{8\text{-}flu}$) (µg·kg^{-1})	
	B	P-Value	*B*	P-Value	*B*	P-Value	*B*	P-Value
Const.	1124.5500	0.0000*	253.2308	0.0000*	3127.3833	0.0000*	28.2981	0.6147
X_1	-22.2681	0.2134	-17.3421	0.1025	-190.0517	0.1258	36.0537	0.2756
X_2	-15.3303	0.3841	1.8754	0.8523	26.0450	0.8261	10.8686	0.7370
X_3	53.2903	0.0080*	77.5502	0.0000*	951.0006	0.0000*	-90.0274	0.0139*
X_4	-12.2764	0.4834	8.2359	0.4192	110.1694	0.3603	16.3693	0.6140
X_1X_2	55.0742	0.0844	-15.2635	0.3883	-206.0633	0.3245	34.4598	0.5408
X_1X_3	5.0500	0.8666	-6.2253	0.7217	-84.3500	0.6819	15.9442	0.7759
X_1X_4	3.4283	0.9092	13.8300	0.4332	152.2583	0.4628	-16.7802	0.7646
X_2X_3	-28.6467	0.3489	12.5049	0.4776	168.3100	0.4180	-12.9705	0.8168
X_2X_4	-86.8200	0.0114*	16.1821	0.3612	225.1417	0.2835	-37.5507	0.5057
X_3X_4	-14.8042	0.6239	26.0960	0.1509	294.8250	0.1667	-97.6830	0.0984
X_1X_1	14.3954	0.5600	-13.2398	0.3603	-158.0111	0.3537	21.2471	0.6431
X_2X_2	-7.2237	0.7688	-24.5712	0.1019	-289.7161	0.1013	42.7031	0.3578
X_3X_3	-57.1146	0.0337*	-9.0183	0.5296	-138.8011	0.4135	42.2623	0.3627
X_4X_4	-9.3604	0.7036	-8.4821	0.5540	-114.6044	0.4978	24.7604	0.5898
Lack of fit		0.6402		0.1719		0.1604		0.0046*
R^2	0.7199		0.8510		0.8603		0.5439	
CV (%)	5.36		14.90		14.29		129.96	

X_1 = specific microwave powers (SP), X_2 = microwave heating times (t_{mw}), X_3 = oven temperatures (T_{oven}), and X_4 = oven heating times (t_{oven})

B = parametric coefficient of the model

* Significant at $p \leq 0.05$

Table 4.7 The fitted model equations in terms of specific microwave powers (X_1), microwave heating times (X_2), oven temperatures (X_3), and oven heating times (X_4) for ΔE-value (Y_1), E_{mw} (Y_2), E_{oven} (Y_3), and E_{total} (Y_4), HMF ($Y_{5\text{-}flu}$), furfural ($Y_{6\text{-}flu}$), furan ($Y_{7\text{-}flu}$) and acrylamide ($Y_{8\text{-}flu}$).

$Y_1 = 45.60 + 10.89X_3 + 2.73X_4 - 0.90X_1X_3 - 1.19X_1X_4 + 1.41X_3X_4 - 1.43X_1^2 - 1.33X_2^2 - 1.09X_4^2$, $R^2 = 0.99$
$Y_2 = 42.08 + 3.82X_1 + 1.24X_2 + 0.11X_1X_2$, $R^2 = 1.00$
$Y_3 = 4685.95 + 674.60X_3 + 2012.07X_4 + 289.11X_3X_4 + 26.63X_3^2$, $R^2 = 1.00$
$Y_4 = 4728.03 + 3.83\ X_1 + 674.60\ X_3 + 2012.07X_4 + 289.11X_3\ X_4 + 26.63\ X_3^2$, $R^2 = 1.00$
$Y_{5\text{-}flu} = 1124.55 - 53.29X_3 - 86.82X_2X_4 - 57.11X_3^2$, $R^2 = 0.72$
$Y_{6\text{-}flu} = 253.23 + 77.55X_3$, $R^2 = 0.85$
$Y_{7\text{-}flu} = 3127.38 + 951.00X_3$, $R^2 = 0.86$

4.4.3 The optimum conditions for producing coffee, chocolate and black malts by combined microwave-hot air roasting based on energy consumption and NFCs content

Tables 4.4 to 4.5 list the regression coefficients for the quadratic models used for predicting the 8 responses (Y_1 to Y_8) as a function of X_1, X_2, X_3, and X_4. The solver module in Microsoft Excel® software was employed to determine optimum conditions for the production of coffee, chocolate and black malt with the right color while minimizing NFCs formation and energy consumption. The optimum roasting parameters and predicted values for optimum conditions are shown in Table 4.8.

Table 4.8 The optimum roasting parameters in terms of specific microwave powers (X_1), microwave heating times (X_2), oven temperatures (X_3), oven heating times (X_4) and predicted values of ΔE, HMF, furfural, furan and E_{tot} for the production of coffee, chocolate and black malt.

Colored Malt	Control parameters				Responses				
	SP ($W \cdot g^{-1}$)	t_{mw} (min)	T_{oven} (°C)	t_{oven} (min)	Color (ΔE)	HMF ($mg \cdot kg^{-1}$)	Furfural ($mg \cdot kg^{-1}$)	Furan ($\mu g \cdot kg^{-1}$)	E_{tot} (kJ)
Coffee	2.68	3.44	206	136	50.41	1083	288	3512	6367
chocolate	2.50	3.48	214	136	54.37	1028	328	3897	6732
black	2.50	3.48	211	150	59.70	993	315	3748	7255

4.4.4 Comparison of the optimum results from fluorometric method and physico-chemical method

Table 4.9 shows HMF, furfural, and acrylamide content obtained from the fluorometric and physico-chemical method. Furan could not be measured by physico-chemical method because of a limited quantity of the samples. The physico-chemical method provided higher HMF, furfural, and acrylamide content than fluorometric method. This might be due to the non-uniformity in size and insufficiency in size reduction which affected the optical properties of the sample that, in turn, affected the result from the fluorometric method. Therefore, grinding step was important for obtained a good result. The differences in values were quite consistent for all samples. Therefore, the correlation of NFCs content obtained from the fluorometric and the physico-chemical methods could be calculated. The % difference of HMF, furfural, and acrylamide content between the fluorometric method and the

physico-chemical method averaged over all 28 treatment conditions was 36%, 31%, and 89%, respectively.

Table 4.9 HMF, furfural, and acrylamide content of malt produced at various treatment conditions according to the Box-Behnken method. The values were obtained from the fluorometric and the physico-chemical method.

Treat-ment no.	HMF[1] ($mg \cdot kg^{-1}$)	HMF[2] ($mg \cdot kg^{-1}$)	Furfural[1] ($mg \cdot kg^{-1}$)	Furfural[2] ($mg \cdot kg^{-1}$)	Acry[1] ($\mu g \cdot kg^{-1}$)	Acry[2] ($\mu g \cdot kg^{-1}$)	D^*_{HMF} (%)	D^*_{fur} (%)	D^*_{acr} (%)
1	1283.20	1996.0	225.86	419.5	80.99	887	36	46	91
2	1089.90	1821.3	174.10	1412.50	230.59	1009	40	88	77
3	1093.34	1880.8	254.51	377.9	20.68	1006	42	33	98
4	1120.33	2384.9	141.69	395.1	308.12	1214	53	64	75
5	1029.73	1939.8	159.36	215.1	128.70	739	47	26	83
6	1181.77	2025.5	172.94	226.9	133.16	718	42	24	81
7	1186.27	1676.8	192.85	202.1	73.21	728	29	5	90
8	1098.27	2028.3	144.65	228.1	169.61	740	46	37	77
9	1048.41	800.1	277.45	299.5	18.11	287	31	7	94
10	968.39	1014.3	306.49	372.2	7.56	240	5	18	97
11	993.009	1241.3	301.50	376.9	11.39	313	20	20	96
12	1002.36	885.3	312.75	335.2	7.14	490	13	7	99
13	1080.31	1868.7	158.57	164.2	123.001	645	42	3	81
14	1060.90	1973.1	227.12	297.2	32.65	1090	46	24	97
15	1176.26	696.1	245.77	307.2	29.82	1039	69	20	97
16	1104.34	1962.9	188.88	308.8	89.24	846	44	39	89
17	1211.03	2105.0	197.60	295.6	149.39	797	42	33	81
18	1032.07	1392.4	307.48	391.6	8.44	935	26	21	99
19	1143.63	1922.0	79.03	219.1	513.26	704	40	64	27
20	1179.63	1537.7	235.34	404.1	46.28	950	23	42	95
21	1116.93	1302.8	254.30	376.2	28.19	1130	14	32	98
22	1058.73	1593.1	252.72	409.7	20.49	885	34	38	98
23	982.49	1439.8	270.54	392.9	12.81	1247	32	31	99
24	1036.17	694.2	332.32	289.4	7.96	150	49	15	95
25	1063.83	1628.2	259.16	352.3	19.18	1150	35	26	98
26	1108.57	1709.0	268.87	346.5	17.44	1260	35	22	99
27	1213.20	1737.6	223.41	349.3	55.81	1238	30	36	95
28	1112.60	1927.9	261.48	372.7	20.76	1169	37	30	98
						Avg.	**36**	**31**	**89**

[1]HMF, furfural, and acrylamide have been quantified by the fluorometric method
[2]HMF, furfural, and acrylamide have been quantified by the physico-chemical method

$$^{*}D = \frac{\left| Y_{fluorometric\ method} - Y_{physico-chemical\ method} \right|}{Y_{physico-chemical\ method}} \times 100$$

HMF, furfural, and acrylamide were quantified by HPLC, HPLC, and HPLC-MS-MS (the physico-chemical method), respectively. The results were used to optimize the conditions for producing coffee, chocolate, and black malt and the obtained optimal conditions were compared with the results obtained from the fluorometric method, as discussed in section 4.4.3. Regression and variance analysis results of HMF, furfural, and acrylamide contents, determined by using the regression module of Microsoft Excel® software are shown in Appendix A, Tables A.10-A.12. Table 4.10 lists the regression coefficients for the quadratic models used for predicting 8 responses (Y_1 to Y_8) as a function of specific microwave powers (X_1), microwave heating times (X_2), oven temperatures (X_3), and oven heating times (X_4). It can be seen in Table 4.10 that oven temperature (X_3) was the most influencing effect with regard to HMF and acrylamide content. This result agrees with a previous study as mentioned in section 4.4.2. To find the optimal settings by using the solver module of Microsoft Excel® software allowing minimization of NFCs formation and energy consumption for production coffee, chocolate, and black malt. The optimal conditions based on the NFCs results obtained by the physico-chemical method and those obtained by the fluorometric methods are shown in Table 4.11. The optimum parameters; SP, t_{mw}, $T_{hot\ air}$, and $t_{hot\ air}$ which were based on the NFCs results obtained by the fluorometric method were close to the optimum conditions which were based on the NFCs results obtained by the physico-chemical method for producing chocolate, coffee and black malt with the exception of the optimum parameters; $T_{hot\ air}$, and $t_{hot\ air}$ for producing coffee and black malt. The difference may be a missing value of furan which was quantified by the physico-chemical method. The NFCs content obtained from both methods were likely to change in the same trend. Therefore, the

optimal conditions obtained based on the NFCs content determined by the two methods are similar. Since the fluorometric method is a fast and cost effective way, pollution free, nondestructive and does not need any extraction steps (Rizkallah *et al*., 2008), it can potentially be more beneficial in the quantification of NFCs content.

Table 4.10 Coefficient and analysis of variance of regression models in terms of specific microwave powers, microwave heating times, oven temperatures, and oven heating times for HMF, furfural, and acrylamide.

Coded Factors	HMF ($Y_{5\text{-}phy}$) (mg·kg^{-1})		Furfural ($Y_{6\text{-}phy}$) (mg·kg^{-1})		Acrylamide ($Y_{8\text{-}phy}$) (µg·kg^{-1})	
	B	P-Value	*B*	P-Value	*B*	P-Value
Constant	1750.6760	0.0000*	355.1794	0.0028*	1204.2500	0.0000*
X_1	147.0697	0.1256	85.4240	0.1490	-2.0833	0.9640
X_2	54.6802	0.5533	-85.2514	0.1497	44.3333	0.3450
X_3	-452.7993	0.0002*	67.4310	0.2474	-154.9167	0.0045*
X_4	-125.6978	0.1852	27.2341	0.6329	-23.8333	0.6072
X_1X_2	169.7056	0.2953	-243.9414	0.0252*	21.5000	0.7881
X_1X_3	143.9370	0.3719	7.3587	0.9403	15.7500	0.8438
X_1X_4	-244.1388	0.1407	7.9769	0.9353	-13.0000	0.8708
X_2X_3	-0.8365	0.9958	5.6901	0.9538	50.5000	0.5305
X_2X_4	-57.4775	0.7178	-2.4059	0.9805	147.5000	0.0824
X_3X_4	-187.8528	0.2489	-39.2614	0.6906	-211.0000	0.0185*
X_1X_1	-16.7933	0.8969	107.3228	0.1960	-133.1250	0.0578
X_2X_2	132.7585	0.3152	93.3045	0.2573	-78.0000	0.2445
X_3X_3	-280.1843	0.0461*	-125.7582	0.1343	-548.8750	0.0000*
X_4X_4	-155.2863	0.2434	-58.8066	0.4685	-82.7500	0.2184
R^2	0.7768		0.86229		0.8843	
CV (%)	28.33		60.19		37.93	

X_1 = specific microwave powers (SP), X_2 = microwave heating times (t_{mw}),

X_3 = oven temperatures (T_{oven}), and X_4 = oven heating times (t_{oven})

B = parametric coefficient of the model

* Significant at $p \leq 0.05$

Table 4.11 The optimal conditions for producing coffee, chocolate, and black malt based on results obtained from the physico-chemical method and the fluorometric method.

	Coffee malt		Chocolate malt		Black malt	
	physico-chemical method	Fluorometric method	physico-chemical method	Fluorometric method	physico-chemical method	Fluorometric method
SP ($W \cdot g^{-1}$)	2.50	2.68	2.84	2.50	3.00	2.50
t_{mw} (min)	3.46	3.44	3.30	3.48	3.30	3.48
$T_{hot\ air}$ (°C)	214	206	216	214	220	211
$t_{hot\ air}$ (min)	60	136	150	136	110	150

4.4.5 Model validation

In order to check the validity of the proposed quadratic models given in Table 4.7, the calculated data are compared with the experimental results for the same operating condition.

A validation experiment could not be performed at the optimum condition because the hot air temperature could only be adjusted in increments of 5 °C, therefore experiments were carried out using the following two conditions:

- Condition 1: SP = 2.68 $W \cdot g^{-1}$ for 3.44 min, T_{oven} = 205 °C for 136 min for coffee malt production.
- Condition 2: SP = 2.50 $W \cdot g^{-1}$ for 3.48 min, T_{oven} = 215 °C for 136 min for chocolate malt production.

Each experimental condition was conducted in duplicate. Table 4.12 shows the comparison between measured ΔE, E_{mw}, E_{oven}, E_{total}, HMF and furfural contents and predicted ΔE, E_{mw}, E_{oven}, E_{total}, HMF and furfural contents by quadratic

equations shown in Table 4.7. The prediction of ΔE, E_{mw}, E_{oven}, E_{total}, HMF and furfural were comparable to the actual values obtained from the experiment. Acceptable difference (%D) values of less than 20%, except in condition 1 for HMF (-29.75%) and furfural (-36.68%), were obtained. The low %D values for the other response models particularly ΔE indicated the adequacy of the predictive models. The predicted ΔE, E_{mw}, E_{oven}, E_{total}, HMF and furfural contents show a good agreement with the experimental data.

Table 4.12 Predicted and observed responses for ΔE, E_{mw}, E_{oven}, E_{total}, content of HMF and furfural of coffee and chocolate malts produced using two roasting conditions

Responses	condition1*			condition2**		
	Predicted	Measured	*D* (%)	Predicted	Measured	*D* (%)
ΔE	49.87	48.16 ± 0.93	4.99	55.19	50.71 ± 0.09	8.83
E_{mw} (kJ)	41.51	41.49	0.05	39.09	39.15	-0.15
E_{oven} (kJ)	6292.38	6136.24	2.504	6756.86	6618.95	2.08
E_{total} (kJ)	6333.89	6177.73	2.503	6795.95	6658.10	2.07
HMF - physico-chemical method (mg/kg)	1082.62	1541.10 ± 47.50	-29.75	1007.12	835.10 ± 55.65	20.60
Furfural – physico-chemical method (mg·kg^{-1})	272.62	430.51 ± 61.96	-36.68	311.39	344.44 ± 2.75	-9.60

$$^{*}D = \frac{\left|Y_{\mathrm{mod}\,el} - Y_{mesure}\right|}{Y_{measure}} \times 100$$

*condition 1: SP = 2.68 W·g^{-1} for 3.44 min, T_{oven} = 205 °C for 136 min.

**condition 2: SP = 2.50 W·g^{-1} for 3.48 min, T_{oven} = 215 °C for 136 min

4.4.6 NFCs content and energy consumption during roasting malt by hot air and combined microwave-hot air

Table 4.13 shows the total energy consumption (kJ) for the conventional and combined processes. In comparison with conventional processes (oven temperature 180 °C, heating time 2.5, 3.5 and 5 hours for coffee, chocolate and black malts, respectively), combined microwave-hot air reduced energy consumption by approximately 40, 26, and 26%, respectively.

Table 4.13 Total energy consumption (kJ) for conventional and combined microwave-hot air process.

Colored malt	Roasting process		% energy reduction
	hot air-only	combined microwave-hot air	
coffee malt	5204.82	3122.89	40
chocolate malt	7286.75	5425.42	26
black malt	10409.64	7738.04	26

Table 4.14 shows HMF, furfural, furan, and acrylamide content of black malt from conventional and combined process. It was found that HMF, furfural, furan and acrylamide levels in black malts processed by the combined process were 40%, 18%, 23% and 95% lower than by the conventional process. The reduction was a consequence of reduced roasting time because of the microwave pre-heating step.

Table 4.14 HMF, furfural, furan, and acrylamide content of black malt from conventional and combined process.

	Roasting process		
NFCs	Hot air-only	combined microwave-hot air	%NFCs reduction
HMF ($mg \cdot kg^{-1}$)	1717.66	1036.17	40
Furfural ($mg \cdot kg^{-1}$)	403.74	332.32	18
Furan ($\mu g \cdot kg^{-1}$)	5248.08	4029.77	23
Acrylamide ($\mu g \cdot kg^{-1}$)	153.53	7.96	95

4.5 CONCLUSIONS

Combined microwave-hot air was proven in this research study to be an effective method for the production of coffee, chocolate and black malt with reduced energy consumption (26% to 40% reduction) and the NFCs content of malt (18%-95% reduction) when compared with conventional roasting processes. The reduction was a consequence of reduced total roasting time due mainly to the microwave pre-treating step. Such combined roasting processes could potentially be applied to products such as roasted coffee which is usually processed at high temperature for an extended period, in order to reduce energy consumption and NFCs formation. The prediction of color, E_{mw}, E_{oven}, E_{total}, HMF and furfural contents by the proposed quadratic model, showed a close agreement to the experimental data.

CHAPTER V

SIMULATION OF THE TEMPERATURE DISTRIBUTION IN MALT DURING THE MICROWAVE HEATING

5.1 INTRODUCTION

Microwaves can directly generate heat inside dielectric matters. This heating is related to the absorption of the electromagnetic wave by the molecules constitutive of the matter. Microwaves are thus used at the industrial level for drying, cooking, pasteurization, defrosting, etc. The originality of microwave heating compared to the conventional one is the way in which energy is transmitted to the product. Whereas in a traditional heating, heat is absorbed from the product surface and it diffuses toward the center. In microwave heating, energy is absorbed and heat is produced inside the product, without requiring any medium as a vehicle for heat transfer. A low thermal conductivity product may quickly reach high temperature and this does not occur in conventional heating (Campanone and Zaritzky, 2004). The main advantage of microwave heating is a greater homogeneity in the distribution of heat inside the product. Nevertheless, it can exist in some cases a heterogeneity of treatment, due either to the product itself, or to a bad field distribution inside the microwave cavity. Thus, one can observe phenomena of overheating. It is essential to control the conditions of microwave energy supplying in order to avoid overheating zones during microwave heating of thermo-sensitive products.

Mathematical modeling can play an important role in the design and optimization of the product and process parameters during microwave heating. Mathematical modeling is a fast and effective design tool. Moreover, the method can minimize laborious and time consuming work. Modeling of microwave heating of

foods allows better insight into the process as parameters such as electric field and temperature distribution are particularly hard to measure. An understanding of the fundamental mechanisms and knowledge of the temperature distribution within the product is crucial for process design, quality control, product handling and energy saving.

Objectives

The objectives of this study were to simulate energy transfer in a malt bed subjected to microwave heating process and to study the effect of microwave power and weight of malt bed on energy distribution inside a malt bed.

5.2 LITERATURE REVIEW

5.2.1 Mathematical modeling

Modeling represents a phenomenon using set of mathematical equations. The solutions to these equations are supposed to simulate the natural behavior of the material. Modeling of microwave heating process involves two parts; one being the modeling of heat and mass transfer in the food by means of conduction heat transfer inside a malt bed and another being the modeling of electromagnetic field generated inside the microwave oven that leads to heat generation term. The heat generation term in the heat balance equation can be modeled following the Lambert's law or the Maxwell's equations.

5.2.1.1 Mass transfer

Prediction of mass distribution in the food exposed to microwave is done by solving the mass balance equation illustrated in equation 5.1.

$$\frac{\partial M}{\partial t} = \nabla \cdot (D \nabla M) \qquad (5.1)$$

5.2.1.2 Heat transfer

Prediction of temperature distribution in the food exposed to microwave is done by solving the energy balance equation (equation 5.2) with an assumption that heat is transported only by conduction inside the malt bed.

$$\rho c_p \frac{\partial T}{\partial t} = \nabla \cdot (k \nabla T) + Q_{av} \qquad (5.2)$$

The heat generation term (Q_{av}) can be evaluated from solving Lambert's law or Maxwell's equations.

At the surface of food, since the food surface losses temperature to the surrounding by convection, heat loss is modeled by specifying the convective heat transfer following equation 5.3.

$$k \nabla T \cdot n = -h(T_a - T_s) \qquad (5.3)$$

5.2.1.2.1 Lambert's law

To simplify the calculation of power absorption in a microwave field, absorbed power can be calculated by a simple expression assuming that the power decays in the food exponentially. Lambert's law assumes that (1) microwaves are incident perpendicular to the sample surface, (2) every microwave

beam passes through the central axis, and (3) internal reflections are neglected. One-dimensional analysis is considered, the power dissipated at a certain sample depth is given by the exponential decay of the incident power (P_0) along z direction (equation 5.4). Equations 5.5 and 5.6 illustrate attenuation factor (α) and penetration depth (d_p) of microwaves inside a sample.

$$P = P_0 \exp(-2\alpha z) \qquad (5.4)$$

$$\alpha = \frac{1}{2d_p} \qquad (5.5)$$

$$d_p = \frac{\lambda_0}{2\pi\sqrt{2\varepsilon'}\sqrt{\sqrt{1+\left(\frac{\varepsilon''}{\varepsilon'}\right)^2}-1}} \qquad (5.6)$$

Q_{av} in the energy balance equation (equation 5.2) can be expressed in a three-dimensional equation (equation 5.7).

$$Q_{av} = \frac{\partial P_X}{\partial V} + \frac{\partial P_Y}{\partial V} + \frac{\partial P_Z}{\partial V} \qquad (5.7)$$

5.2.1.2 Maxwell's equations

Maxwell's equations calculate the exact microwave electric field configuration within the food by mapping out the electric and magnetic field inside the microwave oven with the knowledge of microwave oven cavity configuration and dielectric properties of the food. Maxwell's equations are solved to determine the absorbed microwave power. The accuracy of Maxwell's equations depends on the knowledge of dielectric properties. Unfortunately, an analytical or exact solution of Maxwell's equations is extremely difficult to solve. Thus, to make

analytical calculations of field configurations and heating patterns, one must make simplifying assumptions that may greatly compromise the usefulness of the results obtained (Buffler, 1993; Rao,1994).

The alternative is to use sophisticated mathematical procedures, known as modeling. This technique breaks down the cavity and food geometries into small regions or cells. Maxwell's equations can be approximated and solved for each cell. The individual cell solutions are combined to form a final solution for the electric field within the entire configuration. The electric field defines the deposition of energy within the sample according to equation 5.2. If the thermal properties and the external cooling conditions of the product are known, the power deposited can be used to determine the temperature rise pattern in the sample. This calculation is done by using heat transfer equations that have also been broken up into the same cells used for Maxwell's equations.

5.2.2 Method of problem solving with mathematical modeling

5.2.2.1 Pre-processing

Pre-processing consists of characteristics of the microwave oven, waveguide, and the product. The pre-processing stages involve:

- Defining the geometry of the region of the computational domain such as the microwave oven cavity and food product configuration.
- Generating the sub-division of the domain into a number of smaller and non-overlapping sub-domains which is called a grid (or mesh) of cells (or elements). The cell size is sufficiently small, usually less than one sixth of the wavelength within the region of interest.
- Selecting the physical and chemical phenomena that need to be modeled.

- Defining food properties such as physical, thermal, and dielectric properties.

- Specifying boundary and initial conditions at cells which coincide with the domain boundary.

The solution to mass and heat transfer problem is defined at nodes inside each cell. The accuracy of solution is governed by the number of cells in the grid. In general, the larger the number of cells the better the solution accuracy. Both the accuracy of a solution and its cost in terms of necessary computer hardware and calculation time are dependent on the fineness of the grid. Optimal meshes are often non-uniform. That is, meshes are finer in areas where large variations occur from point to point and coarser in regions with relatively little change. At present it is still up to the skills of user to design grid that is a suitable compromise between desired accuracy and solution cost (Versteeg and Malalasekera, 1995).

5.2.2.2 Solving

There are two distinct streams of numerical solution techniques, which are finite difference and finite element (Versteeg and Malalasekera, 1995). In outline the numerical methods that form the basis of the solver perform the following steps:

- Approximation of the unknown flow variables by means of simple functions.

- Discretisation by substitution of the approximations into the governing flow equations and subsequent mathematical manipulations.

- Solution of the algebraic equations.

The main differences between two streams are associated with the way which mass and heat variables are approximated and with the discretisation processes.

5.2.2.2.1 Finite Difference Method

In Finite Difference Method (FDM), the region to be studied is divided into cells, usually cubic. Each cell is assigned the value of the complex dielectric constant at its location. The mathematics is easier if a food with uniform complex dielectric constant is assumed. Maxwell's equations are approximated by assuming that there is a linear relationship between the fields on each side of the cell. The incident wave is followed as it propagates into the sample, and new electric fields are calculated along the way. By this means, the electric field build up can be observed (transient state). The advantage of the FDM approach is the simplicity of mathematics required to describe the mesh of cells. For this reason it is the most frequently used technique for microwave modeling. The disadvantage of the technique is the long computer processing time required, because all space must be broken up into cells of regular shape (Buffler, 1993).

5.2.2.2.2 Finite Element Method

Finite Element Method (FEM) is equivalent in principle, to the cells of the FDM, but can be any configuration that best conforms to the geometry to be modeled. FEM allows different-sized elements to be used for different regions. For example, large elements might be used in the cavity where the wavelength is long. Small elements can be used inside the food where the wavelength is short and better pattern resolution is desired. A major advantage to FEM is that the power deposition solution can be performed first and then transferred to a separate computer program where the temperature distribution can be calculated. A major

difficulty of the technique is the difficulty of treating the boundary between air and food. Skill and experience are needed to obtained valid solutions in this boundary region (Buffler, 1993).

5.2.2.3 Post-processing

Result validation can be carried out by comparing temperature data obtained from solving the mathematical model with the experimental data or with high quality data from closely related problems reported in the literature (Versteeg and Malalasekera, 1995).

5.2.3 Relevant research on modeling of microwave heating processes

There have been relevant researches on modeling of microwave heating process in food. Researchers have explored different methods to measure temperature distribution during microwave heating.

Lin *et al.* (1995) simulated microwave heating of solid foods using two-dimensional commercial finite element software (TWODEPEP). The model was experimentally validated by using sodium alginate gel as the test material. Microwave oven was operated at 2450 MHz and the line voltage was 115 V. The temperature predictions by finite element analysis and the experimental measurements were very similar in both of slab-shaped and cylindrical-shape samples. The asymmetrical temperature distribution observed during experimental measurements was not effectively predicted by the model due to incomplete description of the microwave power distribution around the sample. To obtain a more accurate result, it might be necessary to take into account more complicated sample geometries and complex electromagnetic distribution field inside the oven into a three-dimensional finite element model.

Zhou *et al.* (1995) developed a three-dimensional finite element model (FEM) to predict the temperature and moisture distribution in food during microwave heating. The power absorption in a microwave field was obtained by solving the Lambert's law. The FEM was verified using experimental data from microwave oven heated slab- and cylindrical-shaped potato specimens. The absolute temperature differences between FEM predictions and measured values in potatoes with slab geometry and cylindrical geometry were within 8.1 and 8.7 ^{o}C, respectively. The absolute moisture differences between FEM predictions and measured values were 1.97% (wet basis) for slab geometry and 1.85% (wet basis) for cylindrical geometry.

Oliveira and Franca (2002) developed two-dimensional finite element model that incorporated the effect of sample rotation to simulate power distributions for cylindrical shaped mashed potato during microwave heating. The sample was irradiated at 2800 MHz for 1 minute, with sample rotating at 1 rpm. Oliveira and Franca compared the power distribution calculated by Maxwell's equations and Lambert's law. The result showed that Lambert's law could be used to simulate the power distribution for semi-infinite slabs and semi-infinite cylinders with a thickness more than 2.7 and 7.0 times their penetration depth, respectively. But the law failed for thinner samples. The researchers concluded that Maxwell's equations could be used for a more accurate prediction of the actual power distribution.

Campanone and Zaritzky (2005) developed a three-dimensional model using an implicit finite difference method involving the effect of sample rotation during microwave heating of an agar gel cylinder. The heating was conducted in a 1000 W 2450 MHz microwave oven, with a rotating turn table at a rate of one cycle every 12 seconds. The result on the temperature predicted by Campanone and

Zaritzky matched well with the predicted result reported by Zhou *et al.* (1995) who employed a finite element model in solving a similar problem.

Geedipalli *et al*. (2007) studied the role of a carousel in improving uniformity of food in a microwave oven. The model was solved numerically using a three-dimensional finite element based computational software. The model was experimentally validated. The results showed that the carousel helps in increasing the temperature uniformity of the food by about 40%.

From previous works as mention above the process of microwave heating has been mathematically modeled by the FEM. FEM is more versatile and has several advantages. FEM can handle irregular geometrical configurations, suited to non-linear problems, element size can easily be varied. The accuracy of FEM depends on several factors, such as, the type of approximation function used in each element, the number and shape of elements, and the time step used. The sizes of the elements must be chosen to be a small fraction of the minimum wavelength in the material (Lin *et al*., 1995).

5.3 MATERIALS AND METHODS

The calculation of temperature distribution during heating in a microwave oven consisted of 2 steps. Firstly, the distribution of electromagnetic field within the malt bed was calculated by using finite element method. The electromagnetic field distribution and boundary condition inside the microwave cavity and a malt bed is governed by Maxwell's equations, and Lambert's law, respectively, as shown in 5.3.4.1. Then, the results were converted to heat generation which was used in the second step. The second step calculated the temperature distribution within the malt bed using finite element method. The temperature distribution was

solved from the heat transfer equation, boundary condition, and initial condition as shown in 5.3.1-5.3.3.

5.3.1 The heat transfer equation

Heat transfer inside the malt bed was governed by the heat transfer equation as shown in equation 5.2

$$\rho c_p \frac{\partial T}{\partial t} = \nabla \cdot (k \nabla T) + Q_{av} \qquad (5.2)$$

5.3.2 Boundary condition

Since the food surface losses heat to the surrounding, convection heat transfer has to be included in the boundary condition as shown in equation 5.8. Convective heat transfer coefficient (h) for natural convection was set at 10 $W \cdot m^2 \cdot K^{-1}$.

$$k \nabla T \cdot n = -h(T_a - T_s) \qquad (5.8)$$

5.3.3 Initial condition

The malt bed to be simulated was set at a constant initial temperature of 21 °C. Equation 5.9 was used to specify the initial values for heat transfer calculation.

$$T = T_0 (x,y,z) \qquad (5.9)$$

5.3.4 Heat generation

5.3.4.1 Electromagnetic field distribution

The electromagnetic field distribution inside the microwave cavity is governed by Maxwell's equations

$$\nabla \cdot \mathbf{D} = 0 \qquad (5.10)$$

$$\nabla \cdot \mathbf{B} = \mathbf{0} \tag{5.11}$$

$$\nabla \times \mathbf{H} = \mathbf{J} + \frac{\partial \mathbf{D}}{\partial t} \tag{5.12}$$

$$\nabla \times \mathbf{E} = -\frac{\partial \mathbf{B}}{\partial t} \tag{5.13}$$

$$\mathbf{D} = \varepsilon \mathbf{E} \tag{5.14}$$

$$\mathbf{B} = \mu \mathbf{H} \tag{5.15}$$

$$\mathbf{J} = \sigma \mathbf{E} \tag{5.16}$$

Power absorbed per unit volume (Q_{av}) by the malt bed is given by equation 5.17.

$$\boldsymbol{Q}_{av} = \frac{1}{2}\omega \varepsilon_0 \varepsilon'' |\mathbf{E}|^2 \tag{5.17}$$

5.3.4.2 Boundary conditions

At all boundaries except at the symmetrical planes, the perfect electric conductor boundary condition (equation 5.18) was assumed.

$$n \times \boldsymbol{E} = 0 \tag{5.18}$$

At the symmetrical planes, the perfect magnetic conductor boundary condition (equation 5.19) was assumed.

$$n \times \boldsymbol{H} = 0 \tag{5.19}$$

The attenuation of incident power within the malt bed in a beaker is based on Lambert's law (equation 5.3). The exact form of the microwave power source term at any location in cylindrical co-ordinates is obtained by the shell balance method (Lin *et al*., 1995; Pandit and Prasad, 2003), which uses the principle of conservation of energy, where incoming and outgoing microwave energy is considered over a shell to find the microwave energy absorbed. Microwave energy absorption model for malt bed is given in equation 5.20.

$$Q_{av} = \frac{2\alpha R P_c^{''}}{r}\left[e^{-2\alpha(R-r)} + e^{-2\alpha(R+r)}\right] + 2\alpha P_c^{''}\left[e^{-2\alpha(L/2-z)} + e^{-2\alpha(L/2+z)}\right] \qquad (5.20)$$

5.3.5 Determination of physical and thermal properties of malt bed

To simplify the mathematical model of microwave heating, a beaker of malt was considered as a lump of porous matrix (malt bed). The physical, thermal and dielectric properties of malt bed are important parameters in the calculation of electromagnetic field distribution and temperature distribution inside the microwave cavity and malt bed. Bulk density and true density of malt bed were measured for calculation of the porosity. Thermal conductivity, specific heat, dielectric constant and dielectric loss of malt bed were calculated by using the porosity-value, measured moisture content of malts, and measured thermal conductivity and specific heat of ground malt as shown in equations 5.22-5.27.

5.3.5.1 Bulk density

Bulk density (ρ_b) is the ratio of the mass sample of malt to its total volume. It is determine by filling a 500 ml container with malts from a height of

about 15 cm, striking the top level and then weighing the contents (Coskuner and Karababa, 2006; Jha, 1998, and Shafiur, 1995).

5.3.5.2 True density

True density (ρ_t), as a function of water content, was determine using the toluene displacement method in order to avoid absorption of water during experiment. Malts were used to displace toluene in a measuring cylinder after their masses were measured. The true density is found as an average of the ratio of their masses to the volume of toluene displaced by malts (Coskuner and Karababa, 2006; Jha, 1998, and Shafiur, 1995).

5.3.5.3 Porosity

The porosity is the fraction of the space in the bulk malts which is not occupied by the malts. The porosity of malts were calculated from the values of true density and bulk density using the relationship as shown in equation 5.21.

$$\varepsilon = (\rho_t - \rho_b) \times 100 / \rho_t \qquad (5.21)$$

5.3.5.4 Thermal conductivity and specific heat

Thermal conductivity (k) and specific heat (C_p) of malt bed were determined using equations 5.22 and 5.23 (Rao, *et al*., 2005). The thermal conductivity and specific heat of ground malt were determined by the guarded hot plated method (CT meter, SA TELEPH, Meylan, France) as depicted in Figure 5.1.

$$k_{malt\ bed} = k_c(2k_c + k_d - 2\varepsilon_d(k_c - k_d))/(2k_c + k_d + \varepsilon_d(k_c - k_d)) \qquad (5.22)$$

Where, k_c is the thermal conductivity of the continuous phase which is the thermal conductivity of air (0.0314 $W \cdot m^{-1} \cdot K^{-1}$); k_d is the thermal conductivity of the disperse phase which is the thermal conductivity of malt (0.222 $W \cdot m^{-1} \cdot K^{-1}$); ε_d is the porosity of malt bed (34.56%).

$$C_{p,malt\ bed} = C_c(2C_c + C_d - 2\varepsilon_d(C_c - C_d))/(2C_c + C_d + \varepsilon_d(C_c - C_d)) \quad (5.23)$$

Where, c_c is the specific heat of air= 1009 $J \cdot kg^{-1} \cdot K^{-1}$; c_d is the specific heat of malt (969.26 $J \cdot kg^{-1} \cdot K^{-1}$); ε_d is the porosity of malt bed (34.56%).

Figure 5.1 Computer connected CT meter (SA TELEPH, Meylan, France) for measurement of thermal conductivity and specific heat of ground malt.

5.3.6 Dielectric properties of malt bed

5.3.6.1 Dielectric constant and dielectric loss

Nelson (1991) proposed equations 5.24 and 5.25 for calculating dielectric constant and dielectric loss of cereal grains, over the frequency range from 5 MHz to 5 GHz and 8 to 26% moisture range. The average initial moisture content of the malt was 9.15% in wet basis.

$$\varepsilon' = \left[1 + \frac{0.504 M \rho}{\sqrt{M} + \log f}\right]^2 \qquad (5.24)$$

$$\varepsilon'' = 0.146\rho^2 + 0.004615 M^2 \rho^2 \left[0.32 \log f + \frac{1.743}{\log f} - 1\right] \qquad (5.25)$$

Where, M is moisture content in % wet basis; ρ is bulk density in g·cm^{-3}; f is frequency in MHz.

Because malt bed in beaker is a porous matrix, the mixture equation was considered. Equations 5.26 and 5.27 were used to calculate for dielectric constant and dielectric loss of malt bed (Nelson, 1991)

$$\sqrt{\varepsilon'} = \nu_1 \sqrt{\varepsilon_1'} + \nu_2 \sqrt{\varepsilon_2'} \qquad (5.26)$$

Where, ν_1 is the volume fraction of air (0.3456); ν_2 is the volume fraction of malt (0.6544); ε_1 is the dielectric constant of air (1); ε_2 is the dielectric constant of malt (2.057).

$$\sqrt{\varepsilon''} = \nu_1\sqrt{\varepsilon_1''} + \nu_2\sqrt{\varepsilon_2''} \qquad (5.27)$$

Where, ν_1 is the volume fraction of air (0.3456); ν_2 is the volume fraction of malt (0.6544); ε_1 is the dielectric loss of air (0); ε_2 is the dielectric loss of malt (0.138).

5.3.7 Input parameters

In this study, malts samples with different weights (50, 75, and 100 g) contained in a 250 cm^3-beaker roasted by a lab scale microwave oven (Microondes Énergic Système, Villejuif, France) were simulated. A lab scale microwave oven equipped with a 1,860 W-microwave generator (magnetron) and running at 2,450 MHz was used. Malts were roasted at different specific microwave powers (2.50, 2.75, and 3.00 $W \cdot g^{-1}$) for 120 seconds. Schematic drawing of the microwave oven system with 75 g of malt bed in a beaker placed at the center of the turntable is shown in Figure 5.2. To simplify the mathematical model, the simulation was carried out for a heating process without turntable rotation. From preliminary experiments, the reflection percentage of microwaves was 25%. Thus, the model needs to take into account the reflection percentage of microwaves. Input microwave power was calculated by multiplying specific microwave power by the mass of the malt sample and the percentage of absorbed microwaves. The corresponding power inputs were obtained (Table 5.1). Cavity and malt bed properties and initial conditions used in the model used are shown in Table 5.2.

Table 5.1 Input microwave power for a 50, 75, and 100 g-malt bed with the 25% reflection of microwaves during microwave heating at 2.50, 2.75, and 3.00 $W \cdot g^{-1}$ used in the simulation

Specific microwave power ($W \cdot g^{-1}$)	Weight of malt bed (g)	Corresponding input microwave power (W)
2.50	75	140.63
2.75	75	154.69
3.00	75	168.75
2.50	50	93.75
2.50	100	187.50

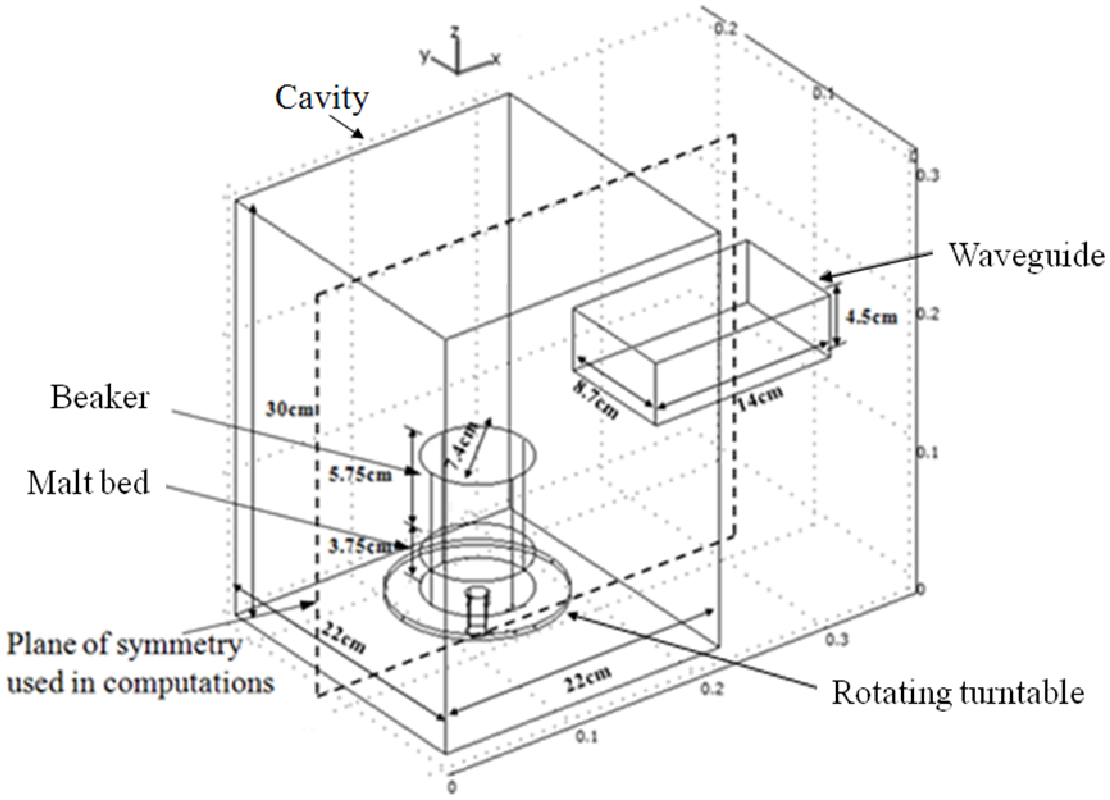

Figure 5.2 Schematic drawing of the microwave oven system with 75 g of malt bed in a beaker placed at the center of the microwave turntable.

Table 5.2 Input parameters

Parameter	Value	Source
Microwave oven interior dimension (cm×cm×cm)	22 × 22 × 30	Experimentally measured in this study
50 g of malt bed dimension (diameter× height) (cm×cm)	7.4 × 2.50	Experimentally measured in this study
75 g of malt bed dimension (diameter× height) (cm×cm)	7.4 × 3.75	Experimentally measured in this study
100 g of malt bed dimension (diameter× height) (cm×cm)	7.4 × 5.00	Experimentally measured in this study
Placement of malt in beaker	Turntable center with no rotation	Experimentally measured in this study
Initial food and air temperature (°C)	21	Experimentally measured in this study
Thermal conductivity of malt bed ($W \cdot m^{-1} \cdot K^{-1}$)	0.027	Experimentally measured in this study

Table 5.2 (Continued)

Parameter	Value	Source
Specific heat of malt bed ($J \cdot kg^{-1} \cdot K^{-1}$)	1003.6	Experimentally measured in this study
Bulk density of malt bed ($kg \cdot m^{-3}$)	604.7	Experimentally measured in this study
Thermal conductivity of air ($W \cdot m^{-1} \cdot K^{-1}$)	$1520.7\times10^{-14}T^3$ $-4857.4\times10^{-11}T^2+1018.4\times10^{-7}T$ -3933.3×10^{-7}	Welty *et al.* (1984)
Specific heat of air ($J \cdot kg^{-1} \cdot K^{-1}$)	$1932.7\times10^{-13}T^4$ $-7999.9\times10^{-10}T^3+1140.7\times10^{-6}T^2$ $-4489\times10^{-4}T+1057.5$	Welty *et al.* (1984)
Density of air ($kg \cdot m^{-3}$)	$4\times10^{-6}T^2-54\times10^{-4}T$ $+2.4451$	Welty et al. (1984)
Heat transfer coefficient ($W \cdot m^{-2} \cdot K^{-1}$)	10	Welty et al. (1984)
Dielectric constant of malt bed	1.6492	Nelson (1991)
Dielectric loss of malt bed	0.0591	Nelson (1991)

Table 5.2 (Continued)

Parameter	Value	Source
Dielectric constant of rotating turntable (polypropylene)	2.40	Rao *et al*. (2005)
Dielectric loss of rotating turntable (polypropylene)	0.0004	Rao *et al*. (2005)
Dielectric constant of air	1	Metaxas (1996)
Dielectric loss of air	0	Metaxas (1996)
Microwave frequency (MHz)	2,450	Default value of the microwave used in this study
Microwave mode type	Transverse electric (TE)	Default value of the microwave used in this study
Waveguide dimension, width (a) × height (b) (cm×cm)	8.7 × 4.5	Default value of the microwave used in this study

5.3.8 Meshing assembly

Meshing assembly of the sample (75-g malt bed) and the microwave oven is shown in Figure 5.3. Since symmetry in the *xz*-plane was assumed, Figure 5.3 shows only half of the studied model. The subdomains were mapped with tetrahedral elements. The total numbers of elements used were 13,441, 16,216, and 19,316 for 50, 75, and 100 g of malt bed, respectively.

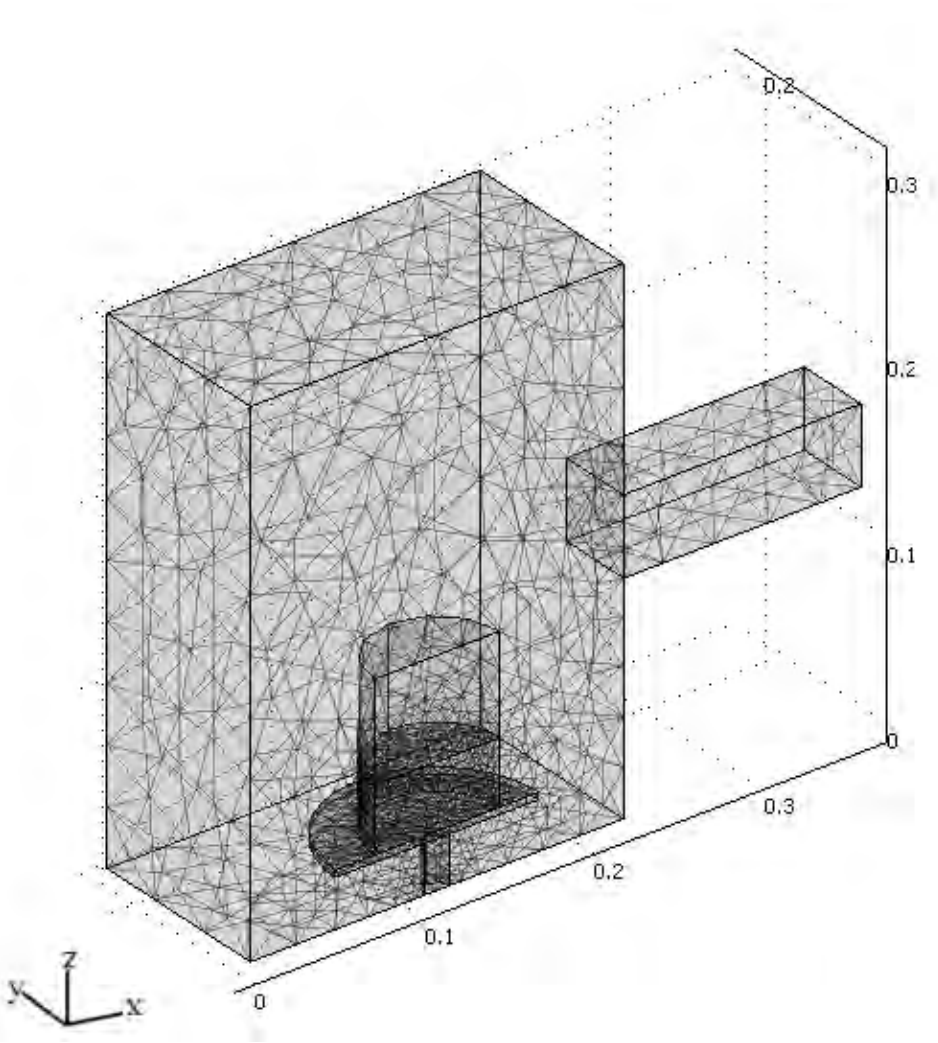

Figure 5.3 Meshing assembly of the sample (75-g malt bed) and the microwave oven.

5.3.9 Problem solving

Problem solving was carried out using a three-dimensional finite element model by commercial program COMSOL 3.5a. Numerical simulation of the differential-algebraic system using backward Euler method with variable time step sizes was carried out.

5.3.10 Model validation

To validate the computational model, experimentally measured temperatures were compared to the calculated values from the model. The experimental verification was conducted using 75 g and 100 g of malt in a 250 cm^3-beaker subjected to microwave treatment at 2.50 $W \cdot g^{-1}$ specific microwave power for 120 seconds. Three fiber optic probes were used to measure temperature at the center of the malt bed during the treatment. All data were collected on a data logger (SA 70, AOIP, Ris Orangis, France) controlled by Labview® supervisor software (National Instruments, Nanterre, France). The experiments were conducted in triplication and duplication for 75- and 100- g malt bed, respectively.

5.4 RESULTS AND DISCUSSION

5.4.1 Model validation

To validate the computational model, experimentally measured temperatures were compared to the calculated values obtained from the model. Figure 5.4 presents the measured and calculated temperature histories at the center of 75 g-malt bed during the microwave heating at 2.50 $W \cdot g^{-1}$ specific microwave power. For the entire duration of heating, the computed temperatures at the center of malt bed were found to be lower than the measured temperatures. The average values of difference $\%D_{avg}$ calculated by equation 5.28, $\%D_{avg}$ were 13.77, 11.97, and 13.16% with respect to experimental number 1, 2, and 3, respectively. The difference between computed and measured temperatures might be resulted from the assumptions that thermal properties and dielectric properties of malt bed were constant and the boundary conditions in the model was not taken into account the evaporation loss at the surface of malt bed. Moreover, the malt bed was considered to be a porous matrix due to limitation in computer memory. Figure 5.5 presents the measured and calculated temperature histories at the center of 100 g-malt bed during microwave heating at 2.50 $W \cdot g^{-1}$ specific microwave power. $\%D_{avg}$ were 5.49 and 3.14% when compared to experimental result number 1 and 2, respectively. Value of $\%D_{avg}$ from 75-g malt bed (Figure 5.4) was higher than 100-g malt bed (Figure 5.5) due to the effect of temperature on physical, thermal, and dielectric properties of malt while the model assumed that physical, thermal, and dielectric properties of malt were constant. Temperature of 75-g malt bed was greater than 100 °C after about 60 seconds heating while the temperature of 100-g malt bed at any location was lower than 100 °C for the entire heating process. The result indicated that changes in physical, thermal, and dielectric properties with temperature had a greater effect on

75-g malt bed than that on the 100-g malt bed. In addition, because the temperature rise in 100-g malt bed did not exceed 100 °C, there is no loss from evaporation.

$$\%D = \frac{\Sigma \left| T_{experiment} - T_{simulation} \right|}{n * T_{experiment}} \times 100\% \qquad (5.28)$$

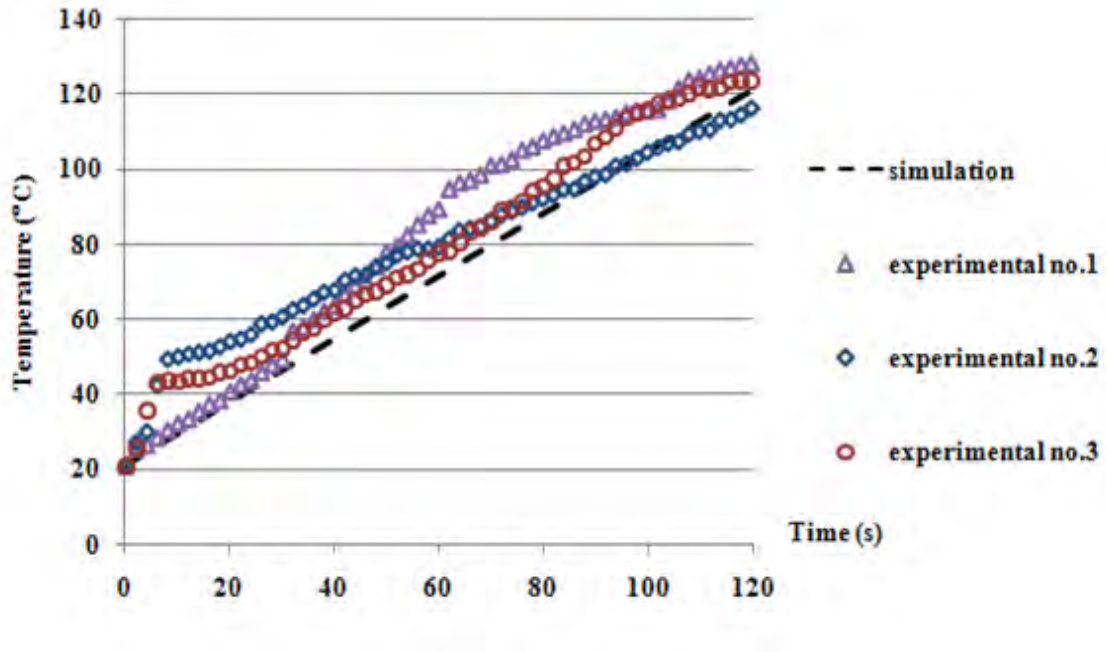

Figure 5.4 Temperature histories at the center of 75 g-malt bed during the microwave heating at 2.50 W·g^{-1} specific microwave power.

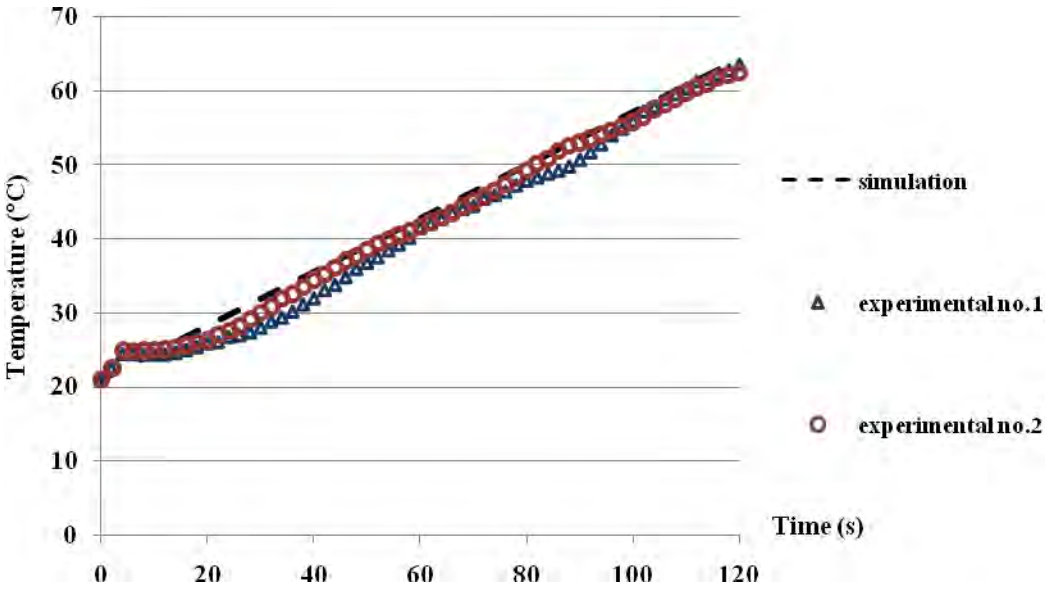

Figure 5.5 Temperature histories at the center of 100 g-malt bed during microwave heating at 2.50 $W \cdot g^{-1}$ specific microwave power.

5.4.2 Distribution of absorbed power in malt bed

Figure 5.6 shows the absorbed microwave power by 75 g-malt bed during the microwave heating at 2.50 $W \cdot g^{-1}$ specific microwave power at any time. Absorbed microwave power will dissipitate as heat in food. The microwave power absorption in malt bed is mainly due to the presence of water molecules. Average initial moisture content of the malt was 9.15% (wet basis). As shown in Figure 5.6, the absorbed microwave power attenuated along radial directions towards the surface. A high concentration of absorbed microwave power existed at the center towards the bottom of the malt bed.

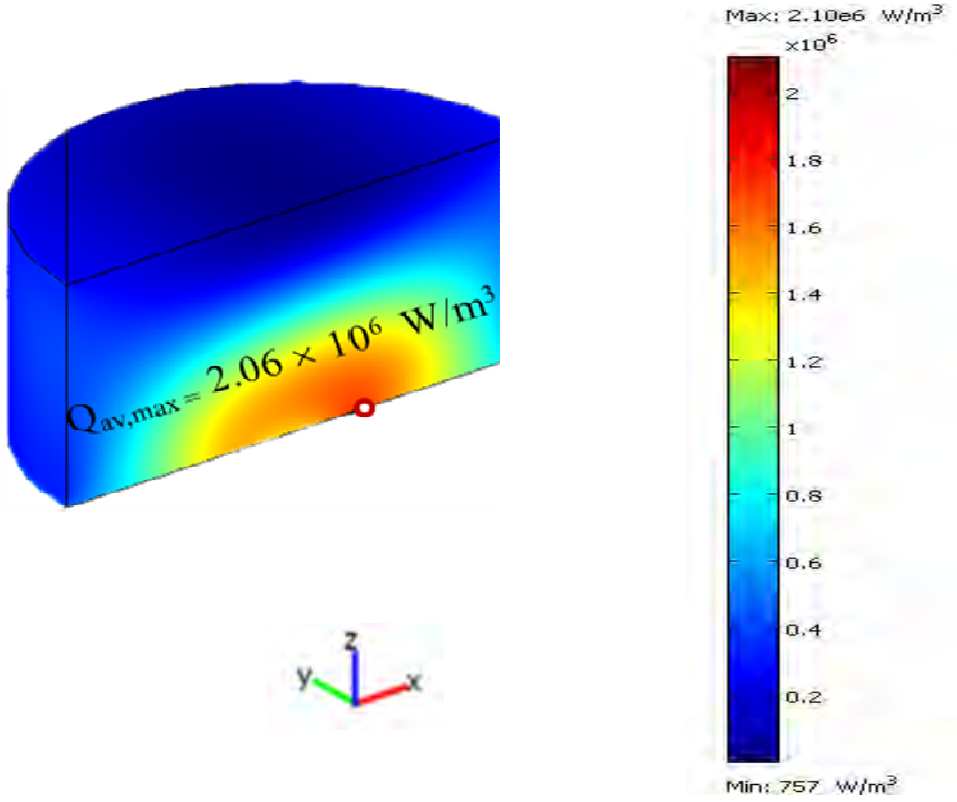

Figure 5.6 Absorbed microwave power by 75 g of malt bed during the microwave heating process at 2.50 W·g^{-1} of specific microwave power at any time.

5.4.3 Temperature distribution in malt bed

The initial temperature of the malt bed was set at 21 °C and the duration of heating was 120 seconds. The boundary condition in the model took into account the convective heat loss at the surface of the malt bed exposing to the surrounding air. Because the malt sample contained only 9.15 % moisture content, low evaporation loss was assumed. Therefore, the model did not take into account the evaporation loss at the surface of malt bed. Energy was used in sensible heating rather than evaporation of moisture in malt. Temperature distribution on the surface of 75-g malt bed during microwave heating at 2.50 W·g^{-1} specific microwave power at various heating times is shown in Figure 5.7. The temperature of hot spot rose from 21 °C

initially to 83.56 °C at 60 seconds of heating time. When the sample is in cylindrical shape, microwave energy enters the bed radially. If the penetration depth is small compared with the food dimensions, most of the energy is absorbed near the surface leaving the center cold. If penetration depth is intermediate, reasonable amounts of energy reach the center and power focusing occurs. Buffler (1993) reported that the microwave energy in cylindrical-shaped foods generates maximum temperature value in the center of food when the penetration depth is more than or approximately 1.5 times the food diameter. From this study penetration depth of malt bed is 40.51 cm which is about 5.5 times the malt bed diameter. Therefore the temperature near the center of the malt bed is much higher than in other parts. The movement of the hot spot is clearly visible from Figure 5.7. During the initial portion of the heating period, the hot spot located near the center towards the bottom of malt bed. As heating proceeded, the hot spot moved towards the center of malt bed. At 120 seconds of heating time, the hot spot located at the center of malt bed approximately 7 mm above the bottom. Figure 5.8 shows temperature distributions at the *xy* plane through the center of 75-g malt bed during microwave heating at 2.50 $W \cdot g^{-1}$ specific microwave power for 120 seconds. Figure 5.8 shows that high temperature values located near the center axis of malt bed.

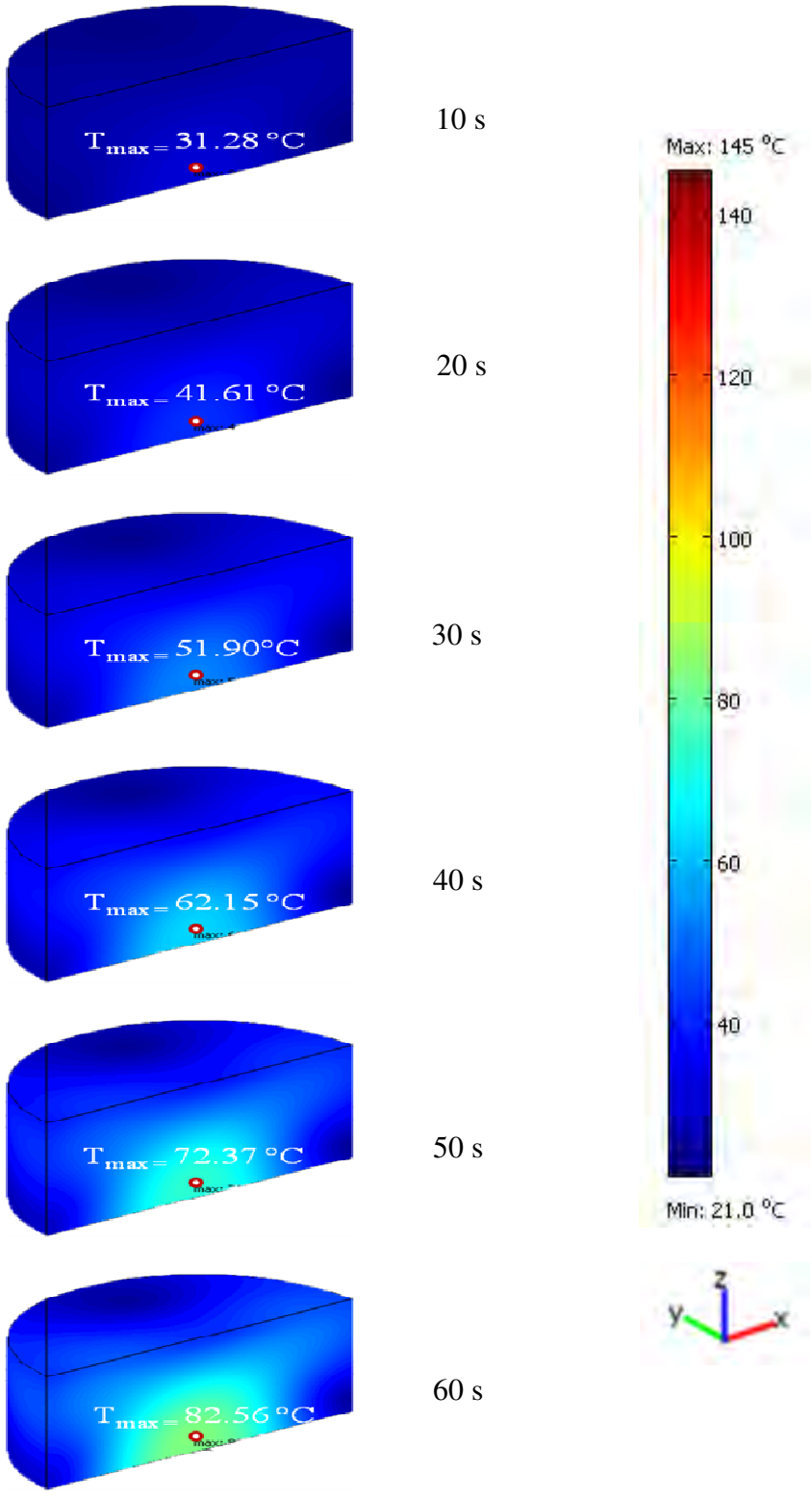

Figure 5.7 Temperature distribution on the surface of 75-g malt bed during microwave heating at 2.50 $W \cdot g^{-1}$ specific microwave power.

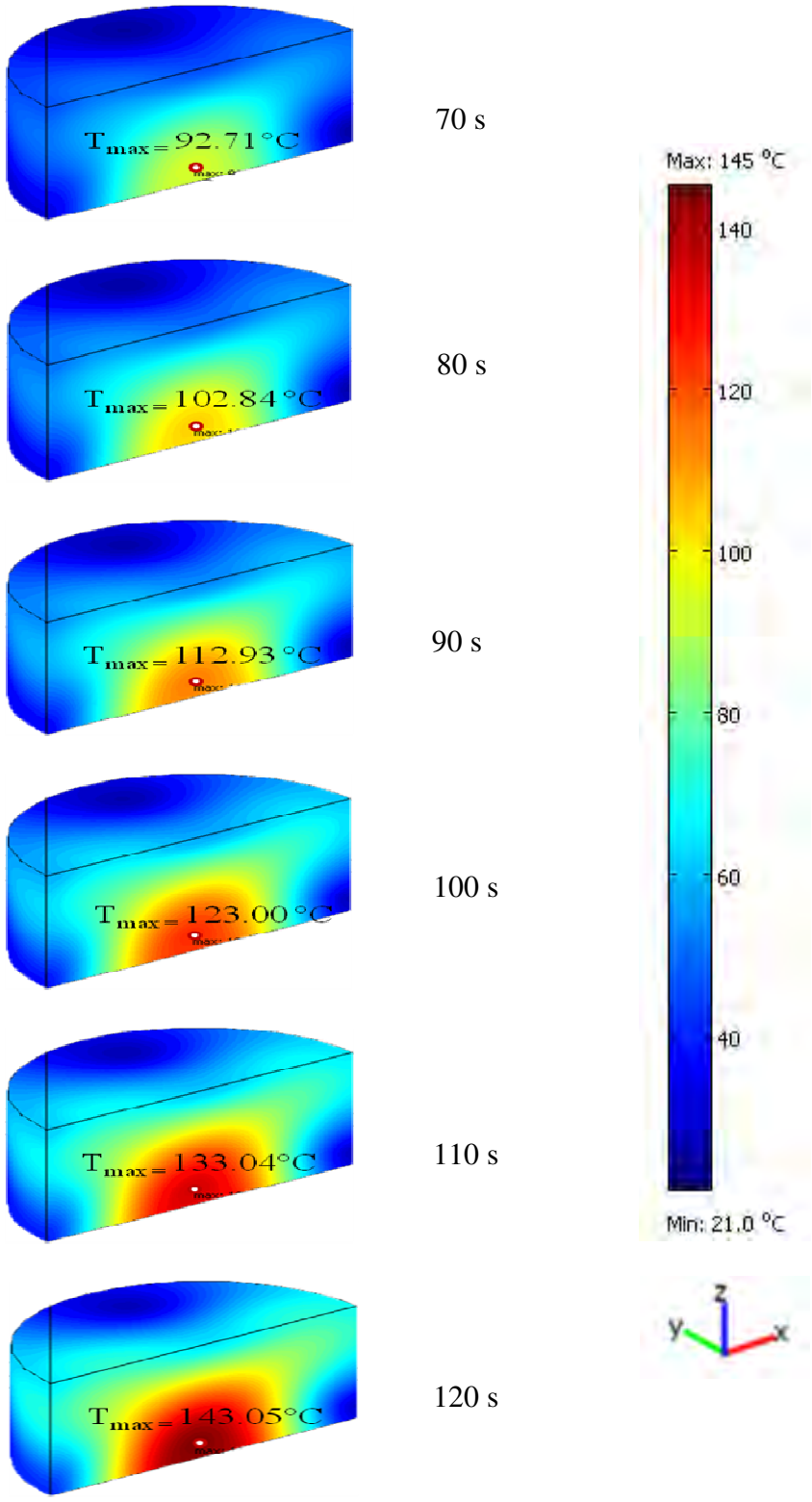

Figure 5.7(cont.) Temperature distribution on the surface of 75-g malt bed during microwave heating at 2.50 $W \cdot g^{-1}$ specific microwave power.

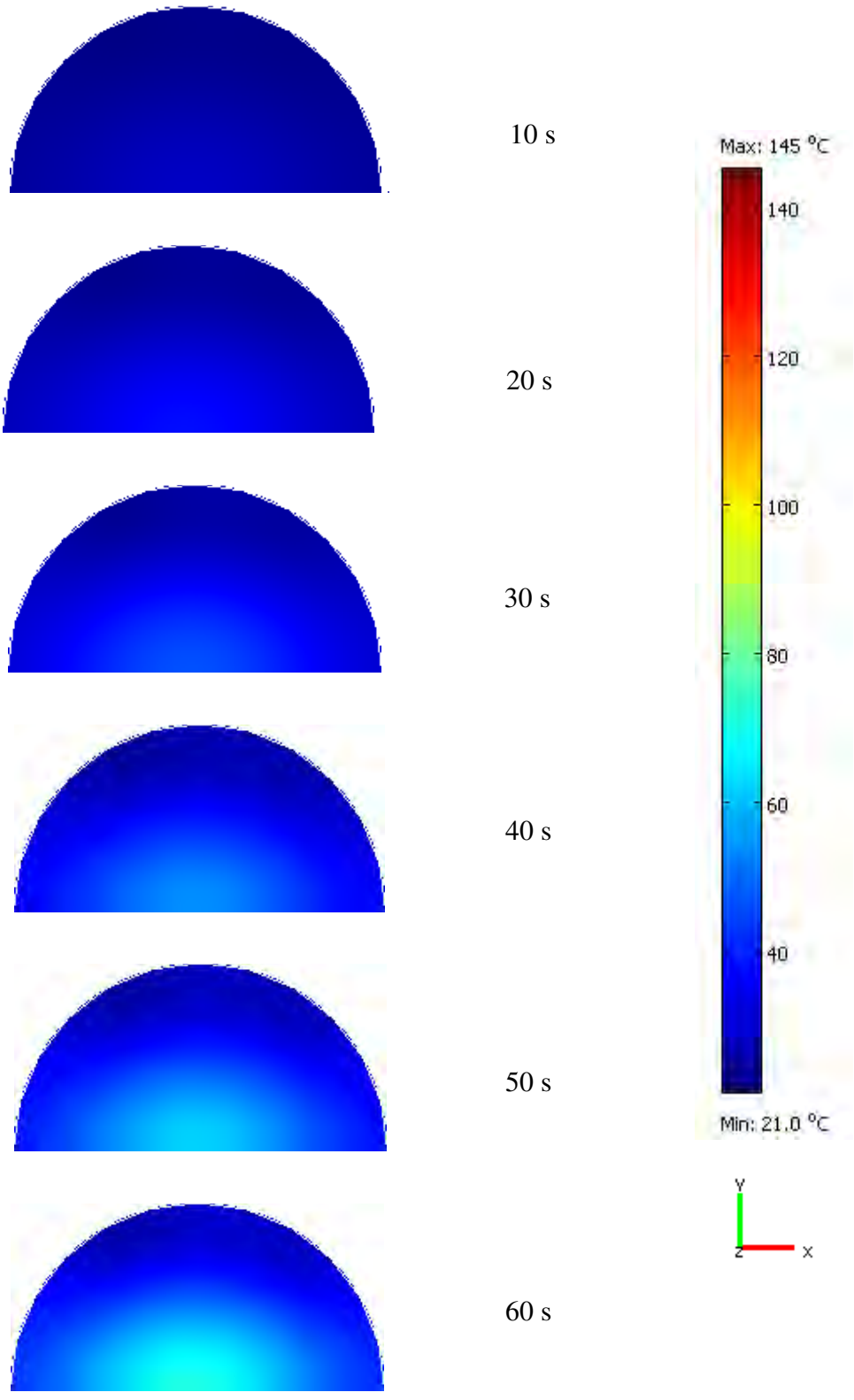

Figure 5.8 Temperature distributions at the *xy* plane through the center of 75-g malt bed during microwave heating at 2.50 $W \cdot g^{-1}$ specific microwave power.

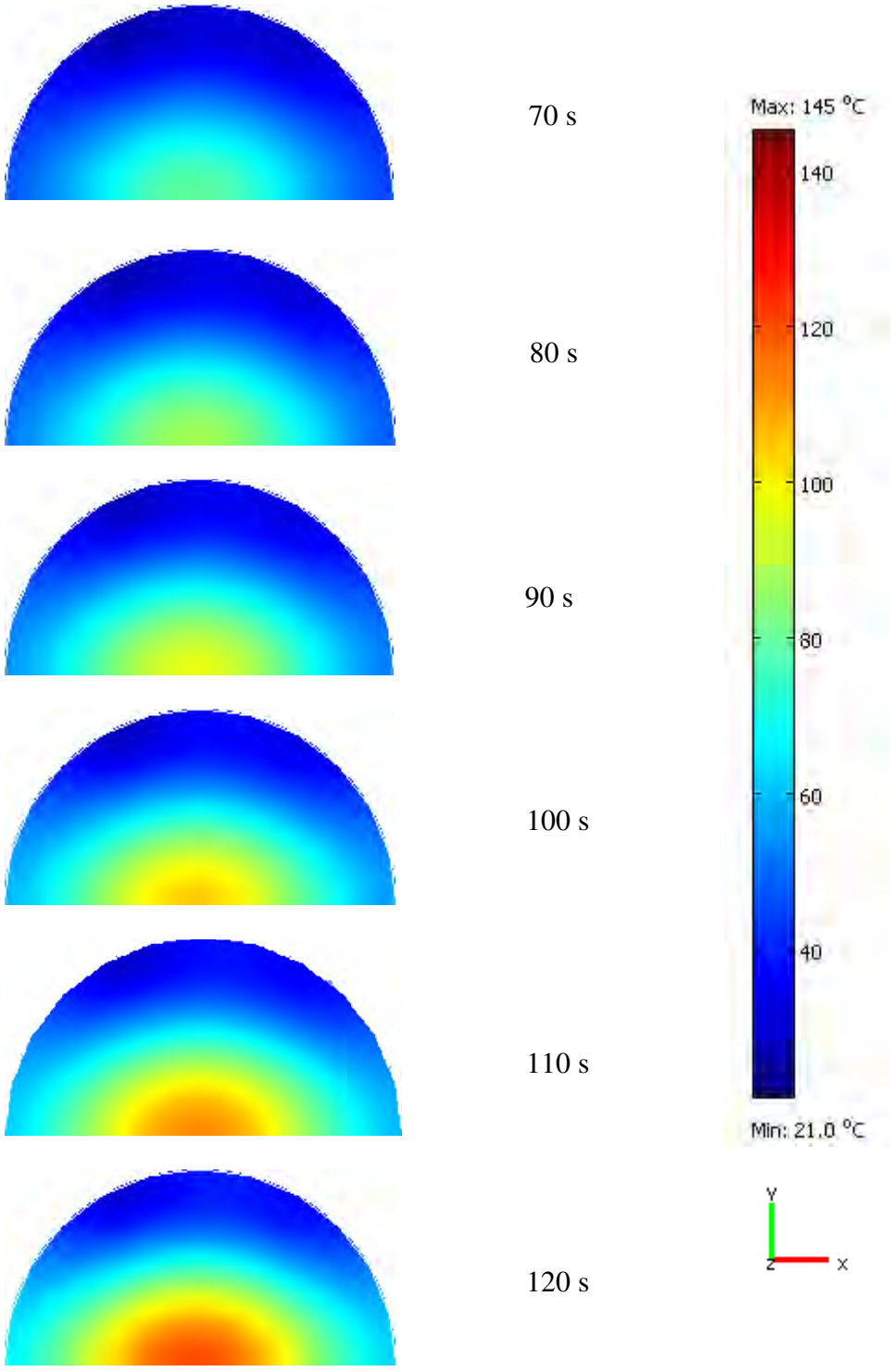

Figure 5.8(cont.) Temperature distributions at the *xy* plane through the center of 75-g malt bed during microwave heating at 2.50 $W \cdot g^{-1}$ specific microwave power

5.4.4 Effect of microwave power on heat distribution

Figure 5.9 shows absorbed microwave power by 75-g malt bed during microwave heating at 2.50, 2.75, and 3.00 $W \cdot g^{-1}$ specific microwave power at any time. As shown in Figure 5.9, the absorbed microwave power attenuated along radial directions towards the surface. From the result, the maximum absorbed microwave powers by 75-g malt bed were 2.06×10^6, 2.27×10^7, and 2.48×10^6 W/m^3 after heating by microwave at 2.50, 2.75, and 3.00 $W \cdot g^{-1}$, respectively. It was apparent that increasing specific microwave power resulted in an increase in the absorbed microwave power. The maximum absorbed power in $W \cdot g^{-1}$ was calculated by dividing the maximum absorbed microwave powers by bulk density of malt bed (604.7 $kg \cdot m^{-3}$). Therefore, the absorbed power by 75-g malt bed were 3.41, 3.75, and 4.1 $W \cdot g^{-1}$ after heating by microwave at 2.50, 2.75, and 3.00 $W \cdot g^{-1}$, respectively. The absorbed microwave powers by malt bed were higher than input microwave power because of power focusing. At the top center of malt bed surface, the absorbed power by 75-g malt bed were 0.014, 0.015, and 0.017 $W \cdot g^{-1}$ after heating by microwave at 2.50, 2.75, and 3.00 $W \cdot g^{-1}$, respectively. It means that some parts of malt bed had higher or lower absorbed microwave powers when compared with the input microwave power. However, the total absorbed microwave power by malt bed must be lower than the input microwave power (total absorbed microwave power by 75-g malt bed were 1.27, 1.39, and 1.52 $W \cdot g^{-1}$ after heating by microwave at 2.50, 2.75, and 3.00 $W \cdot g^{-1}$, respectively). Temperature distributions in 75 g-malt bed during microwave heating at 2.50, 2.75, and 3.00 $W \cdot g^{-1}$ specific microwave power at 120 seconds are shown in Figure 5.10. Figure 5.11 shows the computed temperature histories at the center of a 75 g-malt bed during microwave heating at 2.50, 2.75, and 3.00 $W \cdot g^{-1}$ specific microwave power. The temperature at the center of the bed rose

from 21 °C initially to 71.50, 76.56, and 81.62 °C at 60 seconds of heating. Temperature rose during microwave heating was found to be linear over the entire heating time. At 2.50, 2.75, and 3.00 $W \cdot g^{-1}$ specific microwave power, the heating rate were 0.84, 0.92, and 1.00 $°C \cdot s^{-1}$, respectively.

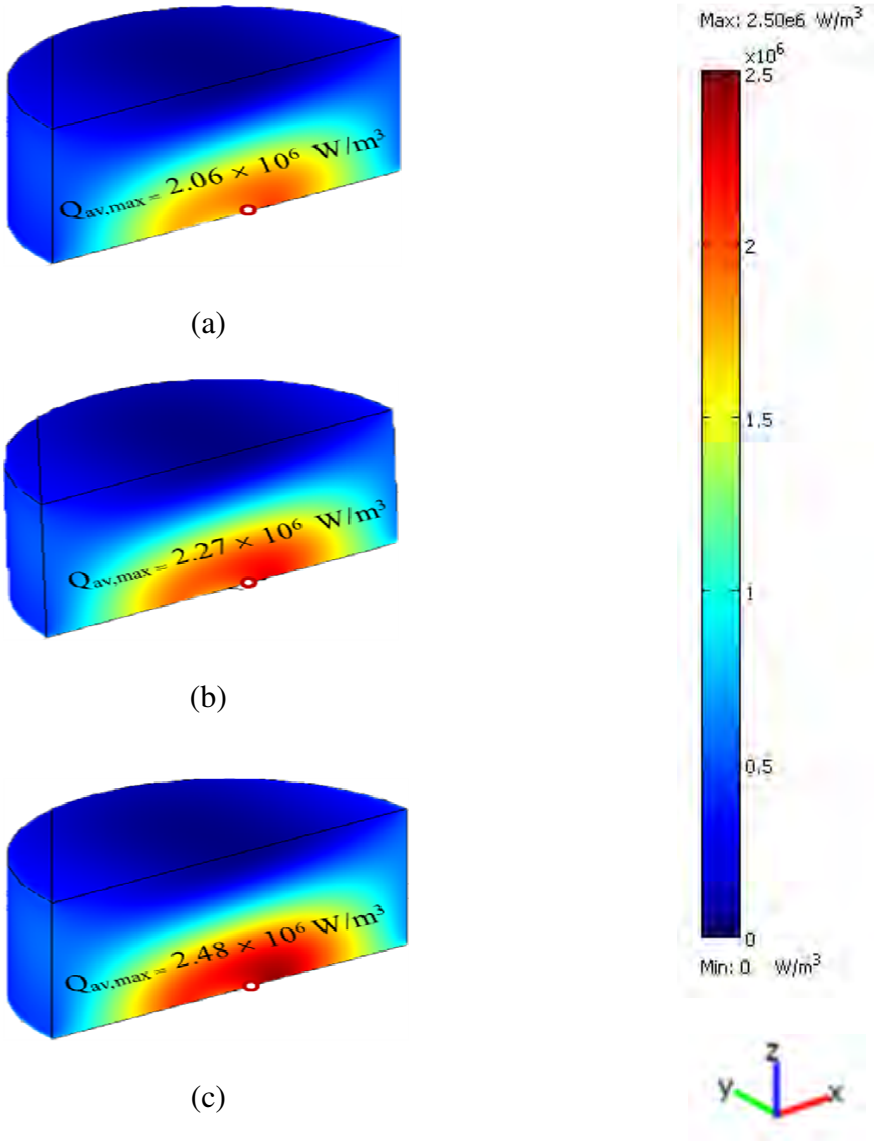

Figure 5.9 Absorbed microwave power by 75-g malt bed during microwave heating at 2.50 (a), 2.75 (b), and 3.00 (c) $W \cdot g^{-1}$ specific microwave power at any time.

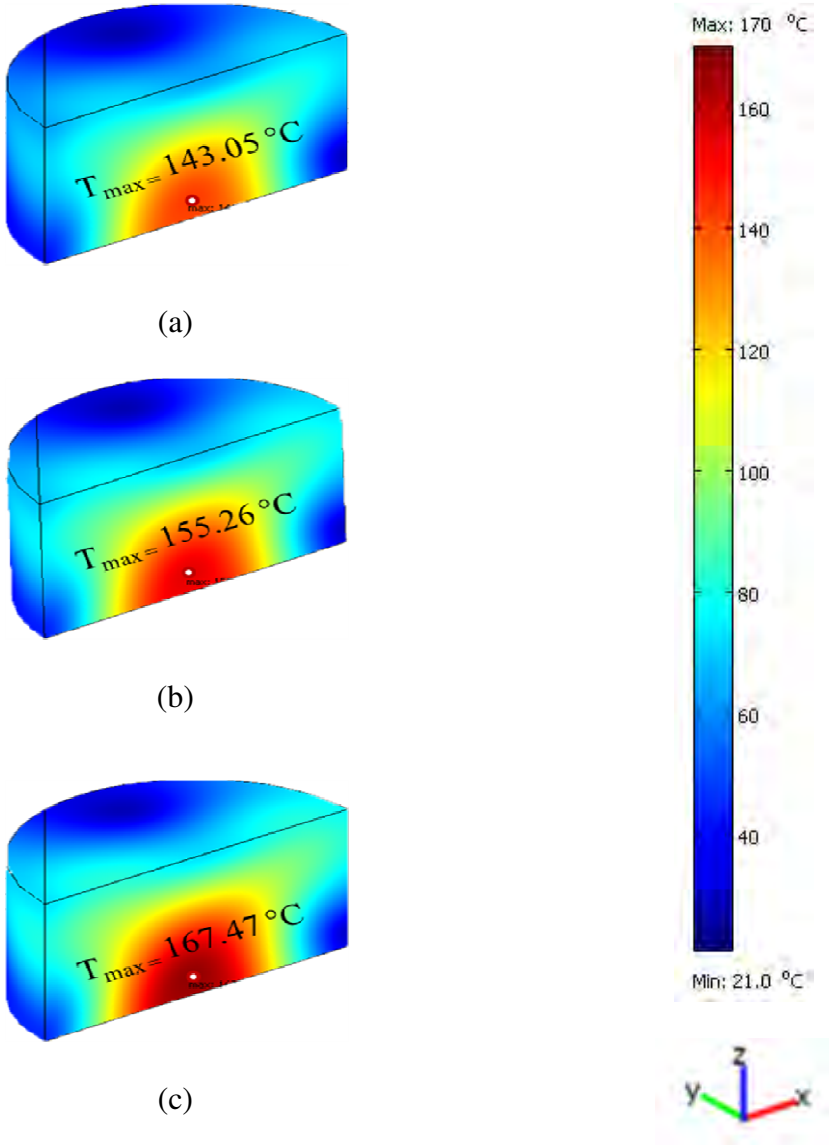

Figure 5.10 Temperature distribution in 75 g-malt bed during microwave heating at 2.50 (a), 2.75 (b), and 3.00 (c) $W \cdot g^{-1}$ specific microwave power at 120 s.

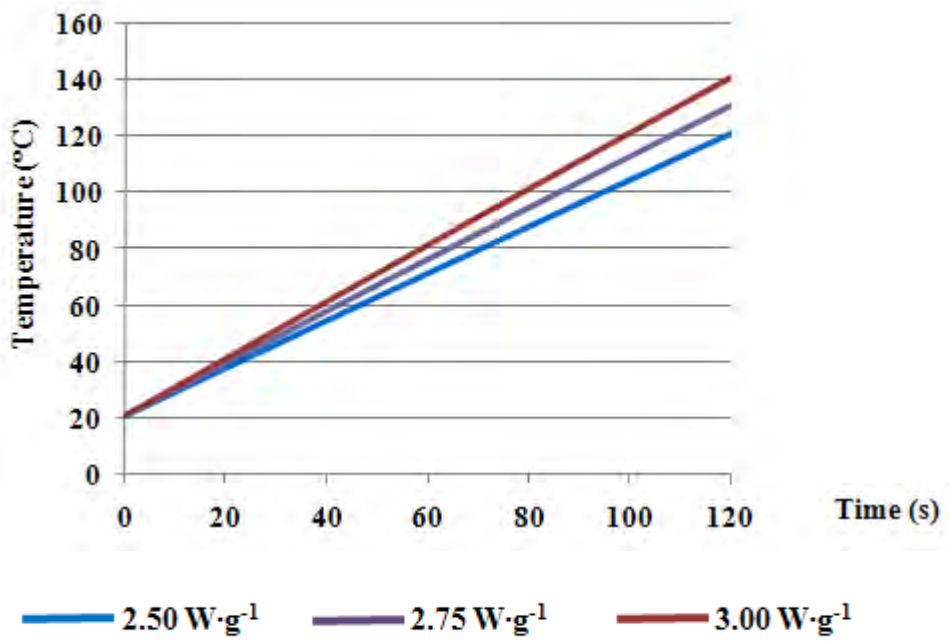

Figure 5.11 Computed temperature histories at the center of a 75-g malt bed during microwave heating at 2.50, 2.75, and 3.00 $W \cdot g^{-1}$ specific microwave power.

5.4.5 Effect of sample weight on heat distribution

Figure 5.12 shows the amount of absorbed microwave power by malt beds having different weights during microwave heating at 100 W input microwave power at any time. Figure 5.13 shows the corresponding temperature distribution in the bed processed at the same condition. These results show that, for 75, 100, and 125-g malt bed values of absorbed microwave power in malt bed were 1.18×10^6, 1.15×10^6 , and 1.13×10^6 $W \cdot m^{-3}$, respectively. In fact the absorbed microwave powers should have the same value because of the unit is per volume. The difference was due to error from calculation. The temperature distribution in malt bed was dependent on the weight of the sample, as weight of malt bed increased, the heat resistance of malt bed increased. Increasing weight from 75 g to 125 g resulted in a

decrease in maximum temperature in malt bed from 288.17 °C to 53.11 °C as shown in Figures 5.13a and 5.13c. Temperature of hot spot and cold spot in a 75-g malt bed were 288.17 and 21 °C, respectively. Figure 5.14 presents computed temperature histories at the center of 75, 100, and 125-g malt beds during microwave heating at 100 W input microwave power. At 60 seconds, temperature at the center of the bed rose from 21 °C initially to 142.42, 47.36, and 32.09 °C for 75, 100, and 125g of weight. For 75-, 100-, and 125-g malt bed, the heating rates were 2.00, 0.44, and 0.18 $°C \cdot s^{-1}$, respectively.

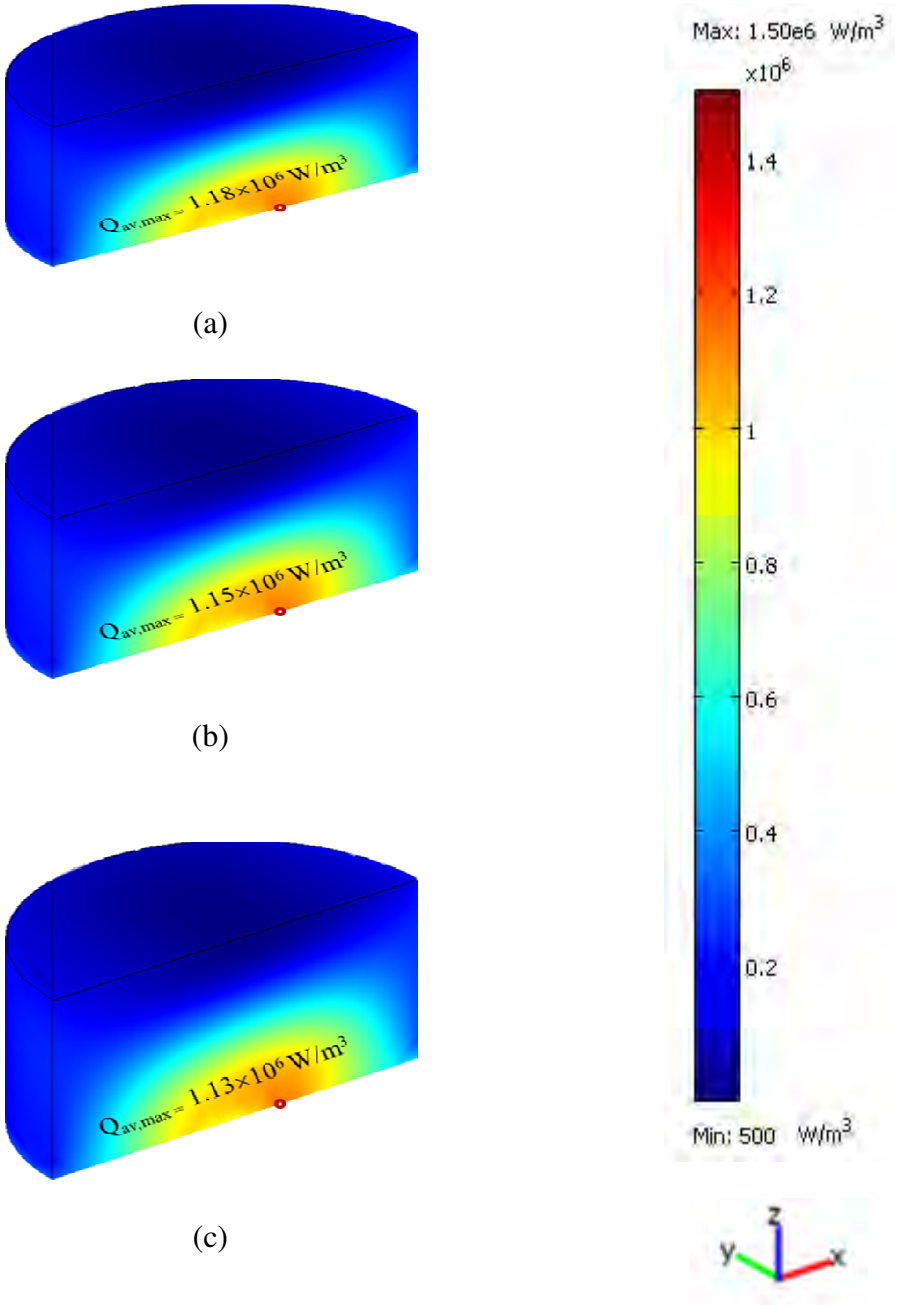

Figure 5.12 Absorbed microwave power by 75- (a), 100- (b), and 125- (c) g malt bed during microwave heating at 100 W input microwave power at any time.

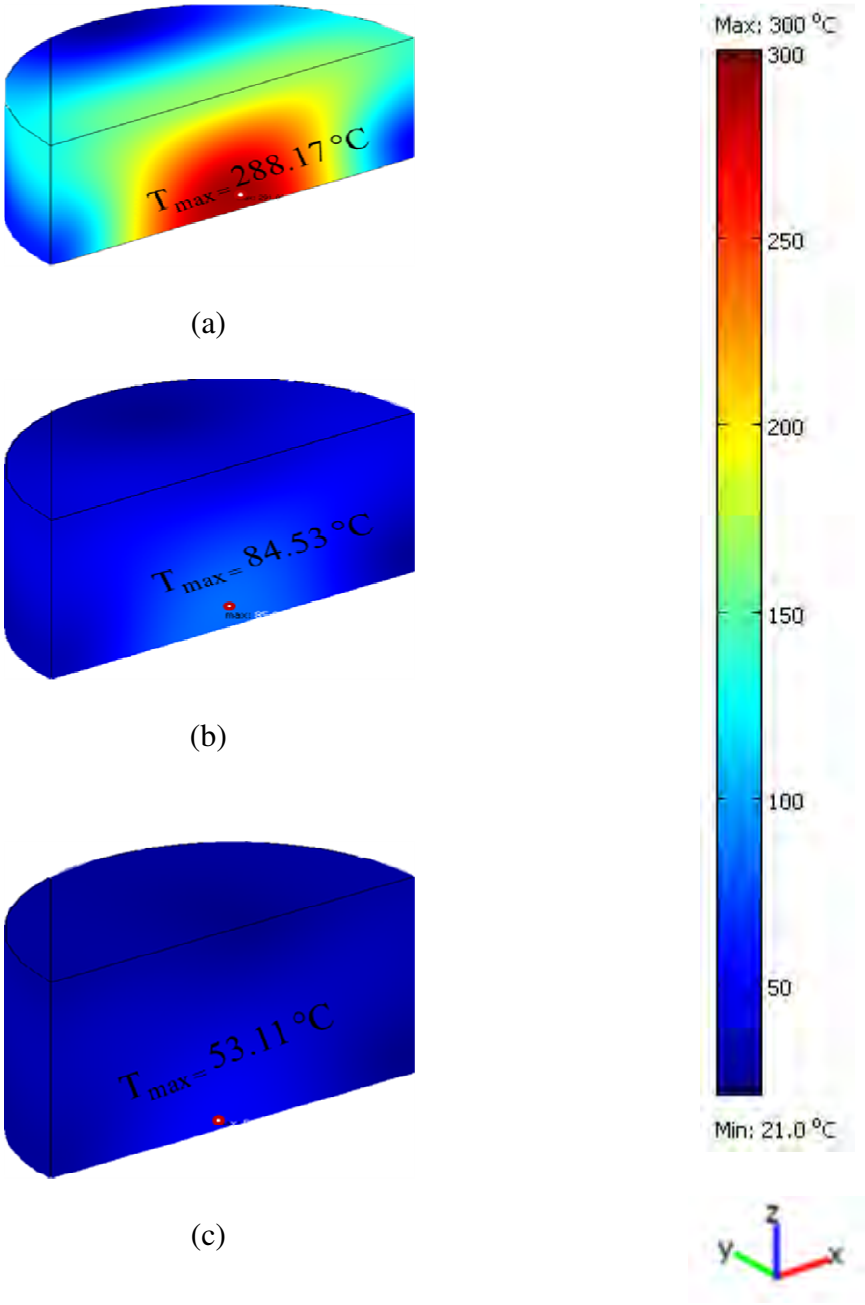

Figure 5.13 Temperature distribution in 75- (a), 100- (b), and 125- (c) g malt bed during microwave heating at 100 W input microwave power at 120 s.

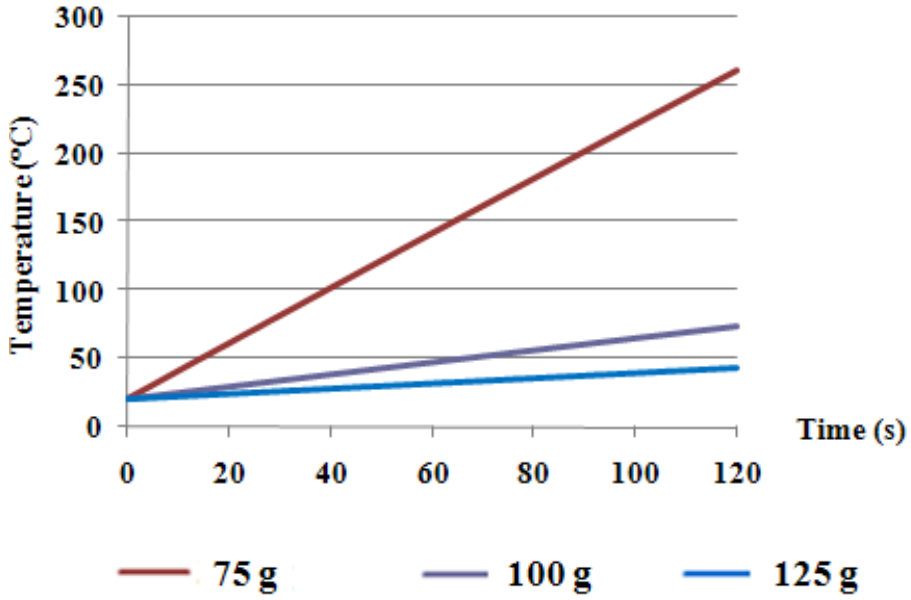

Figure 5.14 Computed temperature histories at the center of 75-, 100-, and 125-g malt bed during microwave heating at 100 W input microwave power.

5.4.6 Predicted HMF and acrylamide formation during microwave heating

From computed temperature histories at the hot spot, the NFCs formation during microwave heating could be calculated. HMF and acrylamide formation followed a first order kinetic (Ameur *et al*., 2006; Claeys *et al*., 2005a). Tables 5.3 and 5.4 show the rate constants (k) at various temperatures (T) for HMF and acrylamide formation used for the prediction. From the rate constants, the activation energy (E_a) for the formation of HMF and acrylamide can be calculated using an Arrhenius relationship (Figure 5.15 and 5.16). The E_a for HMF and acrylamide was found to be 24.64 kJ·mol^{-1} and 167.74 kJ·mol^{-1}, respectively, while k_0 for HMF and acrylamide was 1.60exp(-2963/*T*) and 8.00E+16exp(-20173/*T*), respectively.

Table 5.3 The rate constants at various temperatures for HMF formation in cookies (Ameur *et al*., 2006)

T (°C)	rate constant (s^{-1})
200	0.0028
250	0.0067
300	0.0082

Table 5.4 The rate constants at various temperatures for acrylamide formation in asparagines-glucose model system (Claeys *et al*., 2005a)

T (°C)	rate constant (min^{-1})
140	0.0000
160	0.0005
180	0.0035
200	0.023

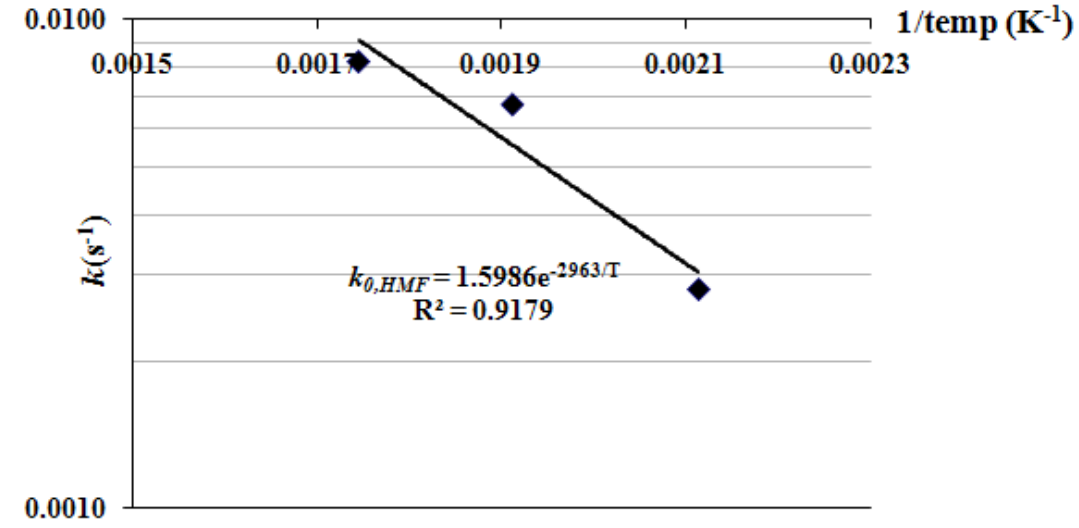

Figure 5.15 The rate constant for the formation of HMF at 200, 250, and 300 °C. (Data taken from Ameur *et al*., 2006)

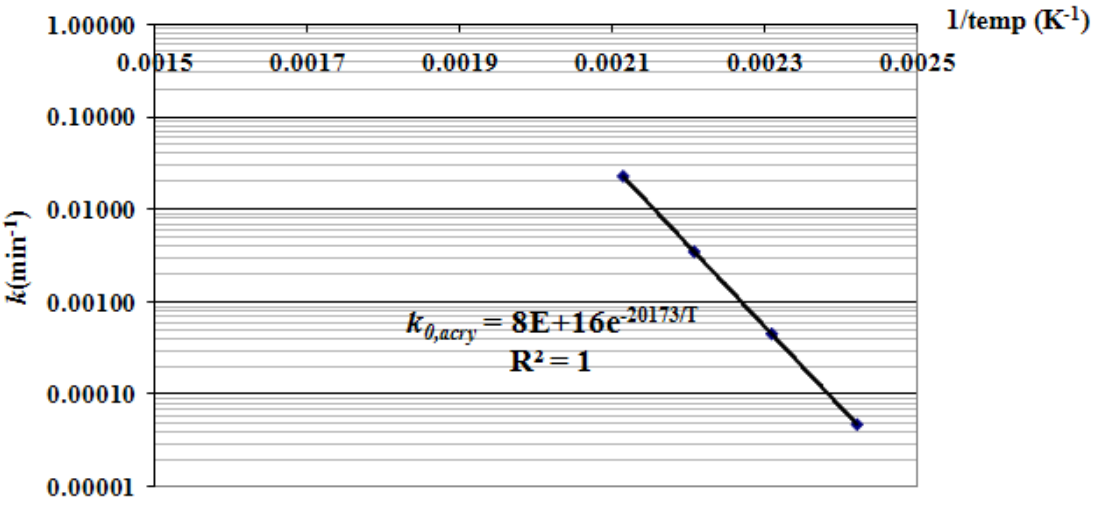

Figure 5.16 The rate constant for the formation of acrylamide at 140, 160, 180, and 200 °C. (Data taken from Claeys *et al*., 2005a)

Figures 5.17 and 5.18 show the predicted accumulation of HMF and acrylamide content, respectively, at hot spot of 75-g malt bed. It is apparent that both HMF and acrylamide were formed as a function of roasting time and increasing specific microwave power.

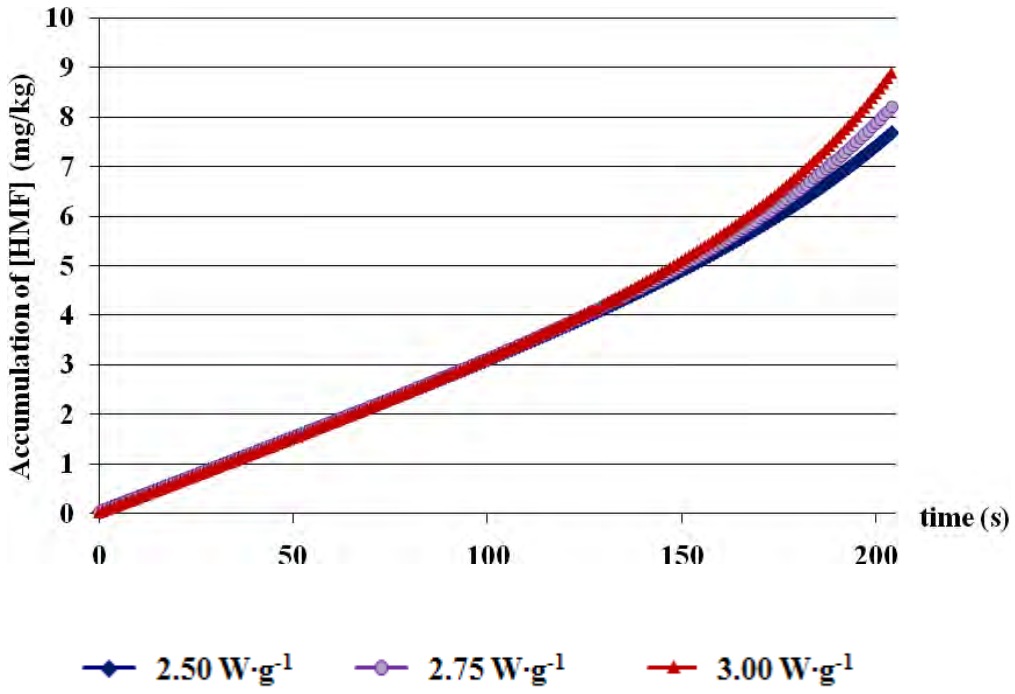

Figures 5.17 Accumulation of HMF content at hot spot of 75-g malt bed.

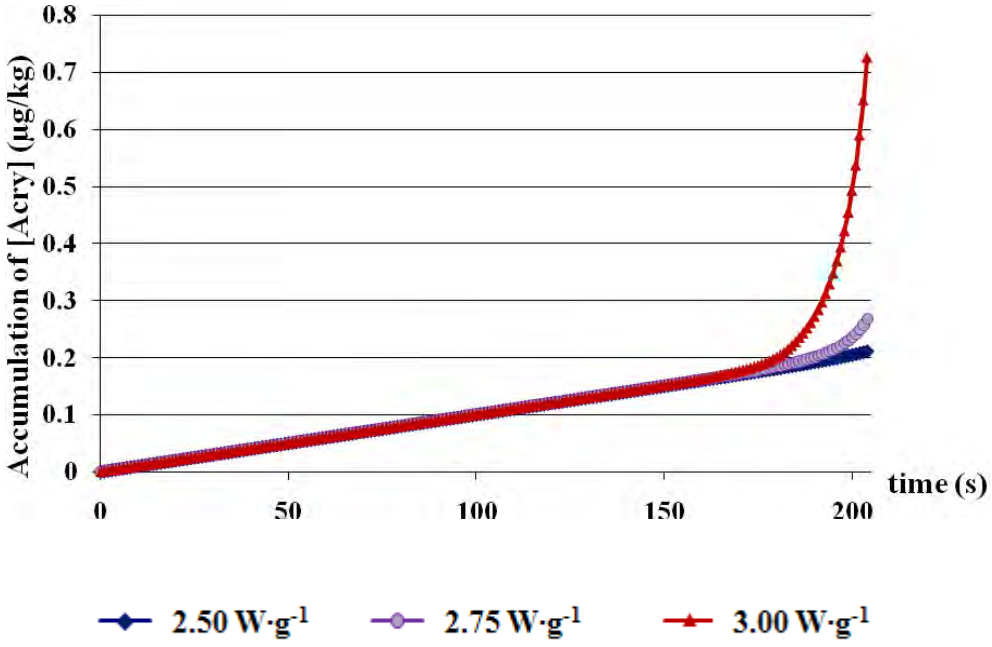

Figures 5.18 Accumulation of acrylamide content at hot spot of 75-g malt bed.

Table 5.5 shows the predicted and the measured HMF and acrylamide content in 75-g malt bed subjected to microwave heating at 2.50, 2.75, and 3.00 $W \cdot g^{-1}$. The results showed that the measured HMF content was about 10 times higher than the predicted HMF content. Conversely, the predicted acrylamide content was in close proximity with the measured acrylamide content. Therefore, at this stage, the model developed in this study can be used to predict the formation of acrylamide quite satisfactorily. The great difference between the predicted and the measured HMF content might be from the fact that the kinetics data used for the prediction was taken from cookies (Ameur *et al*., 2006) which comprises different compositions when compared to malts.

Table 5.5 The predicted and the measured HMF and acrylamide content in 75-g malt bed subjected to microwave heating at 2.50, 2.75 and 3.00 $W \cdot g^{-1}$ specific microwave power.

NFCs content	Specific power ($W \cdot g^{-1}$)	Predicted	Measured*
HMF** ($mg \cdot kg^{-1}$)	2.50	7.69	60.37
	2.75	8.21	110.59
	3.00	8.90	127.35
Acrylamide*** ($\mu g \cdot kg^{-1}$)	2.50	0.21	0.16
	2.75	0.27	0.19
	3.00	0.73	0.24

* Measured by physico-chemical method
** Using kinetic data from Ameur et al., 2006
*** Using kinetic data from Claeys et al., 2005

5.5 CONCLUSIONS

Microwave heating of malt grains in a beaker was simulated using finite element method in 3 D with symmetry in *xz*-plane. The model validated with experimental measurements. The average value of difference $\%D_{avg}$ were 10%. The mathematical model could predict electromagnetic field distribution and temperature distribution in a malt bed. The simulation results showed that absorbed microwave energy concentrated near the center of malt bed. During microwave heating at 2.50 $W \cdot g^{-1}$ for a 75-g malt bed, hot spot moved from location near the center bottom of malt bed towards the center of malt bed approximately 7 mm above the bottom. The simulation results presented that microwave heating is dependent on microwave power input and weight of malt bed. Increasing microwave power resulted in an increase in absorbed power. As the malt weight increased, the maximum temperature of malt bed decreased. HMF and acrylamide content could be predicted from kinetic

parameters and temperature of malt bed. The model developed in this study can be used to predict the formation of acrylamide quite satisfactorily.

REFERENCES

Al-Duri, B., and McIntyre, S. 1992. Comparison of drying kinetics of foods using a fan-assisted convection oven, a microwave oven and a combined microwave/convection oven. Journal of Food Engineering 15 : 139-155.

Alibas, I. 2007. Microwave, air and combined microwave-air-drying parameters of pumpkin slices. LWT-Food Science and Technology 40(8) : 1445-1451.

Ames, J.M., Bailey, R.G., and Mann, J. 1998. Recent advances in the analysis of coloured maillard reaction products. In J. O' Brien, H.E. Nursten, M. James, C. Crabbe, and J.M. Ames (eds.), The Maillard Reaction in Foods and Medicine, pp. 76-82. London : Royal Society of Chemistry.

Ameur, L.A., Mathieu, O., Lalanne, V., Trystram, G., and Birlouez-Aragon, I. 2007. Comparison of the effects of sucrose and hexose on furfural formation and browning in cookies baked at different temperatures. Food Chemistry 101 : 1407-1416.

Ameur, L.A., Trystram, G.L., and Birlouez-Aragon, I. 2006. Accumulation of 5-hydroxymethyl-2-furfural in cookies during the baking process: validation of an extraction method. Food Chemistry 98(4) : 790-796.

Arts, J.H.E., Muijser, H., Appel, M.J., Kuper, C.F., Bessems, J.G.M., and Woutersen, R.A 2004. Subacute (28-Day) toxicity of furfural in fischer 344 rats: a comparison of the oral and inhalation route. Food and Chemical Toxicology 42 : 1389-1399.

Association of Official Analytical Chemists . 1990. Official Methods of Analysis of the Association of Official Analytical . 12th ed. Washington. DC : AOAC.

Biedermann, M., Biedermann-Brem, S., Noti, A., Grob, K., Egli, P., and Mändli, H. 2002. Two GC-MS methods for the analysis of acrylamide infoodstuffs. Mitteilungen aus Lebensmitteluntersuchung und Hygiene 93 : 638-652.

Birlouez-Aragon, I., Morales, F., Fogliano, V., and Pain, J.P. 2010. The health and technological implications of a better control of neoformed contaminants by the food industry. Pathologie Biologie 58(3) : 232-238.

Boekel, M.A.J.S. 2006. Formation of flavor compounds in the Maillard reaction, biotechnology advances. Biotechnology Advances 24(2) : 230-233.

Bouraoui, M., Pichard, P., and Durance, T. 1994. Microwave and convective drying of potato slices. Journal of Food Process Engineering 17 : 353-363.

Briggs, D.E., Boulton, C.A., Brookes, P.A., and Stevens, R. 2004. Brewing Science and Practicel . England : Woodhead Publishing Ltd.

Broyart, B., Trystram, G., Duquenoy, A. 1998. Predicting color kinetics during cracker baking. European Food Research and Technology 228 : 311-319.

Buffler, C.R. 1993. Microwave Cooking and Processing: Engineering Fundamentals for the Food Scientist. New York : Academic Press, Inc.

Carabasa-Giribet M., Ibarz-Ribas A 2000. Kinetic of colour development in aqueous glucose systems at high temperatures. Journal of Food Engineering 44 : 181-189.

Campanone, L.A., and Zaritzky, N.E. 2005. Mathematical analysis of microwave heating process. Journal of Food Engineering 69 : 359-368.

Capuano, E., Ferrigno, A., Acampa, I., Ameur, L.A., and Fogliano, V. 2008. Characterization of the Maillard reaction in bread crisps. European Food Research and Technology 228 : 311-319.

Chemical Research in Toxicology. 2009. In This Issue-Chemical Research in Toxicology [online]. Available from: http://pubs.acs.org/doi/pdfplus/10.1021/tx900140x [2010, March 17].

Claeys, W.L., Vleeschouwer, K., Hendrickx, E. 2005a. Effect of amino acids on acrylamide formation and elimination . Biotechnology Progress 21 : 1525-1530.

Claeys, W.L., Vleeschouwer, K., Hendrickx, E. 2005b. Quantifying the formation of carcinogens during food processing: acrylamide. Trends in Food Science and Technology 16 : 181-193.

Coskuner, Y., and Karababa, E. 2006. Physical properties of coriander seed (*Coriandrum sativum L.*). Journal of Food Engineering 80 : 408-416.

Crews, C., and Castle, L. 2007. A review of the occurrence. Formation and analysis of furan in heat-processed foods. Trends in Food Science and Technology 18 : 365-372.

Datta, A.K., and Ni, H. 2002. Infrared and hot-air-assisted microwave heating of foods for control of surface moisture. Journal of Food Engineering 51 : 355-364.

Decareau, R.V. 1985. Microwaves in the food processing industry. Microwaves in the Food Processing Industry. Orlando : Academic Press. Inc.

Delgado-Andrade, C., Seiquer, I., Haro, A., Castellano, R., and Navarro, M.P 2010. Development of the Maillard reaction in food cooked by different techniques intake of Maillard-derive compounds. Food Chemistry 122(1) : 145-153.

Dybing, E., Farmer, P.B., Andersen, M., Fennell, T.R., Lalljie, S.P.D., Müller, D.J.G., Olin, S., Petersen, B.J., Schlatter, J., Scholz, G., Scimeca, J.A., Slimani, N., Törnqvist, M., Tuijtelaars, S., and Verger, P. 2005. Human exposure and internal dose assessments of acrylamide in food. Food and Chemical Toxicology 43 : 365-410.

Dybing, E., and Sanner, T. 2003. Forum risk assessment of acrylamide in food. Toxicology Science 75 : 7-15.

Eichner, K., and Wolf, W. 1983. Maillard reaction products as indicator compounds for optimizing drying and storage conditions. In: G.R. Waller, M.S. Feather, (eds), The Maillard Reaction in Foods and Nutrition, pp. 317-333. Washington, D.C. : American Chemical Society.

Erdoğdu, S.B., Palazoğlu, T.K., Gökmen, V., Şenyuva, H.Z., and Ekiz, H.I. 2007. Reduction of acrylamide formation in french fries by microwave pre-cooking of potato strips. Journal of the Science of Food and Agriculture 87 : 133-137.

Eriksson, S. 2005. Acrylamide in Food Products: Identification, Formation and Analytical Methodology. Doctoral dissertation Department of Environmental Chemistry Faculty of Science Stockholm University.

Eskin, N.A.M. 1990. Biochemistry of food processing: browning reactions in foods. In N.A.M. Eskin (ed.), Biochemistry of Foods, pp. 240-295. London : Academic Press, 557 p.

Fendor, A.O., Meulenaer, B., Scholl, G., Adam, A., Lancker, F.V., Yogendrarajah, P., Eppe, G., Pauw, E., Scippo, M.L., and Kimpe, N. 2010. Furan formation from vitamin C in a starch-vased model system: influence of the reaction conditions. Food Chemistry 121 : 1163-1170.

Ferreira, S.L.C., Santos, W.N.L., Quintella, C.M., Neto, B.B., Bosque-Sendra, J.M. . 2004. Doehlert matrix: a chemometric tool for analytical chemistry-review. Talanta 63 : 1061-1067.

Food and Agriculture Organization/World Health Organization Consultation on Health Implication of Acrylmide in Food. 2002. Report of a Joint FAO/WHO Consultation Geneva. Switzerland. 25-27th June 2002[online]. Available from: http://www.who.int/fsf/Acrylamide/SummaryreportFinal.pdf [2010, January 8]

Food and Drug Administration. 2004. Federal Register - 69 FR 25911 May 10, 2004: Furan in Food, Thermal Treatment; Request for Data and Information[online]. Available from: http://www.fda.gov/Food/FoodSafety/FoodContaminantsAdulteration/ChemicalContaminants/Furan/UCM078469 [2010, January 8]

Food and Drug Administration. 2005. June/July 2007 Ask the Regulators: Acrylamide, Furan, and the FDA. Available from: http://www.fda.gov/Food/FoodSafety/FoodContaminantsAdulteration/ChemicalContaminants/Acrylamide/ucm194482.htm [2010, March 7]

Food and Drug Administration. 2006. Determination of Furan in Foods[online]. Available from: http://www.fda.gov/Food/FoodSafety/FoodContaminantsAdulteration/ChemicalContaminants/Furan/UCM078400 [2010, March 8]

Funebo, T., and Ohlsson, T. 1998. Microwave-assisted air dehydration of apple and mushroom. Journal of Food Engineering 38 : 353-367.

Gaspar E.M.S.M., and Lopes, J. 2009. Simple gas chromatographic method for furfural analysis. Journal of Chromatography A 1216(14) : 2762-2767.

Geedipalli, S.S.R., Rakesh, V., and Datta, A.K. 2007. Modeling the heating uniformity contributed by a rotating turntable in microwave ovens. Journal of Food Engineering 82 : 359-368.

Gökmen, V. 2006. Rapid Determination of Hydroxymethyfurfural in Foods using Liquid Chromatography-Mass Spectrometry[online]. Available from: http://www.chem.agilent.com/Library/applications/5989-5403EN.pdf [2010, March 17]

Gökmen, V., Palazoğlu, T.K., and Şenyuva, H.Z. 2006. Relation between the acrylamide formation and time-temperature history of surface and core regions of french fries. Journal of Food Engineering 77(4) : 972-976.

Gunasekaran, N. 2002. Effect of Fat Content and Food Type on Heat Transfer during Microwave Heating. Master's thesis Department of Biological system engineering Faculty of Engineering Virginia Polytechnic Institute and State University.

Heldman, D.R., and Lund, D.B. 1992. Handbook of Food Engineering. New York : Marcel Dekker Inc.

Hodge, J.E. 1953. Assessing the Maillard reaction development during the toasting process of common flours chemistry of browning reactions in model systems. Journal of Agricultural and Food Chemistry 1(15) : 928-943.

Hough, J.S., Briggs, D.E., and Steven, R. 1971. Malting and Brewing Science. Great Britain : Richard Clay (The Chaucer Press) Ltd.

International Agency for Research on Cancer . 1994a. furfural[online]. Available from: http://monographs.iarc.fr/ENG/Monographs/vol63/mono63-17.pdf [2010, March 7]

International Agency for Research on Cancer . 1994b. Furan[online]. Available from: http://monographs.iarc.fr/ENG/Monographs/vol63/mono63-16.pdf [2010, March 7]

International Agency for Research on Cancer . 1994c. Monographs on the Evaluation of Carcinogen Risk to Humans: Some Industrial Chemical[online]. Available from: http://monographs.iarc.fr/ENG/Monographs/vol63/mono63-17.pdf [2010, March 7]

International Agency for Research on Cancer Monographs on the Evaluation of Carcinogenic. 1995. Volume 63 Dry Cleaning, Some Chlorinated Solvents and Other Industrial Chemicals[online]. World Health. Available from: http://monographs.iarc.fr/ENG/Monographs/vol63/volume63.pdf [2010, March 7]

Jha, S.N. 1999. Physical and hygroscopic properties of makhana. Journal of Agricultural Engineering Research 72 : 145-150.

Kaldor, J.M. 1992. Quantitative assessment of human cancer risk. Scandinavian Journal of Work, Environment and Health 18 : 90-96.

Knol, J.J., Vikulnd, G.A.I., Linssen, J.P.H., Sjoholm, I.M., Skon, K.I., and Boekel, M.A.J.S. 2009. Kinetic modeling: a tool to predict the formation of acrylamide in potato crips. Food Chemistry 111 : 103-109.

Kroes R. 1999. World Health Organization, Geneva, 1999 IPCS - International Programme on Chemical Safety: Furfural[online]. Available from: http://www.inchem.org/documents/jecfa/jecmono/v042je03.htm [2010, March 7]

Levenspiel, O. 1972. Chemical Reaction Engineering. 2nd ed. New York : Johnson Wiley & Sons.

Lewis, M.J., and Young, T.W. 2002. Brewing. 2nd ed. New York : Kluwer Academic / Plenum Publishers. 398 p.

Lin, Y.E., Anantheswaran, R.C., and Puri, V.M. 1995. Finite element analysis of microwave heating of solid foods. Journal of Food Engineering 25 : 85-112.

Lingnert, H., Grivas, S., Jagerstad, M., Skog, K., Tornqvist, M., and Aman, P. 2002. Acrylamide in food: mechanisms of formation and influencing factors during heating of foods. Scandinavian Journal of Nutrition 46 : 159–172.

Liu, S.C., Yang, D.J., Jin, S.Y., Hsu, C.H., and Chen, S.L. 2008. Kinetics of color development, pH decreasing, and anti-oxidative activity reduction of Maillard reaction in galactose/glycine model system. Food Chemistry 108 : 533-541.

Lo Coco, F., Valentini, C., Novelli, V., and Ceccon, L. 1994. High performance liquid chromatographic determination of 2-furaldehyde and 5-hydroxymethyl-2furaldehyde in processed citrus juice., p.411. Cited in International Agency for Research on Cancer . Monographs on the Evaluation of Carcinogen Risk to Humans: Some Industrial Chemical. 1994. 560 p.

Mark, J., Pollien, P., Lindinger, C., Blank, I., and Mark, T. 2006. Quantitation of furan and methylfuran formed in different precusor systems by proton transfer reaction mass spectrometry. Journal of Agriculural and Food Chemistry 54(7) : 2786-2793.

Martins, S.I.F.S., and Boekel, M.A.J.S. 2005. A kinetic model for the glucose/glycine Maillard reaction pathways . Food Chemistry 90 : 257-269.

Matins, S.I.F.S., Jongen, W.M.F., and Boekel, M.A.J.S. 2001. A review of Maillard reaction in food and implications to kinetic modelling. Trends in Food Science and Technology 11 : 364-373.

Maskan, M. 2000. Microwave/air and microwave finish drying of banana. Journal of Food Engineering 44(2) : 71-78.

Metaxas, A.C., Meredith, R.J. 1993. Industrial Microwave Heating. London : Peter Peregrinus LTD. 357 p.

Mlotkiewicz, J.A. 1998. The role of the Maillard reaction in the food industry. In J. O. Brien , H.E. Nursten, M. James, C. Crabbe, and J.M. Ames (eds.), The Maillard Reaction in Foods and Medicine, pp. 19-28. London : Royal Society of Chemistry. 415 p.

Montgomery, D.C. 1997. Design and Analysis of Experiments. 4th ed. New York : John Wiley and Sons. Inc.

Mozzo, G 1990. Les plans d' experiments. Revue de Statistique Appliquée 38(3) : 23-34.

Mudgett, R.E. 1995. Electrical properties of foods. Chapter 8. In M.A. Rao, and S.S.H. Rizvi (eds.), Engineering Properties of Foods, pp. 389-455. New York : Marcel Decker, Inc. 531 p.

Mujumdar, A.S. 2000. Drying Technology in Agriculture and Food Sciences. Enfield, New Hampshire : Science Publishers. Inc

National Science Foundation. 2005. Microwave Oven[online]. Available from: http://www.colorado.edu/physics/2000/microwaves/hotspots.html [2010, March 18].

Nelson, S. 1991. Dielectric properties of agricultural products. IEEE Transaction on Electric Insulation 26(5) : 845-869.

Nursten, H.E. 2005. The Maillard Reaction: Chemistry, Biochemistry, and Implications. Cambridge : Royal Society of Chemistry. 214 p.

Oliveira, M.E.C., and Franca, A.S. 2002. Microwave heating of foodstuffs. Journal of Food Engineering 53 : 347-359.

Parkash, M.K., and Caldwell, J. 1994. Metabolism and excretion of furfural in the rat and mouse. Food and Chemical Toxicology 32(10) : 887-895.

Prabhanjan, D.G. Ramaswamy H.S. Raghavan G.S.V. 1995. Microwave-assisted convective air drying of thin layer carrots. Journal of Food Engineering 25 : 283-293.

Puris, E. 2010. Browning develpment in bakery products- a review. Journal of Food Engineering[online]. Available from: http://linkinghub.elsevier.com/retrieve/pii/S0260877410001172

Rao, M.A., Rizvi, S.S.H., and Datta, A.K. 2005. Engineering Properties of Foods. 3rd ed. New York : Taylor & Francis Group.

Rizkallah, J., Morales, F.J., Ait-ameur, L., Fogliano, V., Hervieu, A., Courel, M., and Birlouez-Aragon, I. 2008. Front face fluorescence spectroscopy and mutiway analysis for process control and NFC prediction in industrially processed cookies. Chemometrics and Intelligent Labloratory Systems 93 : 99-107.

Romano, V.R., Marra, F., and Tammaro, U. 2005. Modelling of microwave heating of food stuff: study on the influence of sample dimensions with a FEM approach. Journal of Food Engineering 71 : 233-241.

Rufián-Henares, J.A., Delgado-Andrade C., and Morales, F.J. 2006. Analysis of heat-damage indices in breakfast cereals: influence of composition. Journal of Cereal Science 43 : 63-69.

Rufián-Henares, J.A., Delgado-Andrade C., and Morales, F.J. 2008. Assessing the Maillard reaction development during the toasting process of common flours employed by the cereal products industry. Food Chemistry 114(1) : 93-99.

Ryynanen, S. 1995. The electromagnetic properties of food materials: a review of the basic principles. Journal of Food Engineering 26 : 409-429.

Shafiur. R. 1995. Food Properties Handbook. New York : CRC Press. Inc.

Sharma, S.K., Mulvaney, S.J., and Rizvi, S.S. 2000. Food processing engineering, theory and laboratory experiments. New York : John Wiley and Sons, Inc. 348 p.

Sharma, G.P. Prasad, S. 2001. Drying of garlic (*Allium sativum*) cloves by microwave-hot air combination. Journal of Food Engineering 50(2) : 99-105.

Sharma, G.P., Prasad, S. 2006. Optimization of process parameters for microwave drying of garlic cloves. Journal of Food Engineering 75(4) : 441-446.

Simsek, A., Poyrazoglu, E.S., Karacan, S., and Velioglu, Y.S. 2007. Response surface methodological study on HMF and fluorescent accumulation in red and white grape juices and concentrates. Food Chemistry 101 : 987-994.

Sweat, V.E. 1995. Thermal properties of foods. Chapter 3. In M.A. Rao, and S.S.H. Rizvi (eds.), Engineering Properties of Foods, pp. 99-138. New York : Marcel Decker, Inc.

Swedish National Food Administration. 2002. Information About Acrylamide in Food 24th[online]. Available from: http://www.slv.se [2010, January 9]

Symons, S.J., and Dexter, J.E. 1991. Computer analysis of fluorescence for the measurement of flour refinement as determined by flour ash content, flour grade color, and tristimulus color measurement. Cereal Chemistry 68(5) : 454-460.

Taeymans, D., Wood, J., Ashby, P., Blank I., Studer A., Stadler, R.H., Gonde, P., Eijck, P.V., Lalljie, S., Lingnert, H., Lindblom, M., Matissek, R., Muller, D., Tallmadge, D., Brien, J., Thompson, S., Silvani, D., Whitmore, T. 2004. A review of acrylamide: an industry perspective on research, analysis, formation, and control. Critical Reviews in Food Science and Nutrition 44 : 323-347.

Taher, B.J., and Farid, M.M. 2001. Cyclic microwave thawing of frozen meat: experimental and theoretical investigation. Chemical Engineering and Processing 40 : 379-389.

Teixidó, E., Santos, F.J., Puignou L., and Galceran, M.T. 2006. Analysis of 5-hydroxymethylfurfural in foods by gas chromatography–mass spectrometry. Journal of Chromatography A 1135(1) : 85-90.

The Council of the European Union. 2001. Council Directive 2001/110/EC[online]. Available from: http://eur-lex.europa.eu/LexUriServ/LexUriServ.do?uri=OJ:L:2002:010:0047:0052:EN:PDF [2010, March 17].

Ulbricht, R.J., Northup, S.J., and Thomas, J.A. 1984. A review of 5-hydroxymethylfurfural (HMF) in parenteral solutions. Fundamental and Applied Toxicology 4 : 843-853.

University of Maryland Medical Center. 2010. Lysine[online]. Available from: http://www.umm.edu/altmed/articles/lysine-000312.htm# [2010, May 9].

Versteeg, H.K., and Malalasekera, W. 1995. An Introduction to Computational Fluid Dynamics: The Finite Volume Method. Harlow : Longman Scientific & Technical. 257 p.

Westphal, W.B., and Sils, A. 1972. Dielectric constant and loss data., p.417. Cited in Rao, M.A., and Rizvi, S.S.H. Engineering Properties of Foods. New York : Marcel Decker, Inc, 1995.

Yaylayan, V.A., Machiels, D., Istasse, L. 2003. Thermal decomposition of specifically phosphorylated D-glucosed and their role in the control of the Maillard reaction. Journal of Agricultural and Food Chemistry 51(11) : 3358-3366.

Yeyer, Y., Kahpci, E. 2009. The carcinogenic effects of acrylamide formed during cooking of some foods. Journal of Cancer Research 2(1) : 25-32.

Zanoni, B., Peri, C., Bruno, D. 1995. Modeling of browning kinetics of bread crust during baking. Lebensmittel-Wissenschaft und-Technologie 28 : 604-609.

Zhou L., Puri, V.M., Anantheswaran, R.C., and Yeh, G. 1995. Finite element modeling of heat and mass transfer in food materials during microwave heating-model development and validation. Journal of Food Engineering 25 : 509-529.

Zyzak, D.V., Sanders, R.A., Stojanovic, M., Tallmadge, D.H., Eberhart, B.L., Ewald, D.K., Gruber, D.C., Morsch, T.R., Strothers, M.A, Rizzi, G. P., and Villagran, M.D. 2003. Acrylamide formation mechanism in heated foods. Journal of Agricultural and Food Chemistry 51 : 4782-4787.

APPENDICES

APPENDIX A

STATISTICAL RESULTS

Table A.1 Variance analysis result for color (ΔE) of malt roasted at different specific microwave powers (2.50, 2.75, and 3.00 $W \cdot g^{-1}$) for 3.4 min and at 200 °C oven temperature as a function of roasting time.

Source of Variation	*SS*	*df*	*MS*	*F*	*P-value*	*F crit*
Roasting time	322453	4	80613.3	25.6177	0.00013*	3.83785
Specific microwave power	8079.87	2	4039.94	1.28383	0.32843	4.45897
Error	25174.3	8	3146.79			
Total	355707	14				

* Significant at $p \leq 0.05$

Table A.2 Regression analysis result of color (ΔE)

Regression Statistics	
Multiple R	0.9972
R Square	0.9944
Adjusted R Square	0.9884
Standard Error	0.8197
Observations	28

	df	*SS*	*MS*	*F*	*Significance F*
Regression	14	1555.0184	111.0727	165.3163	2.79E-12*
Residual	13	8.7344	0.6719		
Total	27	1563.7528			

* Significant at $p \leq 0.05$

Table A.3 Regression analysis result of *Emw*

Regression Statistics	
Multiple R	1.0000
R Square	1.0000
Adjusted R Square	1.0000
Standard Error	0.0000
Observations	28.0000

ANOVA

	df	*SS*	*MS*	*F*	*Significance F*
Regression	14	193.9950	13.8568	6.23E+30	5.36 E-198*
Residual	13	0.0000	0.0000		
Total	27	193.9950			

* Significant at $p \leq 0.05$

Table A.4 Regression analysis result of *Eoven*

Regression Statistics	
Multiple R	1.0000
R Square	1.0000
Adjusted R Square	1.0000
Standard Error	5.1685
Observations	28.0000

ANOVA

	df	*SS*	*MS*	*F*	*Significance F*
Regression	14	54381186.1757	3884370.4411	1.45E+05	2.18E-31*
Residual	13	347.2739	26.7134		
Total	27	54381533.4496			

* Significant at $p \leq 0.05$

Table A.5 Regression analysis result of *Etotal*

Regression Statistics	
Multiple R	1.0000
R Square	1.0000
Adjusted R Square	1.0000
Standard Error	5.1685
Observations	28.0000

ANOVA

	df	*SS*	*MS*	*F*	*Significance F*
Regression	14	54381380.1707	3884384.2979	1.45E+05	2.18E-31*
Residual	13	347.2739	26.7134		
Total	27	54381727.4446			

* Significant at $p \leq 0.05$

Table A.6 Regression analysis result of HMF (fluorometric method)

Regression Statistics	
Multiple R	0.8485
R Square	0.7199
Adjusted R Square	0.4182
Standard Error	58.9516
Observations	28.0000

ANOVA

	df	*SS*	*MS*	*F*	*Significance F*
Regression	14	116102.6054	8293.00432	2.39E+00	0.0631*
Residual	13	45178.7749	3475.2904		
Total	27	161281.3803			

* Significant at $p \leq 0.05$

Table A.7 Regression analysis result of furfural (fluorometric method)

Regression Statistics	
Multiple R	0.9225
R Square	0.8510
Adjusted R Square	0.6906
Standard Error	34.1993
Observations	28.0000

ANOVA

	df	*SS*	*MS*	*F*	*Significance F*
Regression	14	86844.5297	6203.1807	5.30E+00	0.002*
Residual	13	15204.7277	1169.5944		
Total	27	102049.2574			

* Significant at $p \leq 0.05$

Table A.8 Regression analysis result of furan (fluorometric method)

Regression Statistics	
Multiple R	0.9275
R Square	0.8603
Adjusted R Square	0.7098
Standard Error	402.4573
Observations	28.0000

ANOVA

	df	*SS*	*MS*	*F*	*Significance F*
Regression	14	12963450.7973	925960.7712	5.72E+00	0.002*
Residual	13	2105634.4672	161971.8821		
Total	27	15069085.2645			

* Significant at $p \leq 0.05$

Table A.9 Regression analysis result of acrylamide (fluorometric method)

Regression Statistics	
Multiple R	0.7375
R Square	0.5439
Adjusted R Square	0.0527
Standard Error	109.7265
Observations	28.0000

ANOVA

	df	*SS*	*MS*	***F***	*Significance F*
Regression	14	186653.5042	13332.3932	1.11E+00	4.30E-01
Residual	13	156518.7734	12039.9056		
Total	27	343172.2776			

* Significant at $p \leq 0.05$

Table A.10 Regression analysis result of HMF (physico-chemical method)

Regression Statistics	
Multiple R	0.8814
R Square	0.7768
Adjusted R Square	0.5365
Standard Error	311.2650
Observations	28.0000

ANOVA

	df	*SS*	*MS*	*F*	*Significance F*
Regression	14	4383741.1422	313124.3673	3.23E+00	0.02*
Residual	13	1259516.8494	96885.9115		
Total	27	5643257.9916			

* Significant at $p \leq 0.05$

Table A.11 Regression analysis result of furfural (physico-chemical method)

Regression Statistics	
Multiple R	0.7892
R Square	0.6229
Adjusted R Square	0.2167
Standard Error	192.8843
Observations	28.0000

ANOVA

	df	*SS*	*MS*	*F*	*Significance F*
Regression	14	798746.7052	57053.3361	1.53E+00	2.24E-01
Residual	13	483656.8033	37204.3695		
Total	27	1282403.5085			

* Significant at $p \leq 0.05$

Table A.12 Regression analysis result of acrylamide (physico-chemical method)

Regression Statistics	
Multiple R	0.9404
R Square	0.8843
Adjusted R Square	0.7597
Standard Error	156.7292
Observations	28.0000

ANOVA

	df	*SS*	*MS*	*F*	*Significance F*
Regression	14	2440923.1905	174351.6565	7.10E+00	0.0000*
Residual	13	319332.6667	24564.0513		
Total	27	2760255.8571			

* Significant at $p \leq 0.05$

APPENDIX B

MOISTURE ANALYSIS

Moisture analysis of ground malt was determined according to the method of AOAC (1990, methods 935.29).

B.1 Apparatus

B.1.1 Weighing dish

Use glass bottle, with tight fitting cover, 55 mm diameter.

B.1.2 Oven

Use oven (FB 970 C2/E IX, Ariston, Fabriano, Italy) with automatic control holding temperature.

B.2 Determination

Weight sample to 10 g and place in oven previously heated to a temperature 105 °C. Remove cover of weighing bottle and heat exactly 3 hours at 105 °C**.** Replace cover, transfer to desiccators, cool to room temperature, and weight.

BIOGRAPHY

Suthida Akkarachaneeyakorn was born in Surin, Thailand. She did her Bachelor degree in Chemical Engineering and Master degree in Food Engineering from King Mongkut's University of Technology Thonburi. After graduation, she had instructed at Department of Agro-Industrial Technology, Faculty of Food Science, King Mongkut's University of North Bangkok for 2 years. She entered the Ph.D. program at Food Technology Department, Faculty of Science, Chulalongkorn University in June 2005.